Investigations of Potentially Implantable Glucose Sensors
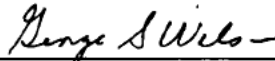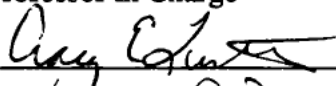
by

Yanan Zhang

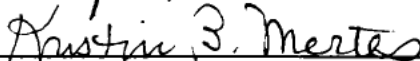B.S., Northeast Normal University, 1981
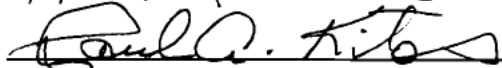
M.S., Jilin University, 1984

Submitted to the Department of Chemistry and

the Faculty of the Graduate School of the University

of Kansas in partial fulfillment of the requirements
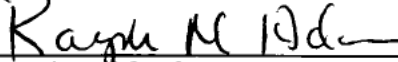
for the degree of Doctor of Philosophy

George S Wilson
Professor in Charge

Gary Quinta

Kristin B. Mertes

Paul A. Kito

Ralph N Dd
Committee Members

Date Defended _Aug. 20, 1991_

Yanan Zhang
C 1991

Investigations of Potentially Implantable Glucose Sensors

Yanan Zhang

Adviser: George S. Wilson

Abstract

The catalytic oxidation of H_2O_2 on Pt and Pt/Ir electrodes in pH 7.4 phosphate buffer was studied. It was found that the electron transfer reaction is more favorable at low concentration and at a well stabilized Pt /Ir electrode the dynamic range can be extended to nearly 1 mM. The oxidation of H_2O_2 is independent of oxygen partial pressure. The electrode surface conditioning was proven to be the most important factor affecting the quantitative measurement of H_2O_2. Covering the electrode surface with cellulose acetate membrane could effectively protect the electrode surface and substantially shorten the stabilization time.

A needle-type miniature glucose sensor for *in vivo* monitoring was developed. Its performance was evaluated both *in vitro* and *in vivo*. A multi-layer inner membrane was demonstrated to successfully eliminate electrochemical interferences. The *in vivo* interference from acetaminophen has been reduced to a minimal level. The sensor could be sterilized and stored in dry state without losing its characteristics, which made clinical applications possible.

A method of sensor toxicity screening was developed using cell culture technique. A freshly prepared sensor was found to have certain toxicity. The toxic substances could be removed by buffer treatment and a non-toxic sensor was readily available.

To evaluate the effect of oxygen on the performance of the glucose sensor, a miniature oxygen sensor was constructed which had identical size and geometry to those of the glucose sensor. It was characterized in buffer and *in vivo* measurements were carried out in rat subcutaneous tissue. Results showed that glucose sensors of low sensitivity were essentially independent of environmental Po_2 while high sensitivity sensors were affected by oxygen fluctuation

To My Parents

Acknowledgement

I wish to express my deep gratitude and appreciation to my academic adviser, Professor G.S. Wilson, for his guidance both in scientific research and social behavior. I have, through years of independent learning in both classroom and research laboratory constantly encouraged by him, gained the necessary confidence and ability to face the challenge of the fast advancing scientific world. A modern scientist will not achieve the due fulfillments without the right attitude and interactions with the outside world.

I would like to acknowledge the faculty of in the Analytical Chemistry Division and the staff in the Department of Chemistry for their support and encouragement. My grateful thanks also due to all the members of Wilson group for their valuable suggestions and friendly help in all aspects of life, which have meant so much in my career of graduate study.

I would like to express my appreciation to Dr. Kitos for his valuable discussion on the toxicity study and for his donation of the fibroblast cell line which made this part of the work easier. In addition, his consent for the access to the ethylene oxide sterilizer gave us excess convenience. I also thank Connie Emerson for her help in the cell culture laboratory. My friend Yibai Hu's cooperation contributed to part of the work in Chapter 4 and his help is gratefully acknowledged.

I also have to express my full hearted gratitude to my wife and my daughter. This task would never have been fulfilled without their love, support, understanding and sacrifice.

Finally, I would like to thank Dr.Gerard Reach in Hotel-Dieu Hospital (Paris) and Dr. Daniel R.Thevenot at the University of Paris XII for their help and friendly collaboration in the past four years.

Preface

This research project has been a multi-party collaboration and involved many people in different fields. The contents included in this thesis is also a partial reflection of the multi-discipline work. It is difficult to arrange the chapters in a sequential way of a text book. Since the work involved is a new area and each subtopic has been actually raised during the course of the sensor development. My assignment in this research was to develop and further improve the implantable glucose sensor and to investigate whatever problems encountered in the process, including both *in vitro* and *in vivo* fields. The chapters are therefore relatively independent of each other and they are more or less written in the form of publishable papers. In fact, some of the chapters have been either accepted or submitted for publication.

There seems to be a gap between Chapters 3 and 4 because the initial "Normal" sensor was jointly developed previously in this laboratory and published(see Bindra, 1991). The protocol for *in vivo* calibration was also a share by other collaborators and published elsewhere (Moatti, 1991; Poitout, 1991). Those contents are therefore not included in detail. This thesis contains only the part of the work for which I am the first author (except for Dr.G.S.Wilson who is my academic adviser).

A general introduction is placed as Chapter 1 in order to outline these topics and an abstract is provided at the beginning of each chapter so that viewers can grasp the basic idea at a glance.

List of Contents

List of Illustrations

Chapter 1. General Introduction

I Biosensors

A biosensor is generally defined as a system of two elements, one biochemical and the other physical, relating the concentration of an analyte to a measurable physical property such as current, potential, optical intensity, conductivity, charge-field effect or enthalpic change. The classification of biosensors can also be based on the characteristics of the physical transducers such as an electrode operated in the amperometric or potentiometric mode. The biocomponent of the sensor distinguishes its characteristics from other chemical sensors which probe the analytes through chemical reactions. Figure 1-1 shows a functional schematic of the biosensor.

In essence, a biosensor is capable of monitoring the concentration of a molecule in a complex matrix continuously with high specificity. The biocomponent is therefore essential for the molecular recognition. Typical examples are enzymes, antibodies, receptors, plant and animal tissues or micro-organisms (Wilson, 1991). Biosensors can also be classified according to application, *in vitro* or *in vivo*. *In vitro* biosensors have found wide applications in biochemical analysis, food processing and clinical diagnostics. *In vivo* sensors are even more promising for therapeutic purposes in disease monitoring and control. The glucose sensor, the most studied biosensor, is a good example for illustrating the functioning of a biosensor. Most implantable glucose sensors have employed enzyme amperometric detection because of its high sensitivity, stability and ease of miniaturization. Figure 1-2 shows two representative configurations of implantable glucose sensors that have been intensively studied. Figure 1-2a shows the O_2 detection mode which measures the consumption of oxygen by the enzymatic glucose oxidation. A cathode is used (usually poised at -600 mV) to measure the reduction of oxygen. The inner polymer layer, typically Teflon, permits

1
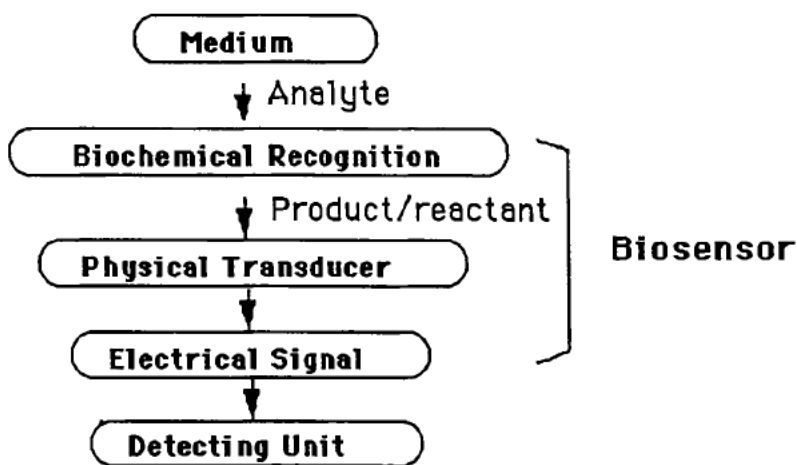
Figure 1-1. Schematic Diagram of Biosensor
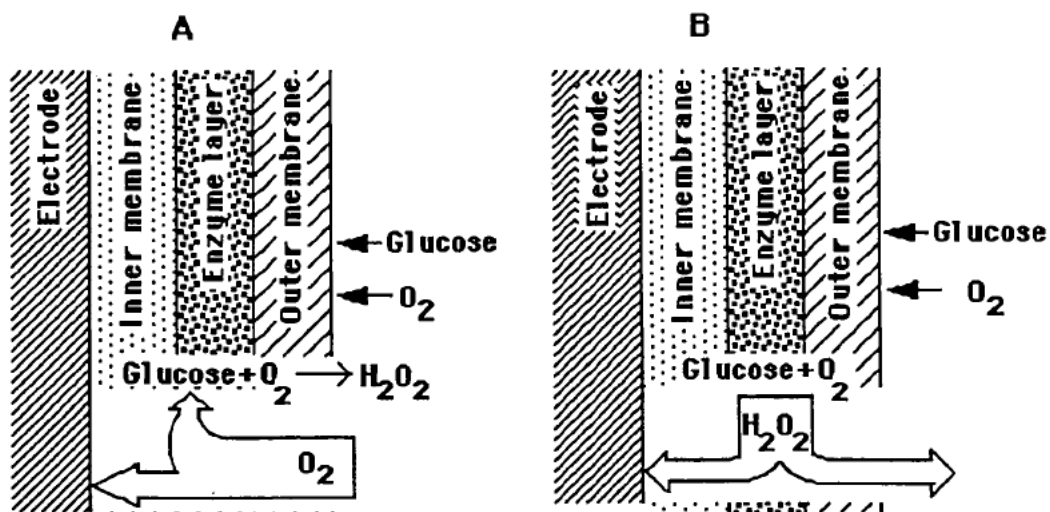
Figure 1-2. Diagram of the O_2 Detecting and H_2O_2 Detecting Glucose Sensors

    A: Oxygen consumption is measured.

    B: H_2O_2 generation is measured.

2

only gaseous oxygen to pass through so that electrochemical interferents in the sample matrix do not reach the electrode. This configuration, however, requires coupling of another identical oxygen electrode without the enzyme layer to differentiate the oxygen consumption between the two electrodes thus avoiding the effect of oxygen fluctuation in the environment. Since the measurement is an indirect method, the sensitivity is essentially uncontrollable once the sensor surface area is fixed. Another restriction is that the sensor couple must be implanted in the blood stream because the external oxygen tension for both electrodes must be identical. This can be approximated only in the intravascular situation. Figure 1-2b illustrates the glucose sensor in the H_2O_2 detection mode. There are several advantages for the H_2O_2-based glucose sensor as opposed to the O_2-based glucose sensor. The overall configuration is simpler and much easier to miniaturize. This is very important because for miniature sensors their dependability in performance is largely determined by the controllability of fabrication. The direct detection mode of this sensor gives higher sensitivity and the sensitivity can be controlled easily by altering the outer membrane permeability to glucose. This sensor is not affected by oxygen fluctuation as long as the overall process is glucose diffusion controlled. Finally, this sensor can be implanted in various sites other than intravascular, which avoids unnecessary surgical implantation and potential systemic infection. One potential disadvantage of the H_2O_2-based sensor, however, is that it can suffer from electrochemical interferences. The inner membrane must be permeable to H_2O_2 and impermeable to other endogenous oxidizable species such as ascorbic acid and widely-used drugs such as acetaminophen. Searching for such a polymer material has been a difficult task and a completely satisfactory film is not yet available.

II Diabetes Mellitus and Its Control

The insulin dependent diabetes mellitus (Type I diabetes) is an autoimmune disease characterized by partial or total damage of pancreatic β–cells by islet-cell antibodies. The loss of insulin secretion capacity results in uncontrolled glycemia and the patients have to depend on external insulin injections to regulate blood glucose. The Type I diabetes involves about 15 % of the diabetic population and occurs primarily in young people. In the United States alone, an estimated 6 million people are known to have diabetes, with an equal number unrecognized. Among them over 1 million are insulin dependent and the net increase is still over 50,000 every year (Galloway, 1988). Current insulin therapy includes monitoring blood glucose and injecting insulin from one to as many as eight times daily. The patients have to be fully aware of the timing for blood test and insulin injection and a strict dietary management is essential.

The concept of closed-loop insulin delivery system, the artificial pancreas, was introduced in early 1970's (Albisser, 1974). It was proposed that a glucose sensor, a computer and an insulin pump could give the patients complete relief. The computer received signals from the glucose sensor, calculated the optimal insulin dosage according to the glucose level and delivered insulin through the pump automatically. There have been several insulin pumps commercialized and the availability of computers capable of performing this task is by no means a problem. But it is still stated in a recent monograph on diabetes mellitus: an implantable glucose sensor is not yet available (Santiago, 1988). For years efforts have been devoted to the development of the implantable glucose sensor. Although steadfast progress has been made, a major breakthrough is yet to be achieved. The glucose sensor is still the "bottleneck" for the artificial pancreas (Reach, 1990).

The difficulties in realizing this goal are the strict requirements for the highly dependable performance of the sensor, including its safety, reliability and durability.

4

Any slightest false signal is not acceptable because in a closed-loop system the insulin infusion is based on the sensor output. The sensor therefore must have stable sensitivity, high selectivity(specificity), and reasonable dynamic range. From the *in vivo* point of view, biocompatibility constitutes another important difficulty. Because living organisms are created to possess self-defense capability by initiating immune response and wound healing, any foreign substance will be recognized and rejected and any damage will be repaired by physiological processes. The degree of those reactions depends to a great extent on the nature of the "invading object". In the case of the glucose sensor, for example, its size, shape and surface chemical reactivities determine the degree of tissue response. Severe tissue damage due to unfavorable shape, large size or high chemical toxicity will induce strong tissue reactions and will result in complete encapsulation of the sensor. Also the surrounding tissue cannot function normally due to the strong perturbation caused by implantation so that the sensor will not sense the normal tissue activity.

III Considerations in the development of an Implantable Glucose Sensor

The following are the general considerations in the development of the implantable glucose sensor for the artificial pancreas.

(1) The artificial pancreas should be wearable to be used by general patients. A bedside instrument is not of great value except for intensive care. This requires that the sensor should have an adequate geometry and small size for the ease of implantation, less tissue damage and patient acceptance. Many designs and geometries have been reported to function *in vivo* (Abel, 1984; Bessman, 1981; Clark, 1982; Pickup, 1985, Gough, 1986, Fischer, 1989; Armour, 1990). A needle shaped sensor is by far the best geometry for these purposes. The first needle-type glucose sensor was tested by Shichiri and co-workers (Shichiri, 1982 & 1984) and monitored subcutaneous glucose

in animals and human diabetics.

(2) The site of implantation should be decided beforehand: blood vessel or tissue. There is no clear answer to this question. An intravenous sensor enables direct *in vivo* calibration because the sensing medium, the blood, can be directly sampled and analyzed. Another advantage is that this sensor is less likely affected by oxygen partial pressure since Po_2 in the blood stream is higher than that in tissue. A critical disadvantage for this sensor, however, is that any infection would be spread systemically, a risk which jeopardizes much of the acceptability. Another disadvantage is that the implantation has to be surgical and the sensor must have long life time to compensate for this shortcoming. The tissue (generally subcutaneous tissue) sensor, on the contrary, is less subject to systemic infection and does not necessarily require surgical implantation. It is therefore readily acceptable by most patients. The subcutaneous tissue for glucose monitoring has been validated by many authors who have shown that the change in tissue glucose follows the blood glucose closely with a lag time of 5 - 10 minutes (Shichiri, 1982; Fischer, 1989; velho, 1989). This sensor also has potential problems. One is that the tissue oxygen supply is lower than that in blood and the fluctuation in oxygen could probably affect the sensor functioning. Although the needle sensor is undoubtedly the best geometry, the size has been unsatisfactory. None of the sensors developed previously could be implanted by patients themselves. In terms of biocompatibility, the size is also important for the tissue reactions. It has to be further reduced.

(3) The configurations of implantable glucose sensors are predominately of the amperometric type. Others such as potentiometric, opto-chemical and FET, etc., are less advantageous due to low sensitivity, long response time, bulky instrumentation or still in an early stage of development. For practical purposes the H_2O_2 amperometric sensor is the favorable choice as opposed to the oxygen type.

(4) The biocompatibility of the sensor is a two sided problem. The host response is the reaction of the physiological system to the implanted device and related damage caused by implantation. The second aspect is the material response resulting in changes in permeability, surface structure,etc of the sensor due to interactions between the sensor and the surrounding tissue. To minimize these interactions, proper methods for reducing sensor surface activity and evaluating the extent of these reactions should be developed. The tissue damage should be minimized by using smallest possible size and modes of implantation which result in minimal tissue disruption.

(5) Much has been said about the size of the sensor. In practice it is very difficult to fabricate a sensor that is less than 0.5 mm in diameter and possesses the required features of sensitivity, stability and, especially, reproducibility. It is a major task to develop a protocol of sensor fabrication to obtain reliable uniform enzyme immobilization and polymer membrane coatings.

(6) From the discussion above it is clear that a H_2O_2 based glucose sensor is much simpler and easier to miniaturize. But there remain some other problems. For example, the autodecomposition of H_2O_2 catalyzed by the Pt surface is a well documented reaction which, if it exists in the case of the glucose sensor, would cause unreliable results because the decomposition

$$2H_2O_2 \ = \ O_2 + 2H_2O$$
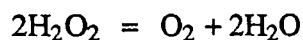
can compete with the electrode oxidation of H_2O_2

$$H_2O_2 \ = \ O_2 \ + \ 2H^+ + \ 2e^-$$
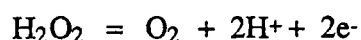
The electrochemical oxidation of H_2O_2 at Pt and Pt-Ir electrodes also has unfavorable kinetics. It has been a common experience that poor reproducibility and unstable responses are frequently encountered in quantitative H_2O_2 detection, and the causes of these problems are largely unknown. The conditions for dependable H_2O_2

measurement at physiological pH as the basis of glucose sensing therefore needs to be established.

(7) Detection of glucose by the sensor is based on the enzymatic reaction

$$\text{Glucose} + O_2 \overset{\text{GOx}}{======} \text{Gluconic acid} + H_2O_2$$
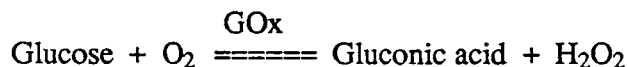
where glucose is oxidized by oxygen to generate H_2O_2 which, in turn, is detected at the electrode, giving a current proportional to the concentration of glucose in the medium. This enzymatic reaction requires a sufficient supply of oxygen, the co-substrate, to proceed. In other words, in order for the overall process to be glucose diffusion controlled, there must be excess oxygen available. Implantable sensors are usually constructed and tested under environmental oxygen partial pressure (~ 150 mm Hg) which is sufficiently abundant to support normal sensor functioning. The *in vivo* P_{O_2} in tissue is obviously much lower (in the range of 20 - 30 mm Hg) than the atmospheric value. The performance of the glucose sensors under such circumstances is very likely to be affected by oxygen. In fact, this has been one of the major criticisms of subcutaneous (sub-Q) monitoring of glucose. Fischer, et al (Fischer,1989) reported a study, attempting to evaluate the oxygen effect on the glucose sensor by implanting an oxygen sensor and a glucose sensor simultaneously in dogs. No oxygen effect was observed. however the oxygen sensor was different in size from that of the glucose sensor. A quantitative relationship between the tissue P_{O_2} and the sensor performance was therefore not obtained. Further work is required to establish quantitative understanding of the *in vivo* oxygen effect since sensor malfunctioning is not allowed in a closed-loop system.

(8) Electrochemical interference has been a major problem for the H_2O_2-based biosensors. A method of eliminating (at least stabilizing) the interferences is definitely

8

required. Further, the extent of *in vivo* interference, its fluctuation and its influence on the sensor performance are not yet known and should be evaluated.

(9) The *in vivo* performance of the implantable biosensor and the impact of the tissue response on the sensor functioning are still largely unknown. Although the concept of biosensor has an important ultimate goal of *in vivo* monitoring, much research work is still at the stage of developing the sensor itself. Systematic and continuous investigation concerning various factors that have potential influence on the sensor performance is indispensable. The final criterion for the performance of a glucose sensor is whether the sensor output has good correlation with glycemia. The decrease in sensitivity after implantation does not affect the sensor's *in vivo* application because it can be corrected with the two point calibration method (Velho, 1989). But the cause of this phenomenon needs to be clarified in order to direct further development. The *in vivo* oxygen effect on the sensor must also be evaluated to validate the application to the tissue measurement. Finally, evaluation of the chemical toxicity of the sensor is another necessary step which constitutes part of a thorough, long-term biocompatibility study.

IV The Research Goal

Success in developing a reliable glucose sensor first rests on the effectiveness of the inner membrane in selectively screening off electrochemical interferences while avoiding excessive resistance to the passage of H_2O_2 and charge carrying ions. Second, high reproducibility and success rate in sensor fabrication depend on a method for uniform and effective enzyme immobilization on the miniaturized sensor. The primary goal of this work is, therefore, to find suitable materials for the electrode surface modification and a reliable method for enzyme immobilization. Sequentially, the behavior of H_2O_2 electrochemical oxidation will be investigated in detail in order to

9

establish a protocol for its amperometric detection. A method for sensor toxicity evaluation will also be developed which serves as an initial screening method to avoid unnecessary massive animal tests. In the field of *in vivo* applications, factors having potential influence on the sensor functioning, such as oxygen effect, background current drift, sensitivity change and interference from endogenous electroactive species, will be addressed individually and systematically to explore the possibility for future clinical application of the implantable biosensors.

Chapter 2. Electrochemical Oxidation of H_2O_2 on Pt and Pt/Ir Electrodes in Physiological Buffer and its Applicability to H_2O_2 Based Biosensors

Abstract

The electrochemical oxidation of hydrogen peroxide on Pt disk and Pt/Ir wire electrodes was studied in physiological buffer at pH 7.40 in order to establish a practical protocol for H_2O_2 based biosensors. The electrode reaction is a two electron irreversible process. The oxidation of H_2O_2 on Pt and Pt/Ir electrode surfaces is a catalytic reaction which is H_2O_2 concentration dependent but O_2 pressure independent at low H_2O_2 concentration. Amperometric detection of H_2O_2 is strongly affected by pH, temperature and electrode surface conditioning. An oxidized surface is required to obtain a stable H_2O_2 response and reductive pre-treatment of the electrode always yields prolonged stabilization time. The application of a cellulose acetate membrane to the surface can protect the oxidized surface and therefore substantially reduce the stabilization time for H_2O_2 measurements.

Introduction

The coupling of H_2O_2 electrochemical oxidation to amperometric biosensors as the signal transducing device has been one of the major successes in the course of sensor development. For example, the most frequently used enzyme sensor to date has been the glucose sensor with glucose oxidase as the biospecific reagent. The reactions involved in the process are:

$$\text{Glucose} + O_2 \xrightarrow{\text{GOx}} \text{Gluconic acid} + H_2O_2 \qquad (2\text{-}1)$$

$$H_2O_2 \xrightarrow{\text{electrode}} O_2 + 2H^+ + 2e^- \qquad (2\text{-}2)$$
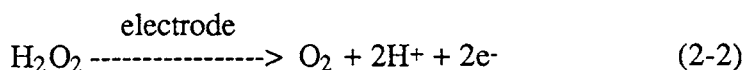
A successful glucose sensor is expected to give a signal linearly proportional to the environmental glucose concentration. The overall process, therefore, has to be glucose diffusion controlled, which requires that the rate of reaction(2-1) should not

depend on oxygen. Reaction (2-2) should be relatively fast such that the rate determining step is reaction (2-1) to ensure that the sensor output is glucose dependent. The enzymatic reaction (2-1) is governed by the enzyme turnover number and its rate is not manipulable. The total enzyme loading can be increased to achieve higher overall turnover rate (in fact, this is the way that most of the glucose sensors have been constructed in order to raise the sensitivity). But when the sensor surface area is fixed, a high density enzyme layer will require an even higher electrode reaction rate to accommodate the enhanced enzymatic reaction. The rate of the electron transfer reaction (2-2) thus becomes crucial.

A full understanding of the electrooxidation of H_2O_2 in neutral pH range is not yet available. Most previous studies were carried out under extreme pH conditions (Huang, 1979; Sandler, 1965; Schuldiner, 1963) (for the study of fuel cells)which simplified the electrode mechanism because either [H+] or [OH-] was high enough to give reproducible results. Further, well defined oxidation behavior of H_2O_2 is more difficult to obtain than its reduction because the oxidation on a solid electrode is hard to reproduce (Prabhu, 1981). Finally, the catalytic decomposition of H_2O_2 on a Pt electrode has been a potential problem for the oxidative detection of H_2O_2 because the current efficiency depends on the rate of catalytic decomposition.

The reactions of the H_2O-H_2O_2-O_2 system in acidic and neutral aqueous solution are as follows:

$$H_2O_2 = O_2 + 2H^+ + 2e^- \qquad (2\text{-}2)$$

$$H_2O_2 + 2H^+ + 2e^- = 2H_2O \qquad (2\text{-}3)$$
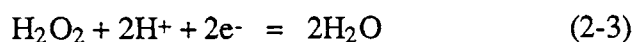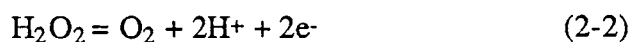
and the addition of these two reactions corresponds to the decomposition of H_2O_2

$$2H_2O_2 = O_2 + 2H_2O \qquad (2\text{-}4)$$

The decomposition reaction is largely a surface conditioning dependent feature and is a

function of the H_2O_2 concentration as well as the oxygen partial pressure.

Nernstian behavior of the H_2O_2-O_2 couple is approximately observed at low H_2O_2 concentration where the $dE/d[H_2O_2]$ and $dE/d\,P_{O2}$ have slopes of -30mV and 30 mV, respectively (Urbach, 1969). This is consistent with reaction (2-2) being the predominant process on the electrode surface when the concentration of hydrogen peroxide in the solution is low (< 1 mM at atmospheric pressure). The situation changes as the H_2O_2 concentration goes up. The electrode potential becomes independent of both H_2O_2 and O_2 concentration because the decomposition of H_2O_2 is significant when the surface $[H_2O_2]$ and P_{O2} are above certain values. The surface adsorption of either H_2O_2 or O_2 leads to saturation such that the surface concentrations are no longer dependent on the bulk concentration. The rate of the Pt catalyzed decomposition of H_2O_2 increases with pH. The evolution of O_2 bubbles on the electrode can be seen with the naked eye in a solution of 0.1 M H_2O_2 at pH > 9 (Bockris, 1955).

The pH dependence of the mixed potential, however, has a value of ~ 60 mV/pH and is relatively constant in the pH range of 2-12 (Bockris, 1955; Honda, 1983), which indicates that the electrode reaction of H_2O_2 is a two electron process throughout this range. This point has been confirmed by the microcoulometric method (Prabhu, 1981).

Although the electrochemical oxidation of H_2O_2 is reported to be quasi-reversible (Prabhu, 1981), it is not clear yet under what conditions a H_2O_2 diffusion controlled process can be approximated and in what situation the electron transfer kinetics and the catalytic decomposition significantly affect its quantitative measurement in the amperometric mode.

A miniaturized sensor, especially one that is developed for the purpose of long

term *in vivo* implantation, requires that the sensor material be robust. Platinum is certainly the best choice not only because of its physical stability but also because of its low overpotential for the oxidation of H_2O_2. Yet pure Pt alone is still too soft when the size of the electrode is reduced to the 0.1 mm range. Any bending of the wire electrode by accident would destroy the modified surface. An alloy of Pt/Ir is therefore adopted which is stable both chemically and mechanically. The electrode thus can be handled with ease.

The methods of solid electrode surface treatment have been well discussed Adams, 1969), In the case of a miniature sensor, however, any rigorous treatment such as strong acid, base or oxidant cannot be used and neither is the polishing method applicable. The surface conditioning for the H_2O_2 sensor is therefore still an important issue to be addressed because the oxidation of H_2O_2 is extremely sensitive to the surface condition. To obtain an "effective surface area" reproducibly is a prerequisite for a successful H_2O_2 based sensor. A study of the effect of surface conditioning thus becomes necessary.

This report deals primarily with the electrochemical oxidation of H_2O_2 on Pt and Pt/Ir electrodes. Factors that might influence the quantitative measurement of H_2O_2 will be addressed in order to establish a dependable protocol for the detection of H_2O_2 in physiological buffer which could also be extended to *in vivo* application of various H_2O_2 based biosensors.

Experimental

The Pt rotating disk electrode with the diameter of 0.5 cm (surface area 0.196 cm^2) and the Model MSR rotator were the products of Pine Instrument Co. (Grove City, PA) and a gold RDE of the same surface area was from Bioanalytical Systems

Inc.(West Lafayette, Indiana). An EG&G Princeton Applied Research potentiostat/galvanostat Model 273 controlled through a computer was used except for the pulsed amperometry and DC amperometry which were performed on a PAR Model 400 EC detector.

Phosphate buffer (0.1 M) containing 0.15 M NaCl was prepared directly from reagent grade Na_2HPO_4, KH_2PO_4 with NanoPure II (Barnstead-Sybron, Rochester, NY) treated distilled water. Sodium azide (0.1 g/L) was added as preservative. Standard solutions of 1.00 and 10.0 mM H_2O_2 were diluted freshly from a 10.00 M stock solution which was standardized by $KMnO_4$ titration and kept in the refrigerator in an amber bottle. The concentration of the stock solution was re-checked periodically and no detectable change was found in three years. Standard solutions that had been exposed to the air and room temperature more than four hours were discarded.

Buffers of various pH were simply obtained by adjusting the pH 7.4 buffer with 5 M HCl or NaOH and a Fisher Accumet Model 910 pH meter was used to monitor the pH change throughout the experiments whenever a pH other than 7.4 was adopted.

Wire electrodes (0.5 mm and 0.17 mm O.D.) were made from Teflon coated Pt and Pt/Ir (10 % Ir; Pt and Pt/Ir for each size) (Medwire, Mount Vernon, NY). A circular cut was made in the Teflon coating perpendicular to its axis 4 mm from one end and a cylindrical cavity of 1 mm length was created by moving this 4 mm Teflon coating to the tip. The excess 1 mm Teflon coating at the tip was then cut off and discarded. The end of this electrode was sealed with silicone rubber glue (Dow Corning). The sureface area was 0.0157 cm² for the 0.5 mm wire and 0.00534 cm² for the 0.17 mm wire.

A cellulose acetate membrane coated wire electrode was made by dip-coating the above electrode into a 6 % cellulose acetate (CA; acetyl content 39.8%, Aldrich)

solution (1:1 acetone : ethanol). The freshly coated electrode was dried in the air for half a minute and dip coated in the cellulose acetate solution two more times using the same procedure. The electrode was then let dry in the air for one minute and put into water for more than ten hours to allow water to replace the residual solvents. This process enabled better permeability control.

A three-compartment electrochemical cell (25 ml capacity) was used for the platinum RDE experiment and another three-compartment cell of 10 ml capacity with a stirring bar on the bottom was used for wire electrodes in the pulsed and DC measurements. The RDE was first polished with 1 μm alumina followed by ultrasonic cleaning and thorough rinsing with distilled water. The electrode was then scanned from -0.4 V to 1.2 V for at least 5 cycles until a reproducible I-E curve was obtained. The cleaning (or conditioning) of the wire electrodes is one of the purposes of this study and will be addressed subsequently.

Amperometric measurements of H_2O_2 were carried out by treating the wire electrodes in various ways and applying a constant potential of 650 mV vs Ag/AgCl. After a stable background current was obtained, a spike of H_2O_2 was then injected into the cell with a micropipet. The i-t behavior was recorded with a Kipp & Zonen BD 40 x-t recorder.

All the experiments were made against Ag/AgCl reference electrodes. The potential values are reported accordingly and will not be reiterated in the text.

Results and Discussion

I. Electrode Materials

It has been pointed out in the Introduction Section that the sensor is developed for the purpose of implantation and only noble metals are considered as the electrode

materials. Voltammetry was run for platinum and gold disk electrodes. Their C-V curves are shown in Figure 1-1. The oxidation of H_2O_2 takes place readily at Pt but not at Au. This is in agreement with the reported work that H_2O_2 oxidation has a higher overpotential on Au than on Pt (Hoare, 1965). The evolution of O_2 from the oxidation of water, on the other hand, has lower a potential on Au, leaving a narrower potential window to manipulate. These two observations demonstrate clearly that Pt is advantageous over Au in terms of H_2O_2 oxidation. The experiments thereafter were carried out on the platinum electrode only.

II. Hydrodynamic study

The general equation for an irreversible electrode reaction contains both kinetic and mass transfer components (Bard, 1980)

$$ i = nFAk_fC^* / (1 + k_f / m) \qquad (2\text{-}5) $$

where k_f is the heterogeneous electron transfer rate constant and m the mass transport parameter which assumes different forms for different electrode geometry and solution hydrodynamics. These two terms can be separated if the following transformation is made

$$ 1/i = 1/i_k + 1/i_d \qquad (2\text{-}6) $$

where $i_k = nFAk_fC^*$ is the kinetic current and $i_d = nFAmC^*$ is the diffusion current.

For a rotating disk electrode, $m = 0.620 \, D^{2/3} \, \nu^{-1/6} \, \omega^{1/2}$, where ν is the kinematic viscosity (~0.01 cm^2/sec for water) and ω the rotation speed in rpm. Equation (2-6) thus becomes

$$ 1 / i = 1 / (nFA \, k_fC^*) + 1 / (0.620nFAC^* D^{2/3} \, \nu^{-1/6} \, \omega^{1/2}) \qquad (2\text{-}7) $$

A plot of $1/i$ vs $1/\omega^{1/2}$ (Koutecky-Levich Plot (K-L)) will yield a straight line
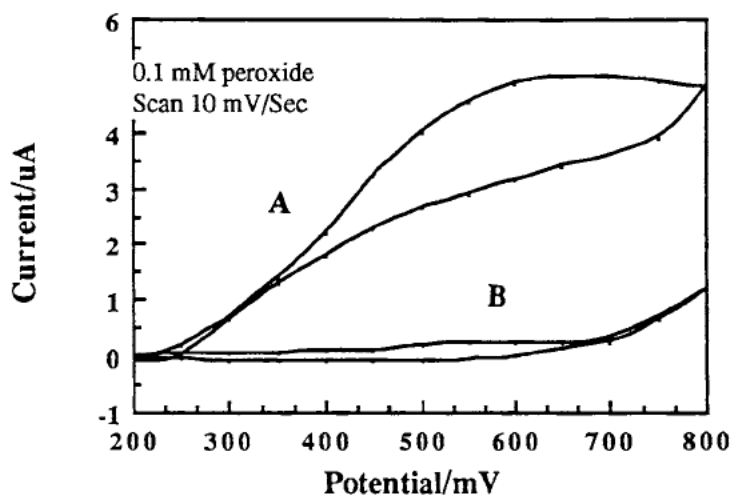
Figure 2-1. The Current-Potential Curves of H_2O_2 on Pt and Au

0.1 mM H_2O_2,   A: Pt and B: Au
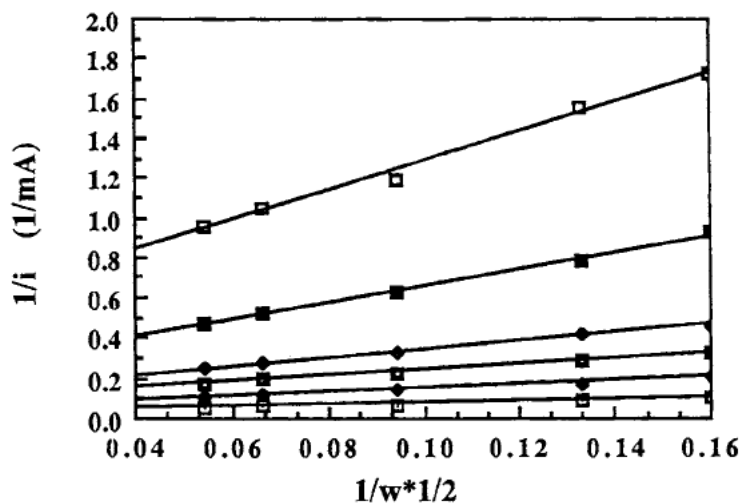
Figure 2-2. Koutecky-Levich Plot of H_2O_2 Oxidation on Pt RDE

Measured at 750 mV vs Ag/AgCl; ⊡:0.1 mM; ■: 0.3 mM;

◆: 0.5 mM; ⊞1.0 mM; ◇2.0 mM; ⊡ 3.0 mM.

2-2 shows the plot of H_2O_2 oxidation on Pt RDE at pH 7.4, in which a typical non-mass transfer controlled process is illustrated.

The kinetic currents (i_k) taken at the intercepts (i.e. $1/i = 1/(nFAK_fC^*)$) are plotted against the bulk concentrations of H_2O_2 in Figure 2-3 and corresponding rate constants (k_f) are given in Table 2-1. Although good fits are obtained for the K-L plot throughout the entire concentration range (10^{-5} - 10^{-2} M), the kinetic current does not vary linearly with concentration because of the variation of the rate constant (Table 1).

Table 2-1. Rate constant (k_f) vs H_2O_2 concentration*

$[H_2O_2]$/mM	0.1	0.2	0.3	0.5	0.7	1.0	2.0	3.0
k_f /10^{-6} cm/sec	7.5	7.1	6.9	6.6	6.3	6.0	5.5	5.5

* Calculated from Figure 2 measured at 750 mV vs Ag/AgCl.

An i-$[H_2O_2]$ curve measured amperometrically on a Pt/Ir wire electrode in a constantly stirred solution exhibits the same trend (Figure 2-4), losing linearity when the concentration is above 1 mM.

These results are similar to those previously reported for the potentiometic measurements of H_2O_2 (Urbach, 1969). The electrode potential of the H_2O_2 - O_2 couple obeyed the Nernst Equation below 1 mM H_2O_2 and became independent of H_2O_2 above that concentration under atmospheric pressure, which was explained by the saturation of the electrode surface by the adsorption of H_2O_2 and O_2. The electrode

19
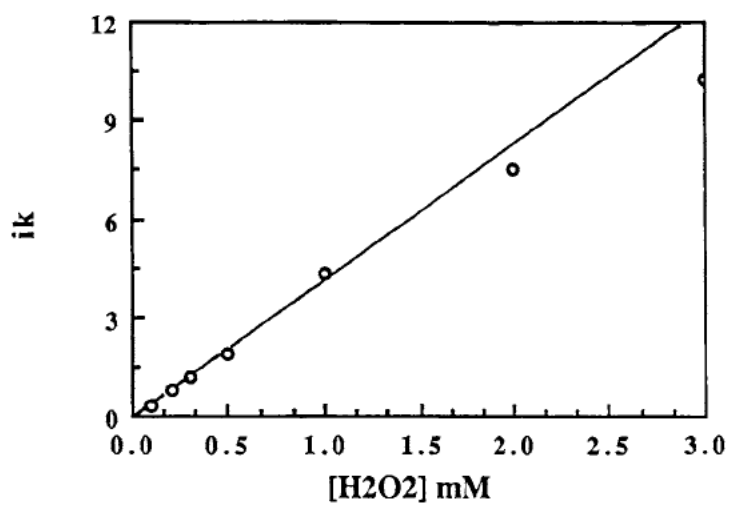
Figure 2-3. Kinetic Current vs H_2O_2 Concentration

(Calculated from Figure 2-2)
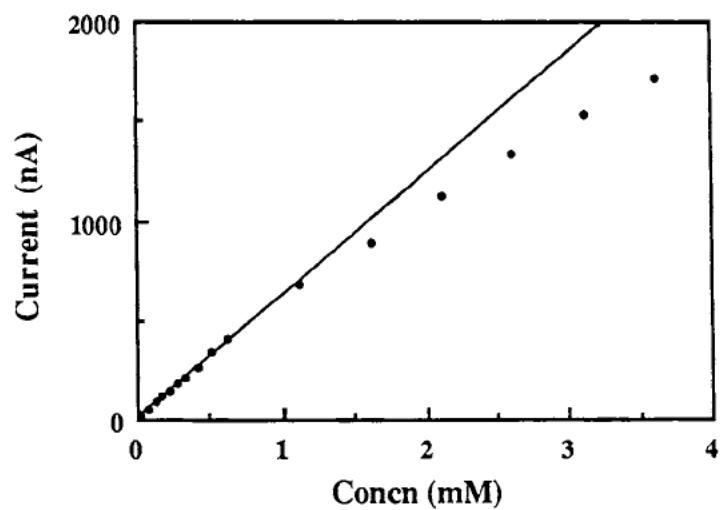
Figure 2-4. Steady State Current of H_2O_2 Oxidation on Pt/Ir wire Electrode

kinetics, as has been observed in this experiment, is certainly a surface condition controlled event and therefore the correlation between the surface properties and the electron transfer reaction is reflected by the rate constant. It is also possible that because of the slow electron transfer the supply of reactant (H_2O_2) easily reaches a state of excess. The current is therefore no longer diffusion controlled.

III. The pH Effect

Since protons are involved in the H_2O_2 oxidation reaction, a strong dependency of both potential and current on the solution pH was observed. Figure 2-5 shows the voltammograms of air saturated H_2O_2 solutions of various pH and Figure 6 shows the mixed potential (E_m) of the H_2O_2 - O_2 couple against pH, where values are taken at the zero current points.

The mixed potential (E_m) follows the relationship of $d(E)/d(pH) \sim 60$ mV within the pH range of 4 - 13, which confirms that the reaction is a two electron process (Reaction 2-2). The rate of the reaction is also pH dependent as demonstrated by the $E_{1/2}$ (half wave potential) vs pH curve (Figure 2-6) which was obtained by the intercept of the i-E scan slope in Figure 5 at the 50 % current points. The $E_{1/2}$ values reflect the relative rate of the electron transfer because the scan rate is constant for all these curves (10 mV/sec). The reaction proceeds faster at higher pH. As pointed out earlier by others (Prabhu, 1981) the oxidation behavior of H_2O_2 is difficult to reproduce. The data shown in Figures 2-5 and 2-6 were obtianed by keeping a Pt RDE and a pH electrode in 25 ml buffer containing 0.1 mM H_2O_2 and adjusting the pH by adding 5 M HCl or NaOH. The i-E curves were measured after each pH adjustment when the pH electrode had a stable reading.

The current - pH curve was measured on a Pt/Ir wire electrode at a fixed potential of 650 mV vs Ag/AgCl under constant stirring as shown in Figure 2-7. The
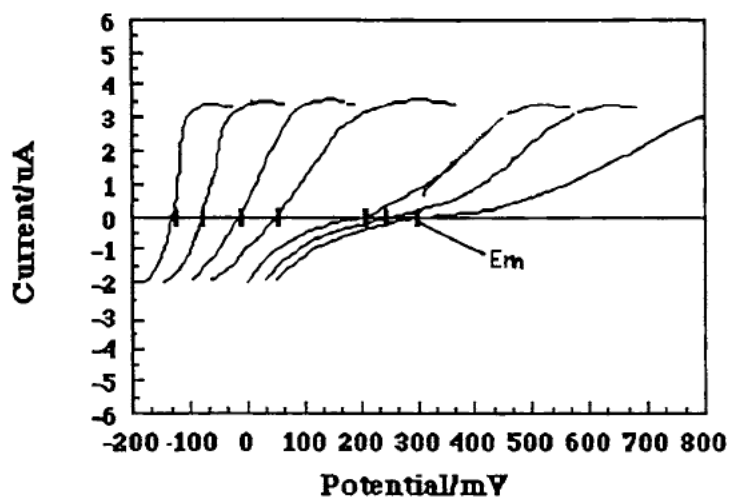
Figure 2-5. Voltammograms of H_2O_2 vs pH on Pt Electrode

pH: 13.0; 12.4; 11.1; 10.2; 7.40; 6.65; 5.81
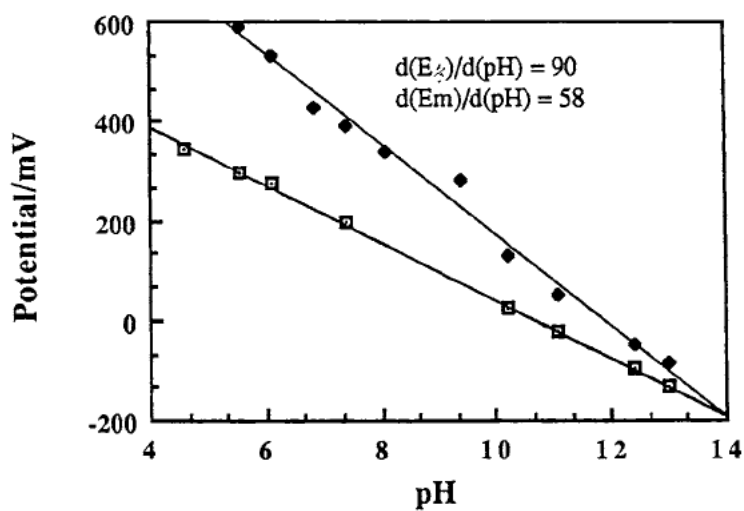
Figure 2-6. Half Wave Potential and Mixed Potential vs pH

Obtained from Figure 2-5. ⊡ : E_m; ◆ : $E_{1/2}$

result shows that the anodic current also has a strong pH dependent feature due to the pH dependence of the potential and reaction rate. The observed pH effect seems to be consistent with Reaction (2-2), although the basic form, perhydroxyl, also has similar pH dependence

$$HO_2^- + OH^- = O_2 + H_2O + 2e^- \qquad (2\text{-}8).$$
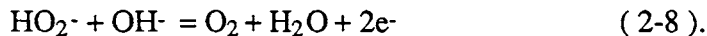
However the pH dependence of the potential for Reaction (2-8) should be -30mV instead of -60 mV. The distribution of the peroxide acid-base forms vs pH is plotted in Figure 2-8 (calculated from the $pK_a = 11.7$). It is illustrated that the dominant form below pH 12 is H_2O_2. This has been well verified throughout the experiment. In the case of pH > 13, however, there is not enough evidence to support the mechanism of Reaction (2-8) perhaps due to the experimental error in measuring high solution pH.

IV. The oxygen effect

Since the redox potential of the H_2O_2 couple is dependent on both H_2O_2 concentration and oxygen partial pressure, it is expected that the behavior of H_2O_2 oxidation would be affected by the environmental P_{O2}. Experiments were carried out for 0.1 mM H_2O_2 solution with air bubbling ($P_{O2} \sim$ 160 mm Hg) and nitrogenbubbling ($P_{O2} < 2$ mm Hg monitored simultaneously with a O_2 sensor). Surprisingly, the resulting CV curves obtained on a Pt disk electrode showed no sign of P_{O2} dependence. Similar measurements were repeated with Pt/Ir wire electrodes (both bare and cellulose acetate coated) in the amperometric mode to ensure a steady state i-E response as shown in Figure 2-9. This result indicates that the oxidation of H_2O_2 on Pt and Pt/Ir surface is a catalytic process in which oxygen is not directly involved in the rate determining step.
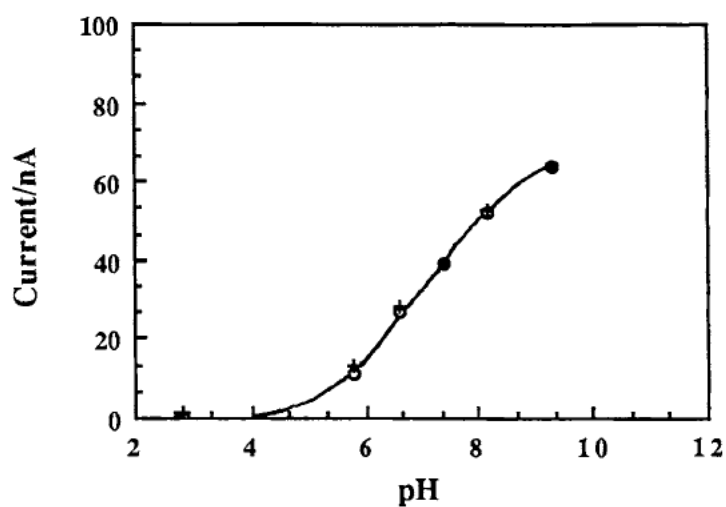
Figure 2-7. Steady State i-pH Curve on Pt/Ir Wire Electrode at 650 mV
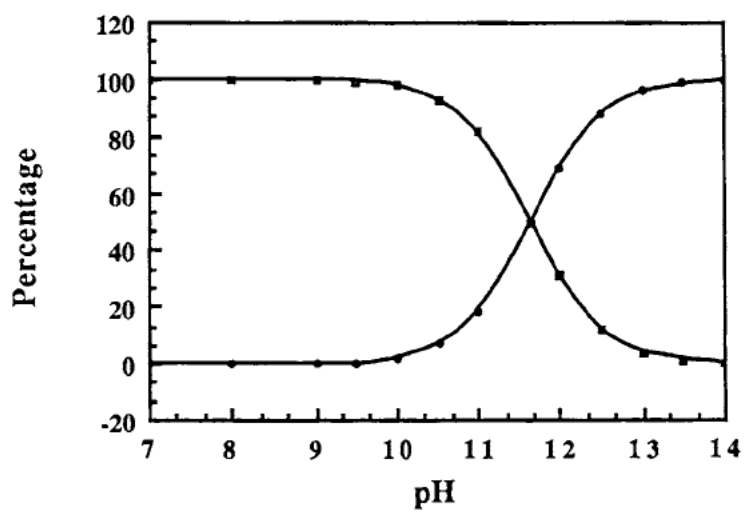
Figure 2-8. Distribution of Peroxide Forms vs pH

(▪ : Peroxide;   ● : Perhydroxyl)

V. The Temperature Effect

The effect of temperature on the electrooxidation of H_2O_2 was measured on both bare Pt/Ir and cellulose acetate coated Pt/Ir wire electrodes in the amperometric mode and a steady state current was achieved for 0.1 mM H_2O_2 solution thermostated at various temperatures. No significant difference was found between the coated and bare electrodes. A temperature parameter of 2.5 % / ^0C was observed as shown in Figure 2-10 in which the current is normalized at 37 ^0C for the ease of comparison.

VI. Chronoamperometry

When the applied potential is sufficiently high (complete concentration polarization) for a planar electrode, the current-time behavior of a diffusion controlled process is given by the Cottrell Equation

$$i = nFAD^{1/2} / \pi^{1/2} t^{1/2} \qquad (2-9)$$

A plot of i vs $1/t^{1/2}$ should be linear. Figure 2-11 shows the i - $1/t^{1/2}$ curves at various H_2O_2 concentrations on a disk Pt electrode in an unstirred solution. The potential step is from 200 mV to 800 mV which is appropriate as indicated in Figures 2-1 and 2-9. It is again observed that a diffusion controlled process prevails at lower concentrations. Cottrell behavior is achieved only for $[H_2O_2] < 1$ mM. Deviation from linearity occurrs at higher concentrations. We regard this phenomenon as the general feature of the low rate of electron transfer (Table 2-1). It is easy for the supply ofreactant to reach a state of excess through diffusion and therefore the overall process deviates from diffusion control.

VII. The surface conditioning of Pt/Ir wire electrode

A brief discussion about the Pt surface condition is helpful in understanding the electrochemical processes that take place on its surface as related to various applied
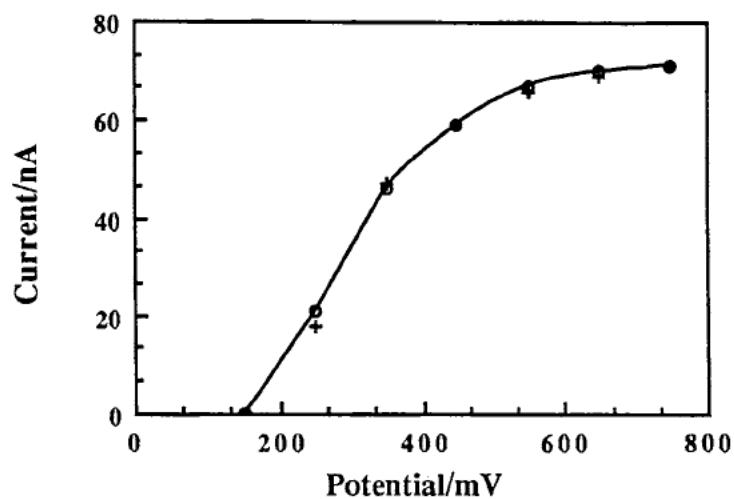
Figure 2-9. Steady State i-E Curves of H_2O_2 Oxidation under Different P_{O_2}

(o: ~160 mm Hg;   +:   < 4 mm Hg)
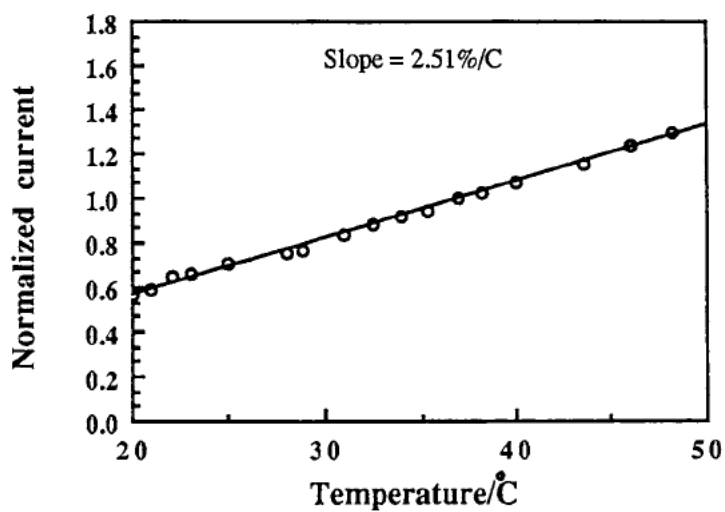
Figure 2-10. Temperature Effect on H_2O_2 Oxidation on Pt/Ir Wire Electrode

potentials. The surface oxidation of platinum begins approximately at 550 mV vs Ag/AgCl at pH 7.4 and the surface coverage of the oxidized form (designated PtO) is a function of potential. The PtO coverage varies from 20% to 60% in the potential range of 600 mV - 1000 mV. The monooxide of Pt turns to the dioxide form (PtO_2) at potential higher than 1600 mV. The conversions between PtO_2, PtO and Pt are chemically reversible with the change of applied potential (Chialvo, 1983), but the processes are not fast and could well be in the scale of tens of minutes and even hours. This feature makes the electrode conditioning very important and the timing should also be taken into account.

The oxidation of H_2O_2 is extremely sensitive to the surface conditioning. A bare wire was treated in different ways and then subjected to amperometric measurement of H_2O_2 at a fixed potential of 650 mV. The time required to stabilize the electrode surface varied to a great extent as illustrated in Figure 2-12. It seems that the potential scanning is the worst approach to electrode pre-treatment. The response to H_2O_2 kept changing for as long as three hours before reaching a stable current when the electrode was scanned five cycles from -200 mV to 1200 mV. Ultrasonication in ethanol for five minutes also produced an unstable surface which took more than two hours to stabilize. It is shown definitely that the the electrode needs to acquire a stable oxidized surface to accommodate the oxidation of H_2O_2. Any reduction on the electrode will lead to a rearrangement of the surface which is a time consuming process related to the degree of surface roughening. The roughening effect on a Pt electrode by potential scan has been visualized by scanning tunnelling microscopy (Itaya, 1990). The potential scan is usually the best way to achieve an "electrochemically reproducible" fresh surface which unfortunately must be avoided for H_2O_2 oxidation. The oxidative treatment, on the other hand, seems to have a favorable effect. Ultrasonic

cleaning in 3 M H_2SO_4 substantially reduced the stabilization time as opposed to ethanol cleaning because H_2SO_4 was believed to give an oxidized surface. This was further supported by the electrooxidative treatments plotted in Figure 2-12 which show that a pre-oxidation at 1200 mV for 5 minutes yielded the shortest stabilization time. This experiment suggests that the oxidative detection of H_2O_2 should be conducted with an oxidized surface and any reductive treatment of the electrode ought to be avoided.

The above experiment was also performed on a cellulose acetate film coated Pt/Ir wire electrode. The results were similar as far as the effect of the electrode oxidation and reduction were concerned. The degree of surface roughening and the stabilization time, however, were greatly reduced as demonstrated in Figure 13.

A general practice in amperometric detection with solid electrode is to stabilize the background current under constant applied potential. The electrode is considered to be stable when the background current decays to a low and constant value. It usually takes anywhere between 10 to 60 minutes, depending on the electrode material, solution composition and hydrodynamics. The time required to obtain stable current is defined here as the background stablization. The stabilization of the electrode surface for the oxidation of H_2O_2, however, is not related to the background current. Addition of H_2O_2 to a system in which the electrode stabilization seems to be complete often results in a response that has a constant decaying pattern as illustrated in Figure 2-14 (A). A true stable surface is obtained only when sufficient time is allowed to achieve a fully conditioned surface recognized by an H_2O_2 response which yields a real steady state as shown in Figure 2-14 (B).

The true stabilization times for the bare and coated wire electrodes as designated by the stable H_2O_2 response shown in Figure 2-14 (B) are given in Tabl 2-2.

28
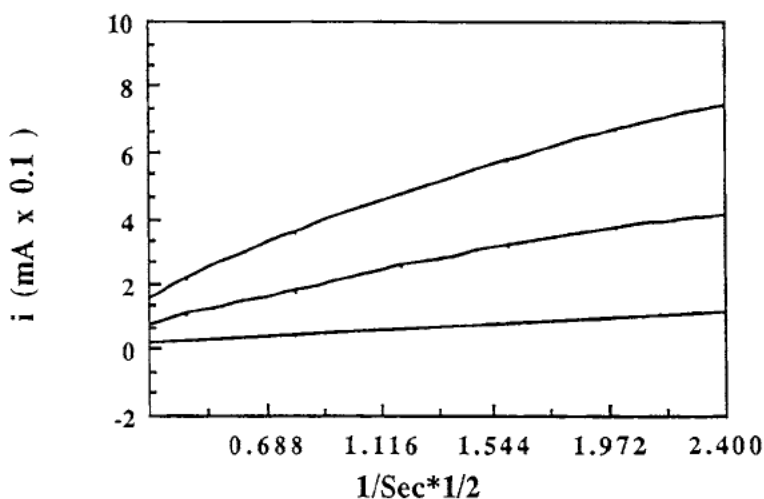
Figure 2-11. i-1/t$^{1/2}$ Plot of H$_2$O$_2$ Oxidation by Chronoamperometry
[H$_2$O$_2$]: 10.0 mM; 5.0 mM; 1.0 mM; E step: 200 - 800 mV vs Ag/AgCl
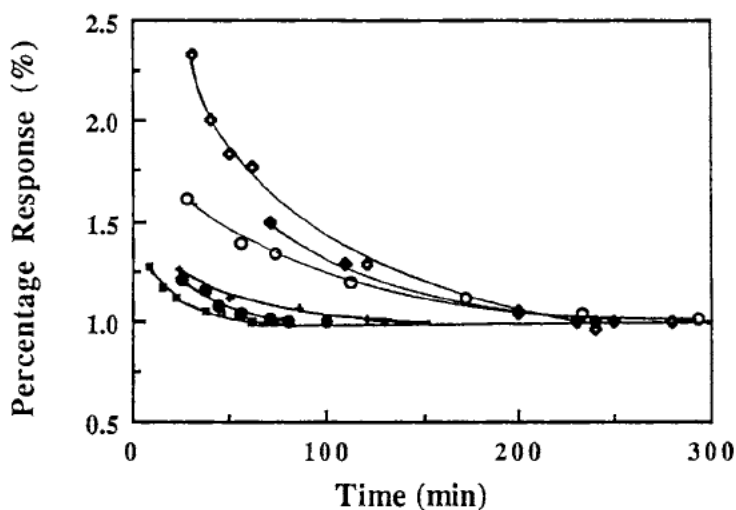
Figure 2-12. The Bare Pt/Ir Wire Electrode Surface Stabilization after Different
Treatments

◇   5 cycles(-200 mV - 1200 mV);   ◆ : 4 cycles (-200 mV - 1200 mV);

○ : 5 min sonication in ethanol;●:no treatment;✦: 5 min sonication in 3 M H$_2$SO$_4$;

▫ : 5 min oxidation at 1200 mV.

29

Table 2-2. Stabilization time for bare and CA coated Pt/Ir wire electrodes*

Method of treatment	Stabilization time (min)	
	bare electrode	CA coated electrode
5 scans/-200 - 1200 mV	220	40
5 scans/-200 - 950 mV	200	30
EtOH/ultrasonic 5 min	180	
Directly apply 650 mV	90	20
5 min oxidation at 950 mV	50	< 10

* The stabilization time was measured by applying 650 mV after different pre-treatments and monitoring the H_2O_2 response until a steady state current as shown in Figure 14 (B) was observed.

The success of quantitative measurement of H_2O_2, as has been demonstrated above, has much to do with the electrode conditioning. Any treatment that involves the reduction of the Pt surface should be carefully avoided not only because much longer stabilization times result but also the surface is rarely reproducible. Reducing the electrode after each measurement always yielded a change in sensitivity even though the same electrode was used. The best conditioning seems to be the pre-oxidation at 950 mV (1200 mV can be used but it has the problem of O_2 evolution) for 5 - 10 minutes which accelerates the oxidation of Pt and therefore reduces the time for the electrode stabilization. More importantly, the pre-oxidation yields a very reproducible
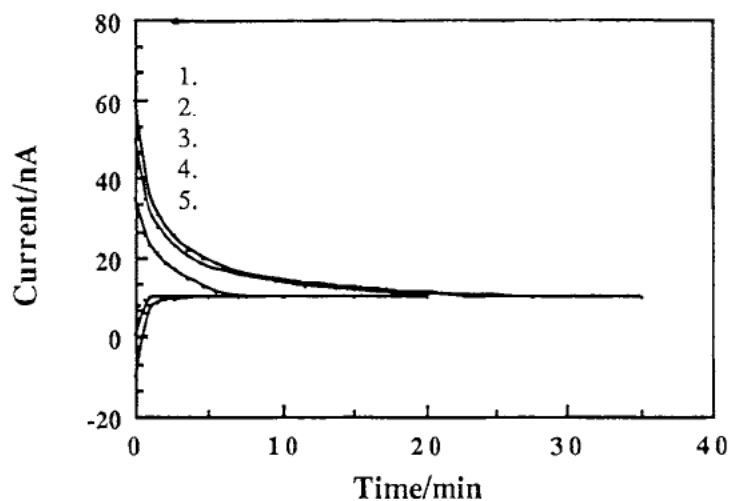
Figure 2-13. Cellulose Acetate Coated Pt/Ir Wire Surface Stabilization
by Pretreatment

(1): 5 cycles(-200 mV - 1200 mV); (2): 5 cycles (-200 mV - 950 mV);
(3): no treatment; (4): 5 min oxidation at 950 mV; (5): 10 min oxidation at 950 mV;)
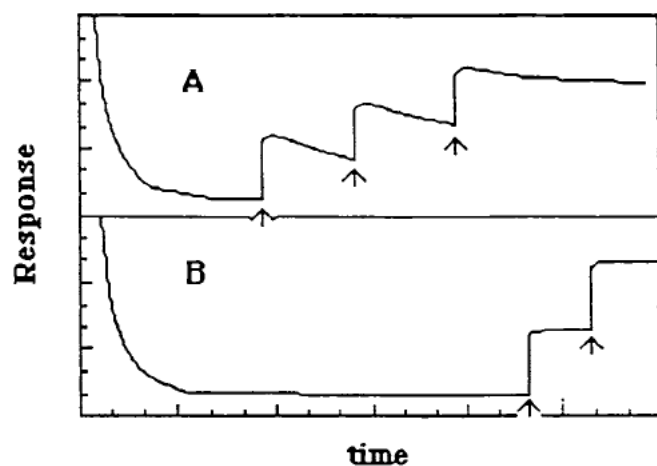
Figure 2-14. Background Stabilization and Surface Stabilization

A: Response pattern when background is stabilized.
B: Response pattern when surface is stabilized.
(Arrows denote where H_2O_2 is added.)

31

surface characterized by stable sensitivity for H_2O_2 detection.

The cellulose acetate polymer film on the wire electrode appears to protect the surface. The history of the surface can be partially preserved by the film for many hours if the electrode is kept in buffer. For example, when a stable surface was obtained at a cellulose acetate coated wire electrode for H_2O_2 measurement in a previous experiment, the stabilization time for the following measurement was much shorter which indicated that the oxidized Pt surface was partially preserved. On the other hand, the same phenomenon is not observed on bare electrodes. The stabilization time was approximately the same whenever the cell was turned off and started again regardless of the past history.

VIII. Pulsed amperometry

The pulsed amperometry involves cycled potential steps which are applied in specific order to clean the electrode surface after each sampling. It has been proven to be a very useful approach in many applications to increase sensitivity, reduce overpotential and even make some electroinactive species detectable electrochemically (Hughs, 1981; Lacourse, 1989). This technique was tried for the electrooxidation of H_2O_2 on Pt disk and Pt/Ir wires of various diameters. Figure 2-15 illustrates the potential form and corresponding current response.

Current is sampled at every E1 which is well above the plateau of the H_2O_2 voltammogram but below the potential of the solvent breakdown as demonstrated in Figure 2-16.

Two major problems were encountered in this experiment, high background and noise. Results obtained for various pulse arrangements and their corresponding background currents are shown in Table 2-3.

Table 2-3. Background currents of various pulse combinations*

E_1 (mV)	E_2	E_3	t_1 (msec)**	t_2	t_3	$i_{b.g}$ (µA)
800	400	0	833	333	500	19
800	400	200	833	333	500	1.7
800	200	200	833	166	833	1.8
800	0	0	833	166	833	33
800	1400	200	833	833	833	2.6
800	1800	200	833	833	833	2.5
800	-400	200	833	833	833	62

* Measured on 0.5 mm diameter bare Pt wire electrode in pH 7.4 buffer. The DC steady state background current is 0.04 -0.05 µA at 800 mV for the same electrode.

** See Figure 15

It is seen that a significant background current results whenever the potential step goes below 200 mV. This is due to the reduction of PtO at the low potential and the evolution of H_2O_2 from the reduction of O_2. These species are oxidized during the positive step and give rise to the background. From Figures 1 and 9 it can be clarified that 200 mV is the zero current point in the ph 7.4 phosphate buffer, below which the electrode process becomes cathodic and surface reduction takes place. From theknowledge obtained previously in the electrode conditioning experiment, this suggests that the pulsed technique is not suitable for the oxidative detection of H_2O_2 because the oxidation of the Pt surface is a slow process which cannot be accomplished in seconds. The step time as shown in Table 2-3 has been as long as 800 msec but the background remains remarkably high which means that the surface cannot be

33
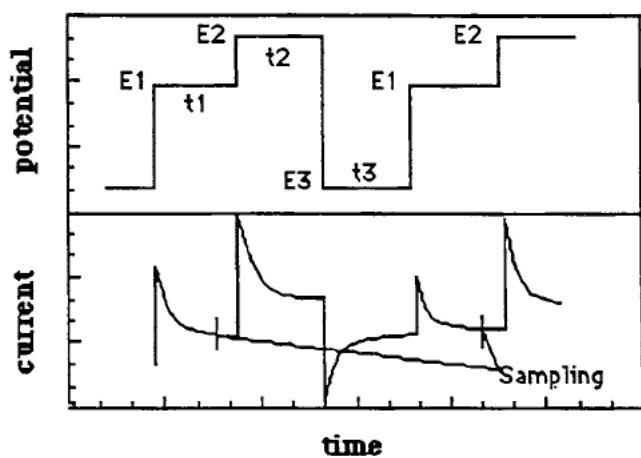
Figure 2-15. Potential Mode and Corresponding Current
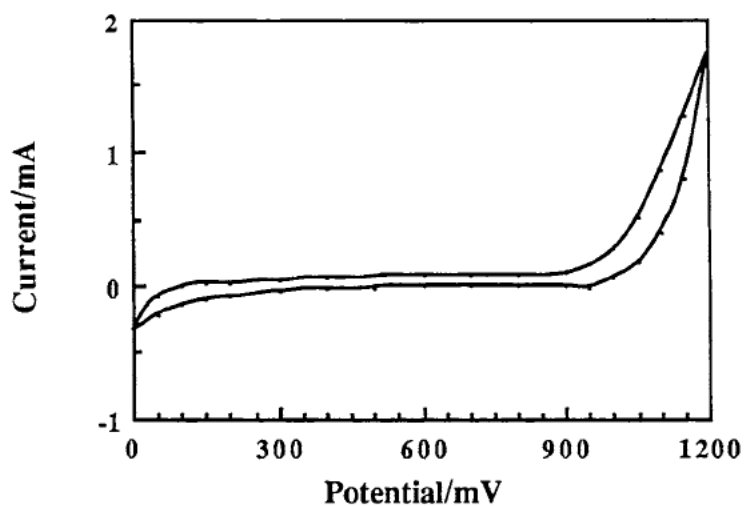
Figure 2-16. Voltammogram of Phosphate Buffer on Disk Pt Electrode

Scan Rate: 10 mV / Sec; Electrode Surface Area: 0.196 cm^2.

stabilized with this technique. Further measurements with various electrodes gave different sensitivity increases varying from 2 fold for the disk electode to 10 fold for a 0.17 mm diameter wire as compared to their corresponding DC sensitivities. The increase in sensitivities, however, was due to the surface area increase accompanied by a concomitant increase in background current and noise level in approximately the same ratio. This is also supported by the fact that the sensitivity and noise increases were inversely proportional to the electrode diameter, which is a normal surface roughening effect.

Considering the background and noise effect, the applicable potential should not be beyond the window of 200mV - 900 mV. This limit eliminated the major advantage of the pulsed technique. Sensitivity increases obtained within this potential range were very limited and were not enough to compensate for the loss in sensitivity due to the increased noise and therefore the S/N ratio.

Conclusion

The electrochemical oxidation of H_2O_2 on Pt and Pt/Ir electrodes is influenced strongly by factors such as pH, temperature and surface conditioning. The electrode reaction is a two electron process as has been established by the Koutecky-Levich plot and the pH dependence characteristics (Figure 6). A diffusion controlled process can be achieved for the concentration range of $10^{-7} - 10^{-4}$ M if careful attention is paid to the control of electrode conditioning. Deviation from linearity occurs when the concentration is higher than 1 mM. The upper limit of the dynamic range depends to a great extent on the electrode surface conditioning. This effect is much more pronounced for a miniature wire electrode and seems to be related to surface

roughening effects. A Pt-Ir wire electrode with a diameter of 0.17 mm was observed to have a linear range only up to ~ 0.04 mM when the surface was not well stabilized (oxidized to a stable condition). On the other hand, the same surface conditioning on the disk electrode had much smaller effect as compared to the miniature wire electrodes.

We have assumed, in employing the Pt-Ir electrode, that the oxidized surface consists of essentially oxides of Pt. The preferential concentration of atomic surface layers of the more stable iridium oxide cannot be ruled out.

Since early studies on the catalytic decomposition of H_2O_2 were mainly carried out at high concentrations (Schumb, 1955), the significance of the decomposition at low concentrations remains a question. Nevertheless, the following common observations are worth mentioning. (a) smooth Pt is less active than a platinized or colloidal Pt surface; (b) alloys are less active than pure Pt; (c) metallic Pt is more likely to serve as an electron shuttle for the H_2O_2 decomposition than is the oxidized state (PtO, etc) and (d) the decomposition is enhanced by the presence of OH- ions.

Recent reports on the study of O_2 reduction confirmed that the rate of the catalytic decomposition of H_2O_2 at low concentration was very low, and had insignificant influence on the reduction of oxygen on a Pt electrode at all pH values (Kaska,1989). There seems to be controversy over the route of oxygen reduction but most of the data show that direct reduction of O_2 to H_2O is the predominant mechanism (Kaska, 1989; Hsuch, 1983). Early study with rotating ring-disk electrodes also demonstrated that only 10 % of O_2 was reduced via H_2O_2 Huang, 1979)· Some useful information about the catalytic decomposition can be drawn from the O_2 reduction study . For example, the catalytic decomposition is driven by the autooxidation of H_2O_2 to O_2, (i.e. Reaction (2)), not the reduction of H_2O_2 (Reaction (2-3)) so that κ_4

in the reaction scheme below determines the rate of the decomposition.

$$O_{2(b)} \; = \; O_{2(*)} \; = \; H_2O_{2(*)} \; = \; H_2O$$

with rate constants κ_1, κ_2, κ_3, κ_{-2}, and κ_4 as labeled.
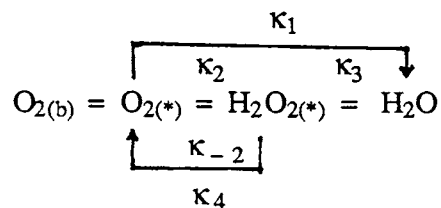
κ_3 is potential independent and has a fairly large value. Since the overall catalytic decomposition has an insignificant rate, it is therefore obvious that the catalytic oxidation of H_2O_2 is the rate determining step for the decomposition. When the oxidation of H_2O_2 in the positive potential range is considered, the competition between κ_{-2} and κ_4 will determine whether the electrooxidation or catalytic oxidation dominates the overall process. To realize the decomposition there must be an excess of H_2O_2 at the Pt surface because the decomposition consists of oxidation of one H_2O_2 molecule and reduction of another H_2O_2 molecule. At steady state the surface concentration of H_2O_2 is zero and there are no accessible extra H_2O_2 molecules available as electron acceptors to accommodate the decomposition. The electrode oxidation, as long as the overall process is mass transfer controlled, will be the major route for the H_2O_2 oxidation.

The electrode oxidation of H_2O_2 is a catalytic electrooxidation catalyzed by the platinum electrode as compared with the experiment on gold. The potential for H_2O_2 oxidation (~ 0.2 V vs SCE) is close to the theoretical value calculated from $E^0 = 0.68$ V (Hoare, 1968) corrected to corresponding pH and atmospheric O_2 partial pressure (0.2 atm) at ~ 1 mM H_2O_2 concentration.

The results in Figure 2-9 also support this argument because the oxidation behavior of H_2O_2 at steady state is P_{O2} independent, which indicates that the oxidation

37

of H_2O_2 at low concentration is a kineticlly controlled and totally irreversible process which is merely a function of Pt surface conditioning, applied potential and pH and does not exhibit normal Nernstian behavior.

The rate of the electrode reaction, however, is very sluggish, having rate constants in the range of 10^{-6} cm/sec (Table 2-1) and is pH dependent, a feature shared with the catalytic decomposition.

The surface conditioning of the electrode, especially the miniature wire electrode, is very important. Pre-oxidation seems to be a preferable strategy and covering the surface with polymer has a remarkably favorable effect on Pt surface stabilization. For successful measurement of H_2O_2, the pH control is the most important aspect because variation in pH causes large errors in the vicinity of pH 7.4.

Chapter 3. Glucose Sensor Fabrication and *In Vitro* Characterization

Abstract

Methods of the miniature glucose sensor fabrication were studied and a protocol was presented which enabled quantitative control of the enzyme loading. The geometry of the cylindrical cavity was confirmed to be favorable for the multi-layer deposition and high success rate. Various polymer materials were investigated and their effectiveness as selective membranes was evaluated. Cellulose acetate has good discrimination against ascorbic acid and very high ratio of electrode response to H_2O_2/ ascorbic acid has been achieved. Acetaminophen, a popular non-prescription medicine for pain relief, is a strong electrochemical interferant to the oxidative detection of H_2O_2 and therefore substantially affects sensor response. Membranes of combined polymer layers (Nafion, cellulose acetate and electrodeposited diaminobenzene) were found to be effective in eliminating the acetaminophen effect. More than 85 % of the acetaminophen interference was eliminated on the improved sensors (compared to the previous "Normal" sensors). It was also found that one week or more was required to stabilize the permeability of the polymer membranes in buffer.

Introduction

It has been pointed out earlier that the optimal geometry for a tissue sensor is a needle shape. Another issue is the location of the sensing element. Shichiri, et al. used a needle sensor with the sensing element at the spherical tip which made direct needle implantation impossible and also required a relatively large diameter (Shichiri,1982, 1984). Matthews and co-workers reported a needle-type sensor with a side window as the sensing element. Ferrocene as the redox mediator was used to fill the hollow tubing of the needle to serve as the matrix for enzyme immobilization and the limitation due to oxygen was reduced (Matthews, 1988). Pickup, et. al. also reported a similar approach, using dimethylferrocene to fill a 22 Gauge cannula which served as the sensor body (Pickup, 1989). The stability of the mediator, however, has always been

a problem and long term performance has not been achieved. To construct an enzyme sensor that has multi-layer structure and long lifetime, Membrane uniformity is essential. The idea of cylindrical cavity on the side of a needle was first adopted in our laboratory and has shown obvious advantage over the former types (Bindra, 1991). It provides a robust structure for the ease in handling and implantation. Its geometry also enables uniform deposition of various polymer layers without sacrificing the overall size of the sensor because the deposition solutions can be confined in a zone of defined geometry.

The most serious problem that the H_2O_2 sensor faces is the electrochemical interference. From a practical point of view, the absolute signal caused by the inteferents should be reduced to a negligible level relative to the sensor response to physiological glucose (~5-6 mM). The bias caused by the false signal will therefore not result in misjudgment. To construct a glucose sensor that has minimal response to acetaminophen, for example, the absolute current caused by the maximum physiological dosage of acetaminophen (0.10 - 0.15 mM) should be depressed to less than the response of 0.5 mM glucose equivalent. The response to 0.1 mM acetaminophen *in vitro* on a bare electrode of the same surface area is about 800 - 1000 nA, which means that 99.95 % of the acetaminophen interference should be eliminated to achieve this goal. For the *in vivo* situation, since the tissue is a poorer diffusion medium, the actual maximum interference is lower. But an effectiveness of 99.9 % is definitely necessary. Normal sensors that have CA (cellulose acetate), GOx (glucose oxidase) + glutaraldehyde and PU (polyurethane) layers can reduce the acetaminophen response to 1-2 % compared to bare electrode, e.g. the absolute current for 0.1 mM acetaminophen is around 10 nA. This sensor, when implanted, could give as high as 200 % error (bias by 0.13 mM acetaminophen / response due to 5 mM glucose). The use of acetaminophen for the sensor users has to be strictly controlled.

There are two general strategies for dealing with this problem. One is the active method in which a chemically active component such as an enzyme, redox reagent or chelating ligand is built into the sensor to destroy the approaching interferents before they reach the electrode surface. The other is the passive method which utilizes a physical barrier to screen off unwanted interferents. The former has been used for modified electrode successfully in several *in vitro* situations. But the approach has the disadvantage of instability. It is difficult to maintain the active species in the membrane effectively and permanently at a reasonable level. Besides, the extra active species in the membrane for long term *in vivo* monitoring must be shown to remain immobilized and not exhibit toxic or other effects. The passive method was therefore adopted in this study

Although there are numerous polymer materials that have been used one way or another as electrode modifiers, molecular filters, ion exchangers, etc., the choice for the H_2O_2 detecting glucose sensor is limited. First, the inner membrane has to be permeable to H_2O_2 to fulfill the task of electrode detection and, second, the membrane has also to allow charge carrier ions to pass in order to accommodate current flow while blocking other electroactive species. This requires that the membrane have the ability to discriminate between smaller ions and other inorganic species such as ascorbic acid and acetaminophen. Size selectivity is the most important feature and chemical or charge selectivities are also required. It has been demonstrated that cellulose acetate is an effective barrier to ascorbic acid and uric acid, but is useless for acetaminophen (Sittampalam, 1983; Bindra, 1991). There are also other polymers with selective features such as Nafion (perfluorinate ion exchanger) and the recently marketed Eastman-Kodak AQ polymers. A series of electrodeposited films have also been reported to possess size and chemical selectivity (Ohsaka, 1987; Geise, 1991).

There are many ways to immobilize enzymes onto the membrane surface. A

chemical method using activated cellulose acetate, parabenzoquinone and bovine serum albumin was reported to effectively immobilize GOx on the surface in more than a monolayer (Sternberg, 1988). In this study, however, for the ease of practical application, glutaraldehyde crosslinking was chosen in order to simplify the procedure and increase the enzyme loading.

The goal of this study is to find suitable polymer materials for the inner membrane to reduce the electrochemical interference and to develop a reliable protocol for the sensor fabrication, including uniform membrane deposition, enzyme immobilization, sensitivity control and storage.

Experimental

Procedures for normal Sensor Preparation

I. Mechanical Preparation

A Teflon coated Pt/Ir wire (Diameter 0.17 mm and overall diameter 0.25; Medwire, Mount Vernon, NY) 40 mm in length was wrapped with 0.1 mm diameter Ag wire starting 5 mm from one end. The Ag wrap covered 6 mm of the Teflon coated Pt/Ir wire. The lead end of the Ag and the Pt/Ir wires were sealed with heat shrinkable Teflon tubing. The wrapped Ag wire was then anodized in a pH 7.4 phosphate(0.1 M) buffer containing 0.15 M NaCl at 0.1 mA constant current for 15 min. and afterwards rinsed thoroughly with distilled water. A circular cut was made (perpendicular to the wire's axis) 1 mm from the tip at the sensing end (totally 5 mm Teflon coated Pt/Ir) and the 1 mm Teflon tubing was removed by sliding it off the tip. Another circular cut was made 4 mm from the tip. The 3 mm Teflon tubing between the first and second cuts was then moved to the tip, leaving a cylindrical cavity of 1 mm in length. The sensor dimension was then, from the tip, 3 mm Teflon coated tip followed by 1 mm cylindrical cavity and then 1 mm more Teflon coated part next to the wrapped Ag/AgCl

reference electrode. The tip was completely sealed with silicone rubber glue (Dow Corning).

II. Cellulose Acetate (CA) Film Deposition

The sensor was dipped into 6 % CA (39.8 acetyl content, Aldrich) solution in 1:1 (v/v) acetone/ethanol up to the front edge of the reference electrode and smoothly pulled out. A surgery scalpel was used to remove the excess CA film on the Teflon coated parts after the CA coating was dried in the air for one minute. The same process was repeated two more times until the thickness of the CA film was great enough to eliminate ascorbic acid response. This CA coated sensor was left in phosphate buffer over ten hours to stabilize the membrane.

III. Glucose Oxidase (GOx) Immobilization

The CA coated sensor was dried in the air at room temperature for 15 minutes and an HPLC syringe was used to deliver 0.4 μl of a 4 % GOx solution (242 U/mg, Biozyme Lab. International Ltd. San Diego, CA) solution (in pH 7.4 phosphate buffer). The entire cavity was first wet with the GOx solution and the remaining drop of GOx solution was delivered to the cavity which due to surface tension held the GOx solution in a spherical shape. The sensor was let dry in the air and in about 15 minutes the GOx became a layer of film attached to the surface of the CA membrane.

A 10 ml bottle was filled with 0.1 ml 12.5 % glutaraldehyde and the periphery of a rubber stopper was cut to provide slots in which the sensor could be held. The stopper with sensor was fixed to the bottle in such a way that the front part of the sensor (mainly the sensing cavity) was sealed inside the bottle (exposed to the vapor of glutaraldehyde). The bottle was then tied to a rotator and rotated (to get rid of gravity effect) at 90-100 rpm for over 7 hours. Glutaraldehyde reacted with the enzyme layer and crosslinking took place during this period. The stopper with sensor was carefully removed from the bottle, dried for ten minutes and put into another bottle of

the same size full of deionized distilled water for one hour to rinse off excessive glutaraldehyde. The sensor was then dried in the air for one hour. A yellow colored film in the cavity indicated an immobilized enzyme layer.

IV. Polyurethane (PU) Coating

A drop of ~20 µl PU (SG 85A, Thermedics Inc. Woburn, MA) solution (4% PU in 98% tetrahydrofuran and 2% dimethylformamide) was hung in a wire loop of 4 mm diameter, forming a liquid film. The sensor was passed through the loop starting from the distal end until all the solution was transferred to the sensor forming a uniform layer on the entire sensor. The sensor was then let dry in the air for ten to fifteen minutes and was soaked in pH 7.4 buffer for stabilization. The sensor response to glucose was checked every two days and, if excessive high sensitivity was found (> 2.5 nA/ mM), an additional PU layer was applied to reduce the sensitivity.

V. Sensor assemblies

(1). G3 Glucose Sensor

A sensor designated G3 was designed for long term implantation. It is relatively flexible and is referred to as the "normal" sensor as shown in Figure 3-1A. Its fabrication has been described above.

(2). G6M Sensor

The G6M sensor is a G3 sensor with reduced diameter (0.13 mm as opposed to 0.17 mm) installed in a 25 Gauge needle. The sensing element is exposed through a window in the side wall of the needle. The tip end of the needle was sealed with silicone glue. The back end of the needle is glued together with the sensor lead wire with super glue and an external skin reference electrode (such as the one used for electrocardiogram) is needed for *in vivo* measurement. A G6M sensor is demonstrated in Figure 3-1B.
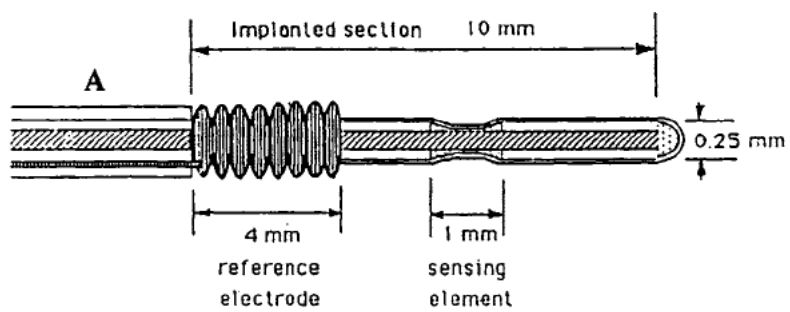
Schematic Diagram of Implantable Glucose Sensor
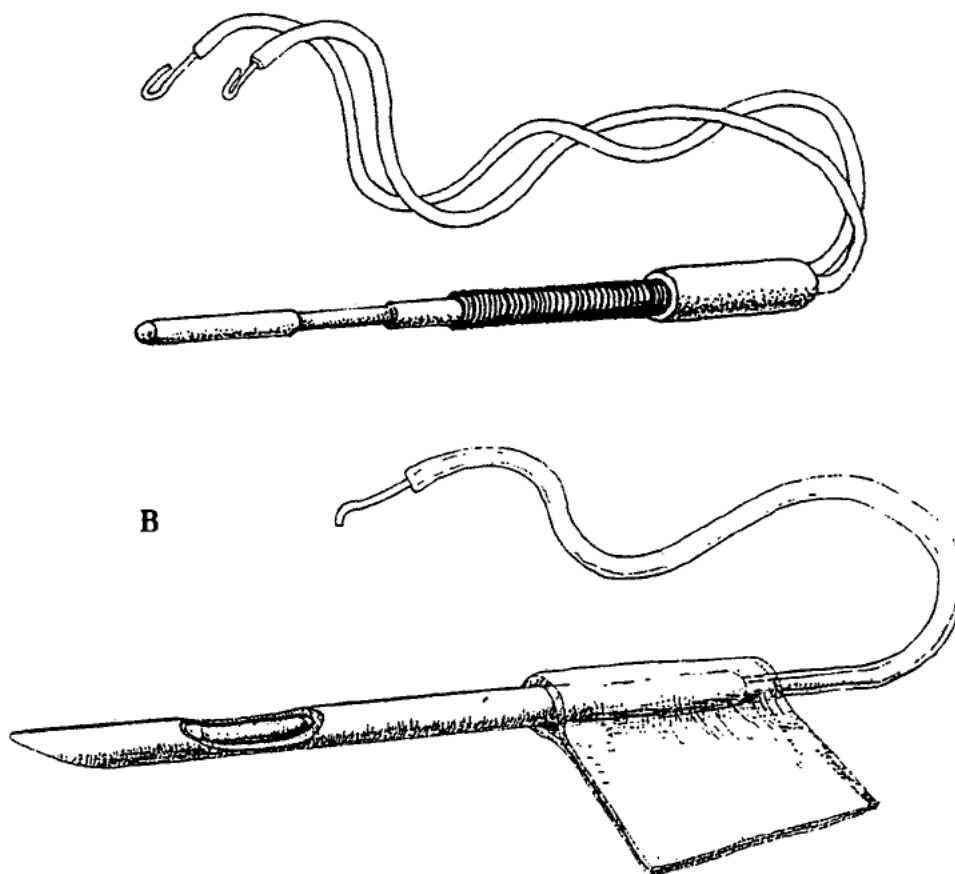
Figure 3-1. G3 and G6M Glucose Sensors

A: G3 Sensor;   B: G6M Sensor

45

Testing of Other Polymer Materials

Cellulose acetate 6 % solution was the same solution used above. Nafion (perfluorinated ion-exchange powder) was a 5 % solution in mixture of lower aliphatic alcohols and 10 % water directly purchased from Aldrich and AQ 55-D (a gift from Dr. Adams, Kansas University. a high molecular weight, amorphous, thermoplastic polyester produced by Eastman-Kodak) was diluted from a 28 % aqueous suspension with a 1:1 (v/v) cyclohexane and acetone to give a 5 % solution. An electrodeposited film was obtained by cycling the bare wire electrode between -100 and 800 mV vs Ag/AgCl in a chloride free 0.1 M phosphate buffer of pH 7.4 containing 10 mM 1,3-diaminobenzene(DAB) (or a mixture of DAB and resorcinol (both from Aldrich), 5 mM each) for over 20 hours under constant N_2 bubbling. A brown colored film forms when DAB polymerizes on the electrode surface.

Nafion and AQ 55D membranes were coated onto the wire electrode with the wire loop described earlier and CA was dip-coated because the solvent evaporation was too quick to use the loop-coating.

In Vitro Measurement

All the measurements were carried out in a single compartment cell of 10 ml capacity with a two electrode system. A coil of anodized Ag wire of 0.5 mm diameter and 0.1 M phosphate buffer of pH 7.4 containing 0.15 M NaCl were used through out the experiment. The use of the two electrode system and anodized Ag wire avoided possible deviation from that of *in vivo* conditions. Sensor response was measured with BAS amperometric detectors (LC 4A, BioAnalytical Systems Inc., West Lafayette, IN) at 600 mV constant applied potential and recorded with Kipp and Zonen BD 40 chart recorders.

Results and Discussion

I. Cellulose Acetate Membrane

To obtain initial insight concerning the film casting process, the following dip-coating methods were compared: (1) Dip-coating followed by complete air-drying; (2) Dip-coating followed by partial air drying (dry in the air after dip-coating for one minute) and water replacement (immersion of the sensor in distilled water before it was totally dry until all the residual solvent was replaced by water); (3) Dip-coating followed by complete water replacement of the solvent (immersing the sensor in water immediately after dip-coating).

The membrane stability was evaluated by measuring the response to 0.05 mM H_2O_2 at various stages of film stabilization. The results are shown in Figure 3-2. It was demonstrated that method (2) produced the most stable membrane. Another criterion for the membrane assessment was to measure the ratio of the equimolar response to ascorbic acid and H_2O_2. Low values indicated that the membrane was more effective in discriminating ascorbic acid. It turned out that Procedure(3) had the poorest ratio (0.7-1.0, n=4) while Procedure (1) had highest (0.1-0.4, n=4) but it also had poorest reproducibility. Measured values changed randomly without control. Procedure (2) was considered adequate due to its high reproducibility (ratio: ~0.4).

Explanation to those results is that the membrane structure and permeability were determined by the ways the solvents leave the film. It was compact and less porous when the solvents directly evaporated in to the air. On the contrary, when the solvents were replaced gradually by water (It took more than ten hours.), a much more porous film resulted which was not only permeable to H_2O_2 but also permeable to ascorbic acid as well.

When two coatings of CA were applied (Procedure(1) followed by Procedure (2)), the ratio was significantly reduced as shown in Table 3-1. It is clearly shown that

multi-layer coating is necessary and very effective. An additional layer of CA reduced the response of ascorbic acid to 2-4 %. While the effect on H_2O_2 was much less, 75-80 % of the response remained after one more CA coating. To ensure a complete elimination of ascorbic acid interference, a third coating was applied and the electrode was essentially not responsive to the addition of ascorbic acid to the buffer. The absolute response to 0.1 mM H_2O_2 was still higher than 10 nA.

Table 3-1. Response to Ascorbic Acid and H_2O_2 after 1st and 2nd CA Coatings

No. of electrode	1st Coating(nA/0.01mM)			2nd Coating(nA/0.01mM)		
	Ascorbate	H_2O_2	Ratio	Ascorbate	H_2O_2	Ratio
1	8	19	0.42	0.55	17	0.032
2	6	17	0.35	0.40	13	0.031
3	12	21	0.57	0.60	15	0.040
4	4	20	0.20	0.45	15	0.030

II. *In vitro* Characteristics of the G3 Glucose Sensor

The glucose sensors needed a certain time to stabilize their sensitivity, typically two to three weeks. Most of the sensors required two or three PU coatings to acquire adequate sensitivity (within the range of 1.0 to 2.5 nA / mM). Figure 3-3 shows the stabilization curves of about twenty sensors after their fabrication. In the first two or three days after fabrication, the sensitivity increased rapidly and was largely unpredictable. It became stabilized after five days and gradually reached a stable value after two to three weeks.
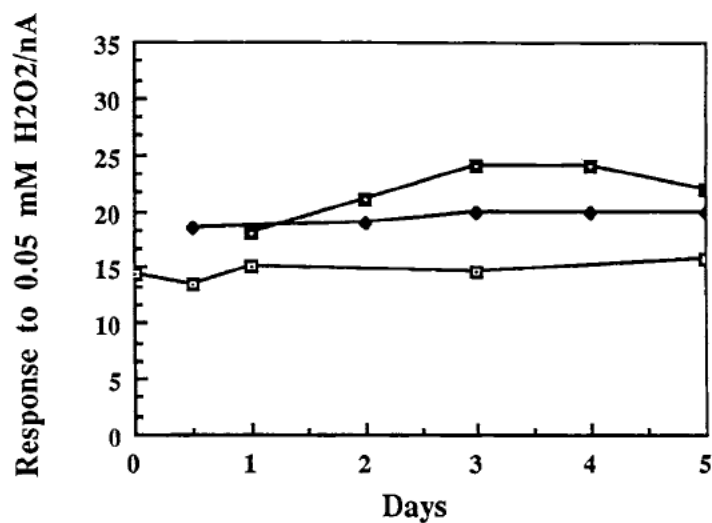
Figure 3-2. Response to H_2O_2 on Different CA Film Coated Electrodes

□: Procedure (1); ◆: Procedure (2); ▣: Procedure (3).
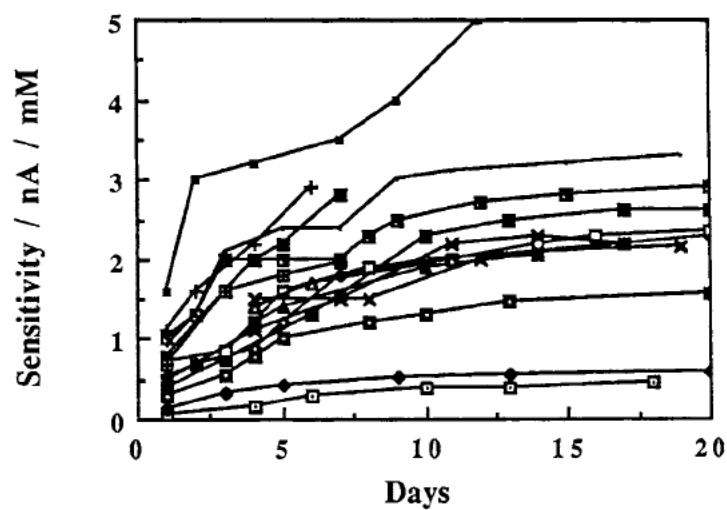
Figure 3-3. Glucose Sensor Stabilization as a Function of Time

Over 200 G3 sensors have been fabricated and tested for their sensitivity to glucose, dynamic range, background current, thermal stability and interference. The sensitivity was usually in the range of 0.8 to 2.5 nA /mM and linearity was in the range of 12 mM to 20 mM with a response time of 3-5 minutes upon an injection of 5.0 mM glucose. The background current was below 0.4 nA when sufficient stabilization time was allowed. The lifetime of the sensors was not systematically tested. It was, however, verified that the sensor could maintain stable sensitivity to glucose for at least three months when stored in pH 7.4 buffer at room temperature. Dry storage in a refrigerator was tested after the sensors were fully stabilized (usually one month after their fabrication). Table 3-2 shows the sensitivity change for these sensors before and after a certain period of storage in dry state at 4 ^{0}C.

The sensors resturned to their original sensitivity when immersed in phosphate buffer and polarized for about 40 - 60 minutes. These results confirmed that the sensors could be packed and stored in dry state so that the fabrication and use can be separated. The life span of the sensor could be actually extended.

III. Study of Polymer Effectiveness on Eliminating Electrochemical Interferences

In order to evaluate the effectiveness of different polymer membranes, ascorbic acid, acetaminophen and H_2O_2 were measured with electrodes coated with different membranes. Figure 3-4 illustrates the response patterns of the three species. The instantaneous increasing current upon an injection indicates that this polymer does not have a discriminating effect on the electroactive species. For example, cellulose acetate does not block acetaminophen and H_2O_2. AQ 55-D does not have effect on any of the three species. The most effective material is Nafion which allows only H_2O_2 to diffuse through. Empirical interpretation of those observations would be that Nafion possesses more strict size selectivity and charge selectivity as well. But cellulose acetate and electrodeposited DAB seem to have the feature of chemical selectivity. Since the

Table 3-2. Sensitivity Change before and after Dry Storage*

Sensor	Before(nA/mM)	After(nA/mM)	Time of storage (day)	% Change
G3-1	0.90	0.90	8	0
G3-2	1.0	0.80	22	20
G3-3	0.94	0.80	6	-15
G3-4	1.20	1.20	22	0
G3-5	2.40	2.60	6	8
G3-6	1.80	2.00	19	11
G3-7	2.00	2.00	23	0
G6M-8	0.56	0.56	41	0
G6M-9	0.50	0.52	40	4
G6M-10	0.60	0.80	36	33
G6M-11	1.50	1.44	42	-4
G6M-12	0.28	0.28	42	0
G6M-13	0.50	0.66	46	32
Average % change				6.8

thickness of the films are not directly measurable, comparison concerning the effects of different thicknesses may not be accurate. A series of electrodes that were sequentially coated up to four times with each of the materials was tested after each coating. The effectiveness of those materials could thus be evaluated with more confidence. Table 3-3 shows the result of the comparison including those of combined polymer layers.
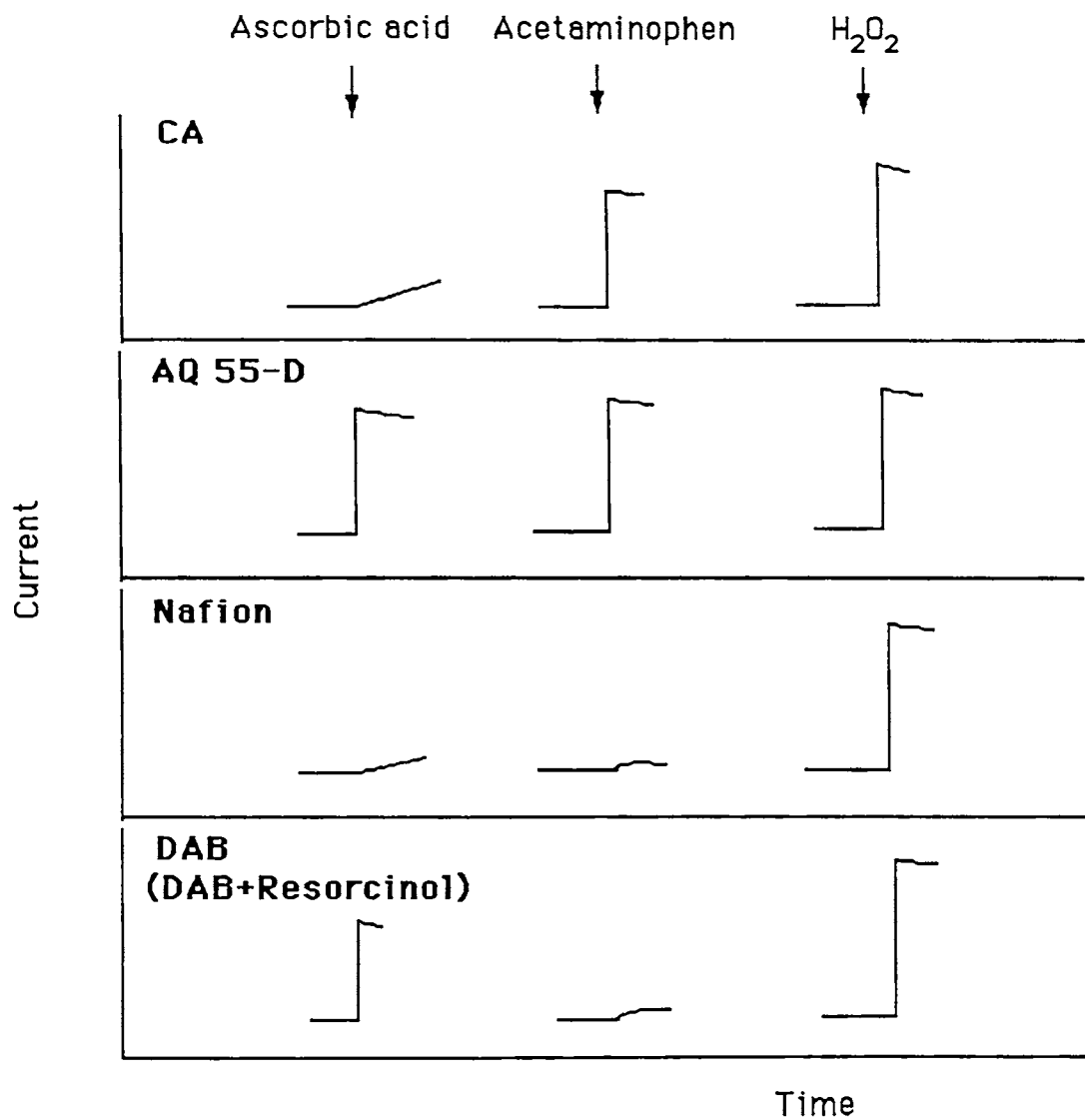
Figure 3-4. Response Patterns on Different Membrane Coated Electrodes

52

It is interesting to note that when a single polymer is repeatedly coated, the efficiency is not proportional to the number of layers. The Nafion membrane, for example, gives a response to acetaminophen which decreases from 97 nA to 63 nA when the number of layers increases from one to three. For AQ 55-D, there is no increased effect as the membrane becomes thicker. The combination of different polymers, on the other hand, shows very impressive selectivity enhancement. The electrodeposited film is a very effective barrier to acetaminophen in the first three or four days after deposition but loses this feature gradually with time. The electrode response to acetaminophen increases every day and reaches a steady state in about ten days where the steady state current for a fixed concentration of acetaminophen is equivalent to ~5-8 % of the response at a bare electrode.

Since in the practical protocol of sensor fabrication CA is the outer most inner layer for enzyme immobilization, the CA layer should be kept unchanged. Modifications are therefore aimed at the domain between the Pt/Ir and the CA layers. A number of multi-layer (or multi-coating because each coating does not necessarily mean a layer) configurations are listed in Table 3-3. It shows clearly that multi-coating is necessary no matter what combination of materials is adopted. Naf-CA-Naf-CA is the simplest structure which still gives 5 nA response to 0.1 mM acetaminophen. The most satisfactory results come from DAB-Naf-CA-Naf-CA and Naf-CA-Naf-CA-Naf-CA. This two configurations have similar response to acetaminophen and H_2O_2. The *in vitro* responses are 1.2±0.5 nA to 0.1 mM acetaminophen and 20±3 nA to 0.1 mM H_2O_2.

The stability of the sensors differs between these two types. The DAB type does not have any response to acetaminophen in the first 4-5 days but gradually increases to a stable value of about 1-2 nA/0.1 mM in ten days. The Nafion type does not have the time dependent feature. It has a response of similar magnitude (1-2 nA /

Table 3-3. Effect of Multi-layer coatings on Different Electroactive Species

Number of layers		Response to 0.1 mM (nA)		
		(Ascorbic acid)	(Acetaminophen)	(H_2O_2)
CA*	0	400	900	350
	1	200	330	340
	2	26	130	210
AQ 55-D**	1	190	320	330
	2	200	360	330
Nafion **	1	10	97	260
	2	10	70	210
	3	9	63	190
DAB*** (day1)1		190	0	300
(day10) 1		190	35	300
Naf-CA-Naf 3		0	7	43
CA-Naf-CA-N 4		0	5	30
Naf-CA-Naf-CA-Naf 5		0	2	23

* Direct dip-coating of 6 % solution;
** Loop-coating with a 4 mm diameter ring of thin wire;
*** Electropolymerized from a 10 mM solution:
CA: cellulose acetate; Naf: Nafion; DAB: electrodeposited1,3-diaminobenzene;
AQ 55-D: Eastman-Kodak Polyester.

0.1 mM) when it is prepared and keeps unchanged. Figure 3-5 shows the stabilization of various glucose sensors with different inner membrane configurations. Each curve represents the average of six sensors. In Figure 3-5 the high current curve represents the normal glucose sensors that have been used previously (CA-GOx/glutaraldehyde-PU). Average for 14 sensors gave the value of 60 nA / 0.5 mM
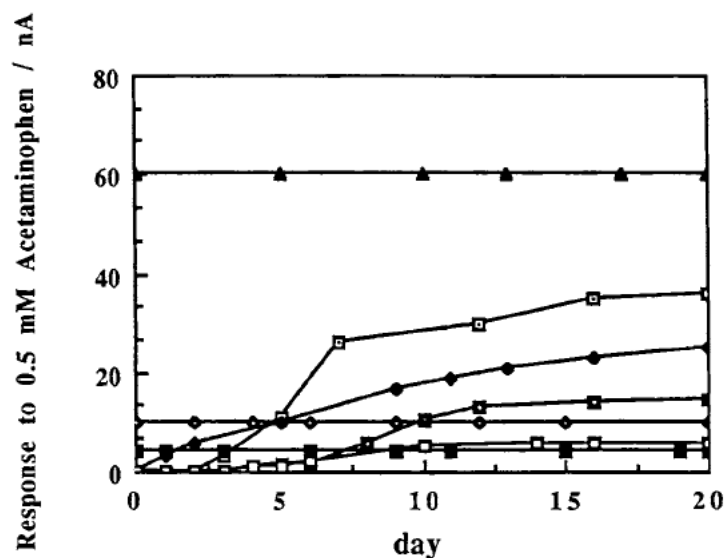
Figure 3-5. Acetaminophen Response on Glucose Sensors with

                Different Inner Membranes

Inner membrane Configurations:

(1): normal sensors;   (2): (DAB/res)-CA-Naf-CA;   (3): (DAB/res)-CA;

(4): (DAB/res)-Naf-CA-Naf-CA;   (5): Naf-CA-Naf-CA

(6): DAB-Naf-CA-Naf-CA-Naf-CA; (7): Naf-CA-Naf-CA-Naf-CA.

acetaminophen (12 nA / 0.1 mM acetaminophen). The actual values for the improved sensors are even lower because those sensors have 1.5 mm cavities while the normal sensors have 1.0 mm cavities. The area corrected *in vitro* improvement is that the new sensors have about 6-8 % of the original acetaminophen interference. The absolute response to 0.1 mM acetaminophen is 1.2±0.5 nA (n=12) (12±3 nA for previous normal sensors, n=14). A vivid comparison is demonstrated among curves(2), (4) and (6) of Figure 3-5. The difference between (2) and (4) is that (4) has one more Nafion layer while the difference between (4) and (6) is that the inner most layer for (6) is DAB and for (4) it is DAB+resorcinol. These results confirm that Nafion is a very effective barrier when combined with other polymers and that DAB alone electropolymerized has more stable structure than the mixture of DAB and resorcinol. This is in controversy with the results reported by Geise, etc. (Geise, 1991) that films deposited from a mixture had better performance than those from DAB alone.

Figure 3-6 shows four different sensors: A and B, Normal sensors that have only CA inner layer; Sensor C is the Nafion type and Sensor D the DAB type. The latter two have only slight response to acetaminophen but a similar response to glucose and H_2O_2.

To summarize this study, the multi-layered inner membrane can reduce the acetaminophen interference to 6-8 % of its original value on the "normal" sensors previously used. This new sensor does not have any response to ascorbic acid and 1.2±0.5 nA absolute response to 0.1 mM acetaminophen in phosphate buffer. Initial experiments showed that the compact inner membrane does not have an observable effect on the sensor response time to glucose and the overall response to H_2O_2 (Figure 3-6), which means that the improved sensor is expected to function similarly to the previous one. Further *in vivo* experiments will be summarized in Chapter 4.

Conclusion

The protocol of sensor fabrication has been improved to yield a high success rate of >80% and the method of dry storage enables the feasible sensor application in clinical or therapeutic fields because the sensor can be fabricated, stabilized, sterilized and packed without losing its characteristics. The sensor can then be directly unpacked and implanted without introducing any infectious artifact. The acetaminophen interference has been substantially reduced by using passive membrane techniques. The *in vitro* characterization seems to be satisfactory and further *in vivo* study will be performed in order to establish the relationship between the *in vitro* and *in vivo* parameters.
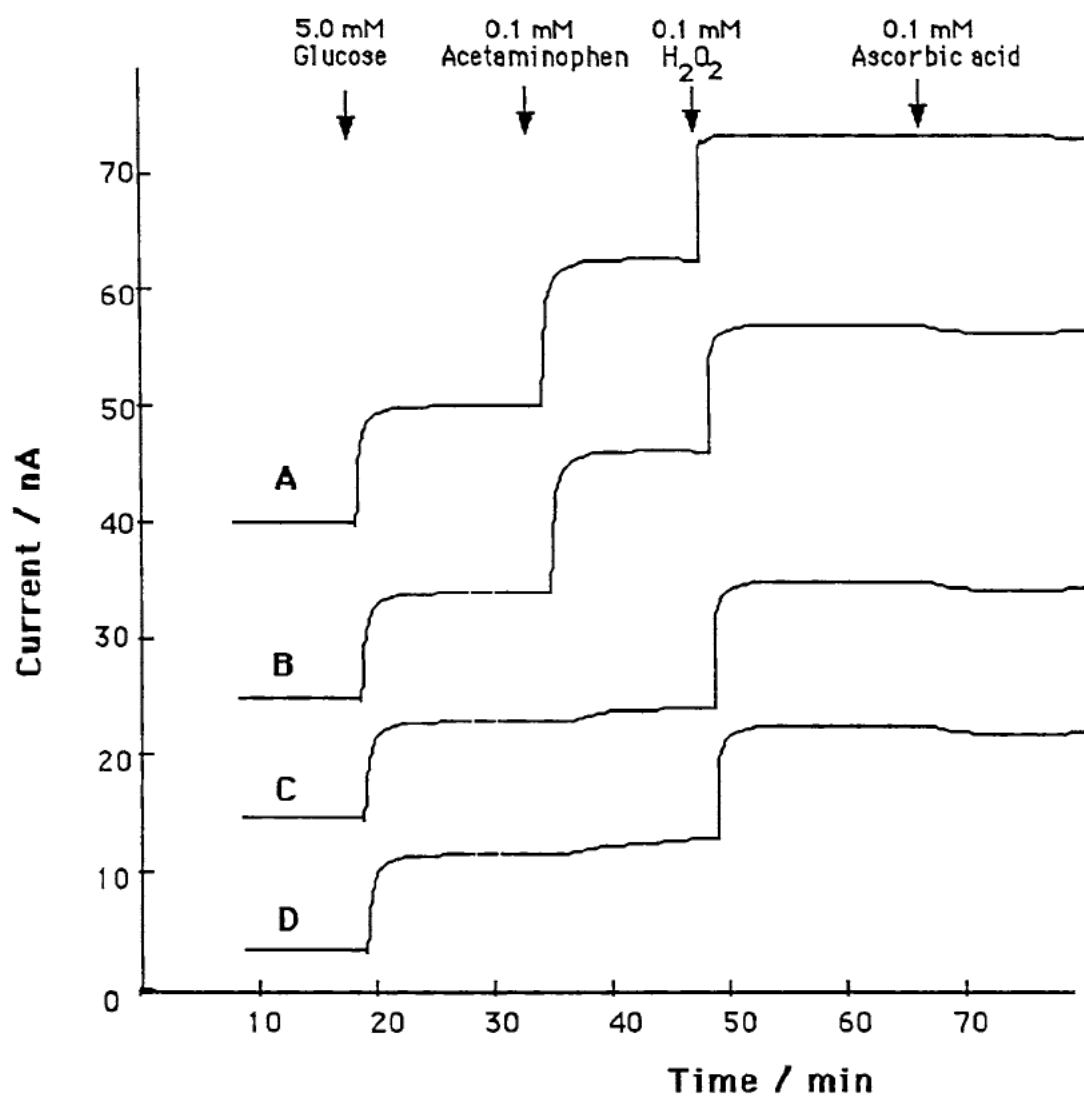
Figure 3-6. Response Patterns of Different Glucose Sensors

A and B: normal sensors (CA inner membranes);

C and D: improved Sensors (inner membrane configurations as in Fig.3-5. (6) and (7))

58

Chapter 4. Evaluation of *In vivo* Performance of the Glucose Sensor

Abstract

The *in vivo* characteristics of the glucose sensor was studied and it was observed that the sensors implanted in subcutaneous tissue followed glycemic change closely with a lag time of 5-10 minutes. A decrease in sensitivity to glucose as calibrated with the two-point calibration method was universally observed and the *in vivo* sensitivity and background current were essentially independent of the *in vitro* behavior. This was mainly attributed to the heterogeneity of the tissue environment and the inflammation and immune reactions, which depending on the location of the implantation and degree of tissue damage varied from sensor to sensor. This feature determined that each sensor must be calibrated individually *in vivo* in order to make accurate glucose measurement. The run-in time was investigated and the cause was initially identified to be the initial gradual decrease in glucose sensitivity rather than electrolysis of electroactive species in the surrounding tissue. The effect of various membranes on discrimination of electrochemical interferences was also studied and the multi-layer inner membrane configuration was found to be advantageous.

Introduction

Various implantable glucose sensors have been tested in animal as well as in human tissues (Shichiri, 1984; Velho, 1989, 1989; Claremont, 1986; Rebrin, 1989; Koudelka, 1991) and most of them were shown to function to different degrees as glucose detection devices. But no systematic, consistent and long term *in vivo* study has been reported satisfactory and none of those sensors has shown reliable, long term stable response to glucose. A common obstacle seems to be the instability of the sensor output which is mainly caused by changes in the outer polymer membrane. The varied permeability in turn influences the sensor sensitivity and results in an unstable signal. A sensor is useless if constant calibration is needed. An intravascular device seems to have less variation (Armour, 1990) probably due to the uniform medium although

insufficient data are presented. If the tissue heterogeneity and inflammatory response are the major causes of sensor instability, the sensor size and surface biocompatibility would be the most important factors in improving the sensor performance.

In principle, a certain decrease in sensitivity between *t*the *in vivo* and *in vitro* environments is expected because tissue is a different medium from an aqueous buffer solution and therefore the sensor characteristics in buffer will not be the same. A stable sensitivity, however, is definitely required so that frequent calibration can be avoided. Studies in this chapter and the following chapters will focus on the *in vivo* behavior of the glucose sensor. The correlation between *in vitro* and *in vivo* characteristics will be investigated and various factors that influence the sensor response (or sensitivity) will be individually addressed in order to establish a general understanding.

Intensive *in vivo* tests have been carried out both in rats and dogs (Moatti, 1991; Poitout,1991). The G3 sensor has been shown to function reliably up to twenty days, giving stable response to glucose. The general behavior of the sensor was that the output assumes a decaying pattern after implantation for three to five hours and then becomes stable, giving precise correlation with glycemia if calibration is made after stabilization.

This correlation is not linear during the run-in period and a valid calibration cannot be obtained. This phenomenon is considered to be one of the major defects of the implantable biosensors because monitoring cannot be made in this period. For long term *in vivo* applications (e.g. more than three days), a 2 to 5 hour initial waiting time is tolerable, but it could be a major drawback for emergency treatment. It is therefore important to find out its cause so that further improvement can be made accordingly.

A major concern about the H_2O_2 based glucose sensor is that it could suffer from endogenous electrochemical interference. *In vitro* study (Chapter 3) has shown that a passive membrane could reduce the interference from ascorbic acid and

acetaminophen to a negligible level. The *in vivo* situation, however, is different from that of *in vitro* because a concomitant decrease in glucose sensitivity occurs and a relative increase in the interference level is possible. This effect will also be addressed in this chapter.

Experimental

An anesthetized rat (Sprague Dawley, body weight 350 - 450 gram) was placed on a thermostated pad circulated with 37 ^{0}C water and a gas mixture of air, oxygen and halothane anesthetic (Halocarbon Laboratory, Inc., North Augusta, SC)) was fed to the rat through a mask. The ratio of the components was controlled by three flowmeters (Cole Parmer, Chicago). The flow rate of air, oxygen and gas bubbling through halothane could all be regulated individually. The back of the rat was shaved and sterilized with 70 % ethanol. A 20 Gauge catheter was inserted into the subcutaneous tissue parallel to the spine and the sensor was fed into the catheter in the opposite direction with the sensing tip first. The catheter was then pulled out of the tissue, leaving the sensor inside. The sensor was connected to an amperometric detector (LC4A BioAnalytical Systems, Inc., West Lafayette, IN) poised at 600 mV vs Ag/AgCl and the current was recorded with a Kipp and Zonen BD 40 chart recorder.

After the sensor output was stabilized, a glucose injection was administered by injecting 1 to 2 ml of 30 % sterile glucose (MCB, Manufacturing Chemists, Inc., Cincinnati, OH) in saline (ip). The blood glucose was simultaneously monitored by sampling blood from the tip of the tail and measuring with an Accu-Chek IIm glucose meter (Boehringer Mannheim Diagnostics, Indianaplis, IN). The *in vivo* calibration was made according to Velho, et. al. (Velho, 1989) by dividing the increment in sensor output by the glycemic increment after a glucose loading. The sensitivity was then expressed as $\Delta i / \Delta C$ Two glucose injections were made sometimes to evaluate the

in vivo sensitivity change.

Evaluation of the acetaminophen effect was performed by a similar method, injecting 1% acetaminophen solution (Aldrich) (ip) at a level slightly higher than maximum human dosage (0.014 - 0.02 mg / 1g body weight, equivalent to 0.09 - 0.13 mM (W/V) concentration). The figure of 0.025 - 0.03 mg / g body weight was usually adopted so that the observed interference was 20 - 50 % higher than the normal dosage.

The sensors were polarized overnight before implantation in order to eliminate misinterpretation due to the stabilization of the electrode itself. *In vitro* calibration was carried out both before and after each *in vivo* measurement using the method described in chapter 3.

Results and Discussion

I.   Study on the run-in period

The long run-in time for the subcutaneous monopolar glucose sensor is observed when a sensor is implanted and its output assumes a continuous decreasing pattern which is not directly related to the blood glucose. This decrease usually occurs in the first three to five hours of implantation. No clear correlation between glycemia and sensor signal is established during this period. This is obviously a major disadvantage and it would be very beneficial if this run-in time were shortened. The cause of this phenomenon could have two sources. One is that the decrease in current is due to decay in the background current which is caused by various endogenous electroactive species present in the physiological fluid. It is possible that these species need some time to establish a kinetic balance and once reached it is relatively stable. The other possibility is that the decay is caused by the decrease in sensor sensitivity (i.e. the sensitivity decrease is a time dependent process). If the sensor assumes

reduced sensitivity in the physiological environment due to tissue reactions, it is likely to be a time dependent phenomenon.

The partial loss of sensitivity in subcutaneous tissue has been long confirmed by the two-point calibration method (Velho, 1989; Moatti, 1991). The reason for the sensitivity decrease should be studied for better understanding of the physiological environment and interactions between the sensor and the tissue. There could be many possible causes. One assumption is that the glucose supply in the subcutaneous tissue is not high enough to accommodate the constant consumption by the sensor. The sensor therefore actually sees a reduced level at the interface between the sensor and the surrounding tissue. Another assumption is that the outer membrane undergoes a series of changes due to tissue reactions, either inflammation or immune response or both. The membrane permeability is altered (presumably reduced) by blockage of the outer layer by endogenous materials resulting in the apparent sensitivity decrease. The monopolar sensor also has another potential problem that an electric field exists at the sensor surface (it is not clear yet if it extends into the tissue) which could cause some reactions of electrolytes and charged species. Doubtless this is a complicated problem and is not easy to resolve.

The first approach was to compare the performance of enzyme sensors and blank sensors (the ones that did not have enzyme but were otherwise identical in overall configuration and geometry) in rat subcutaneous tissue. Two or more sensors (at least one glucose and blank sensor each) were implanted parallel to each other in each rat. Sensors were pre-polarized overnight to eliminate possible effects of prolonged electrode stabilization time. Since the blank sensors did not have enzyme and its output current was purely "background", any change in the sensor output during the run-in period must be due to changes in the endogenous electroactive species.

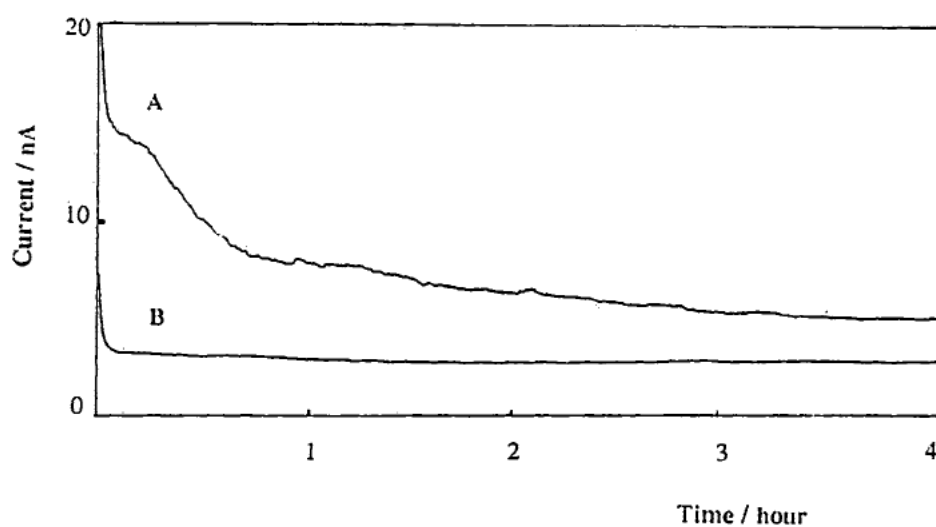Figure 4-1 shows the typical current decaying signals monitored after

Figure 4-1. Decay Patterns of Glucose Sensor and Blank Sensor

A: Glucose Sensor; B: Blank Sensor

64

implantation. Figure 4-1A is the output of a glucose sensor and B the output of a blank sensor. The blank sensor had very low initial current (within the range of 1.5 to 4 nA in the first 10 minutes) while the enzyme sensor had an initial current between 10 and 30 nA. Apparently, the main part of the current was due to the enzymatic reaction of glucose and the high current showed that the sensors had relatively high glucose sensitivity when they were initially implanted. The blank sensors, on the other hand, did not have significant decay in output. The current stabilized within 20 minutes and remained relatively stable. The absolute change in four hours after stabilization was less than 0.3 nA for all the three blank sensors tested repeatedly in different rats. This observation was verified by changing the glycemia more than one time during the current decaying period. It was possible to estimate the sensor sensitivity at different times by roughly estimating a smooth baseline between the two regions before and after the peak. Figure 4-2 shows two curves in an experiment. Two enzyme sensors were implanted in the same rat and two glucose injections were administered (ip) during the course of four hours. For both sensors the first peak of the sensor output had higher sensitivity (nA/mM) than the second peak. It was therefore obvious that the sensitivity decrease occurs gradually during the first few hours of implantation.

According to the results of a large number of *in vivo* experiments in anesthetized rats and conscious dogs (Moatti,1991; Poitout, 1991), the sensitivity became stable after the baseline was stabilized. This has also been observed in our experiments.

Measurement of the sensor sensitivity upon explantation was carried out immediately after the sensors were removed from the tissue. The *in vitro* sensitivities initially were typically close to those of the *in vivo* sensitivity values and sometimes higher. If the sensor was left in buffer stirred for 3-4 hours, the *in vitro* sensitivity prior to implantation could be obtained. This suggested that the loss of sensitivity was
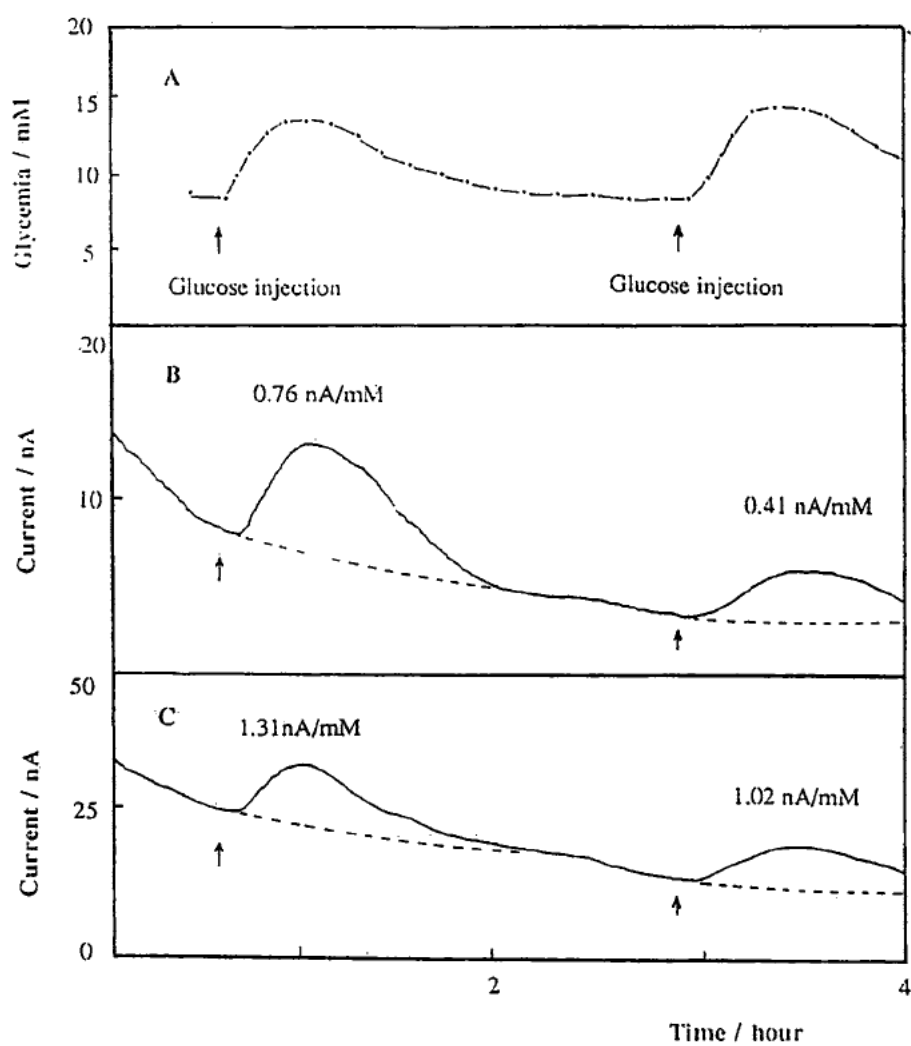
Figure 4-2. Sensitivity Decay during Run-in Period

A: Glycemia;   B and C: Glucose Sensors

66

caused by a reversible process, probably a change in the sensor outer membrane. The membrane lost some permeability to glucose due to adsorption of physiological species.

This experiment suggests that the current decay during the run-in period was most probably due to the decrease in sensitivity caused by partial blockage of the polyurethane membrane. This phenomenon was reversible. The sensitivity could be restored when the adsorbed species were washed off. This also ruled out the possibility of enzyme activity loss because the sensitivity could be completely restored after explantation. The background current due to direct electrochemical oxidation of interfering species decayed rapidly and remained at a low level. It was therefore not the source of the long run-in time. Other possible causes such as the depletion of O_2 cannot be ruled out and should be further investigated.

II. Study on acetaminophen interference

Moatti, et. al. have carried out a study on acetaminophen interference on the "normal" glucose sensors and found that the effect was very pronounced (Moatti, 1991). A similar study was also performed *in vitro* by Bindra, et al. (Bindra, 1991) and a recent report confirmed that the interference was very serious (Shaw, 1991).

The *in vivo* performance of both the original (the normal sensor) and the improved sensors (introduced in the last part of Chapter 3) have been compared in *in vivo* experiments. Larger rats (500 - 550 gram body weight) were used for this study and three or four sensors were implanted simultaneously in each rat in order to compare different sensors under identical cinditions. Acetaminophen (12-14 mg) was injected (ip) at a level about 20 to 30 % higher than the normal adult human dosage. Glucose was also injected to test the sensor's normal functioning.

Figures 4-3 and 4-4 show two sets of experiments. The first injection was acetaminophen and the second was glucose. It was impressive that the interference was
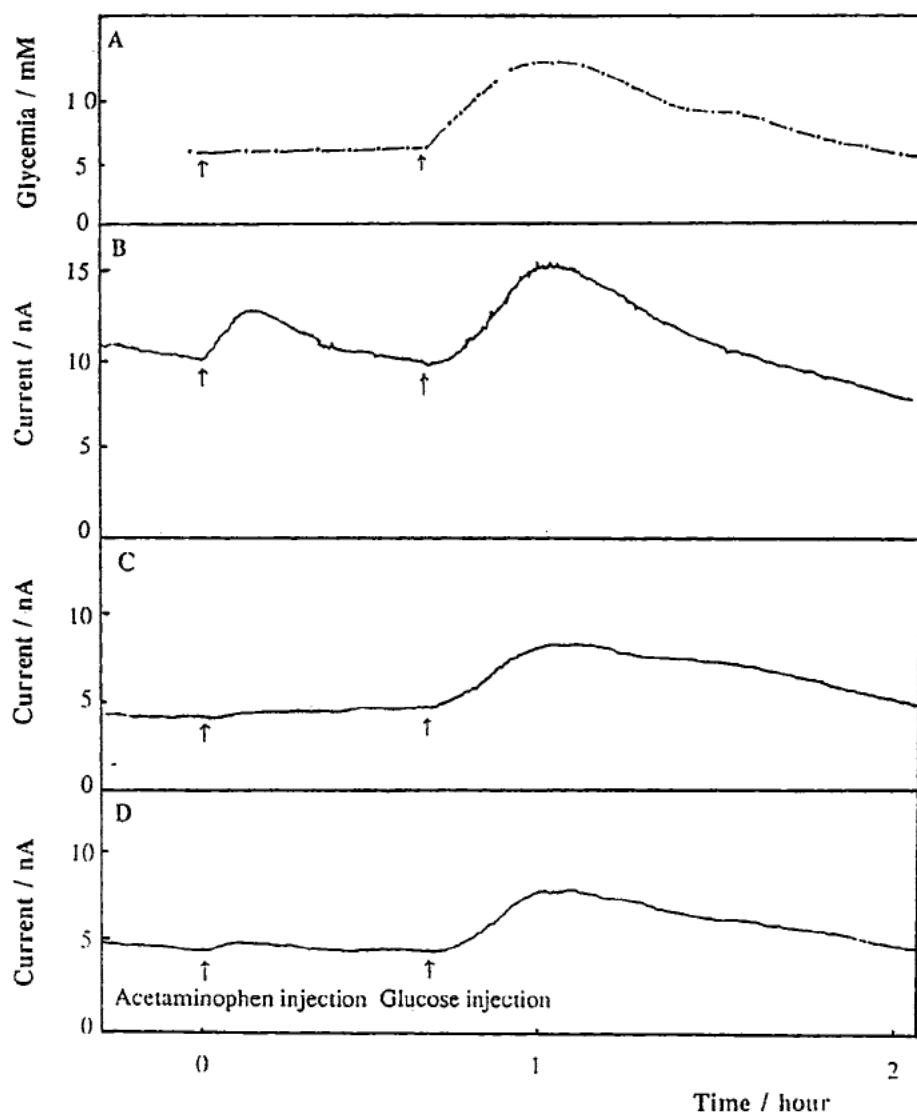
Figure 4-3. Acetaminophen Response *in vivo*

A: Glycemia; B: Normal Sensor; C and D: Improved Sensors

68
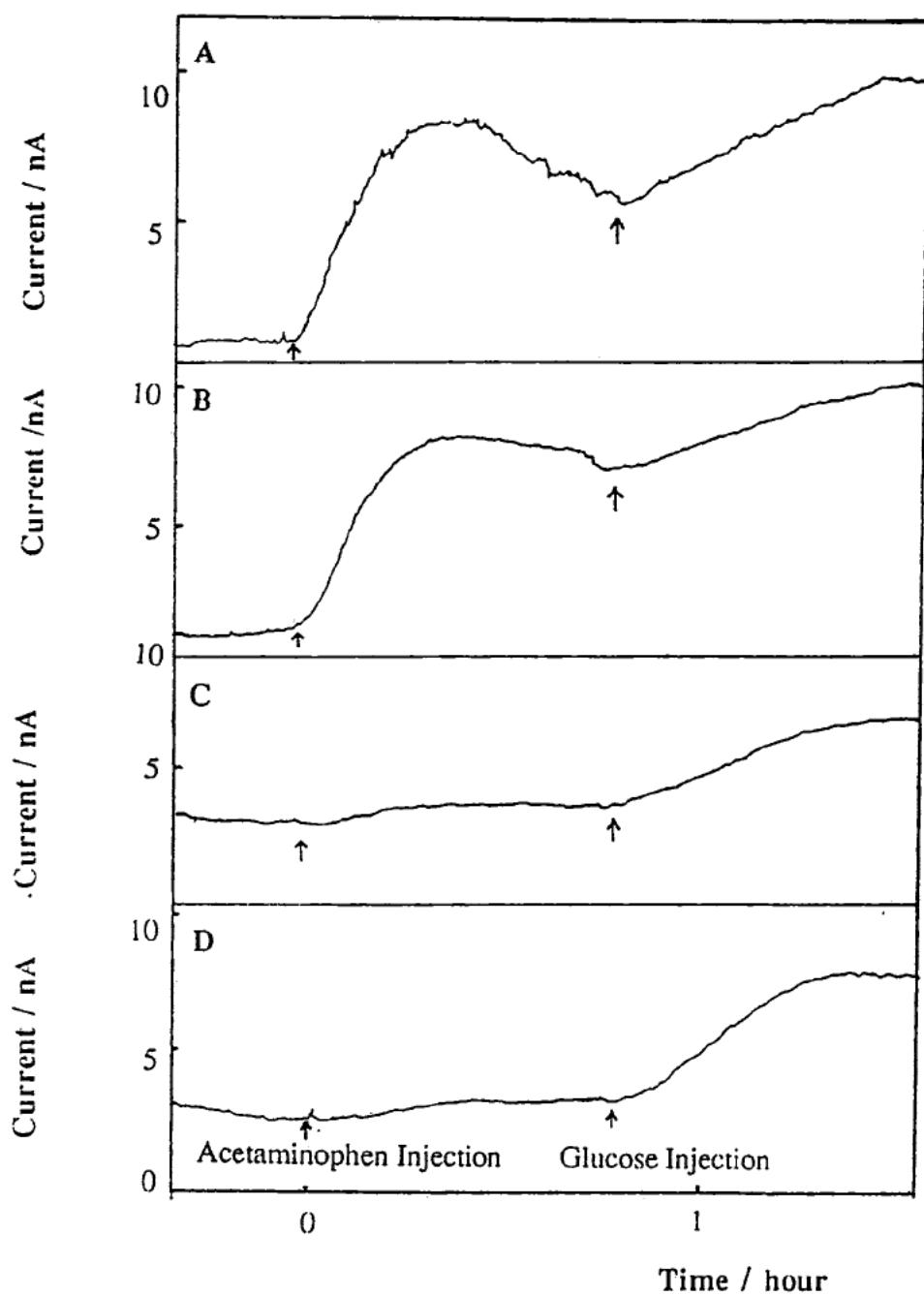
Figure 4-4. Acetaminophen Response *in vivo*

A and B: Normal Sensors;   C and D: Improved Sensors;

significantly reduced. The glycemia curve measured simultaneously showed that the blood glucose was undisturbed when acetaminophen is administered. The bias caused by acetaminophen for the normal sensors was equivalent to 80 - 200 % of 5 mM glucose response (absolute current 3 - 7 nA for 7 sensors) while for the improved sensors it was around 15 to 30 %, depending on the relative sensitivity to glucose.

Table 4-1 shows the improvement between the improved sensors and the normal sensors. The *in vitro* response to acetaminophen for both sensors was

Table 4-1 Percentage Reduction of Acetaminophen Interference on the Improved sensors Compared to the Normal Sensors

Improved sensor / Normal sensor*	*In vitro* %**	*In vivo* %**
N2 / S3	10.0	10.0
D1 / S3	14.0	10.0
D5 / L6	14.7	11.5
N2 / L2	8.6	10.9
D1 / L2	12.0	10.9
D6 / L6	14.7	11.5

* N: sensors with Naf-CA-Naf-CA-Naf CA configuration (Chapter 3);
   D: sensors with DAB-Naf-CA-Naf-CA configuration;
   S: normal sensors with short cavity (1 mm);
   L: normal sensors with long cavity (2 mm).
** Values are the ratios (improved/normal) of response to acetaminophen in the same system.

measured before and after implantation and it was essentially unchanged. The percentage improvement on acetaminophen interference (improved sensor / normal sensor) falls between 10 and 15 percent, which means that the new sensors could have the bias of 8 -30 % caused by acetaminophen at the over dosage level (The normal sensors had 80 - 200 %.). The actual impact should be less because the injected dosage

was higher than the physiological level. The interference by acetaminophen for human will be expected to be well below 20 %.

Conclusion

The cause of the long run-in time after sensor implantation has been identified to be the decrease in glucose sensitivity due to adsorption of certain endogenous species. The adsorption was reversible and the sensitivity could be restored in buffer. Two other potential causes, loss of enzyme activity and background variation, were ruled out. The improved sensors were compared with the normal sensors and significant reduction in acetaminophen interference has been achieved. The relative interference was reduced from 80-200 % to 8-30 % at the physiological (5 mM) glucose level. The performance of the improved sensor was similar in terms of glucose response.

Chapter 5.   Application of Cell Culture Toxicity Tests to
the Development of Implantable Biosensors

Abstract
The methods of cell culture toxicity testing were modified and applied to the development of implantable glucose microsensors. The positive and negative control materials suitable for the microsensor assessment were also established. The location, source and degree of the toxic effect in a multi-component biosensor was spatially visualized with cell monolayers. A freshly prepared sensor showed moderate toxicity, mainly due to the presence of glutaraldehyde and the residual solvents in the polymer layers. It was, however, possible to reduce the toxicity by removing the leachable toxic substances through extraction in phosphate buffer and a non-toxic sensor can be readily obtained.

Introduction
For the past few years efforts have been devoted to the development of implantable glucose biosensors in our laboratory. One aspect of the current work is to study the biological performance of the sensor, i.e. its biocompatibility. When a sensor is implanted in the tissue of a living organism, the sensor output is expected to reflect the concentration of the analyte of interest in the vicinity of the sensor. Strong interactions between the sensor and the surrounding tissue could result in severe disturbance in the tissue as well as in the sensor, so that the sensor is not able to monitor the concentration accurately. The interactions between an implant and the surrounding tissue generally fall into two categories: the host response (tissue response) and the material response (sensor response in this case). The evaluation of biocompatibility for an implantable device is usually carried out both *in vitro* and *in vivo* (Black, 1981; Bruck,1980). The *in vitro* methods include tissue culture and blood

contact. As the sensor is being developed for subcutaneous monitoring, the tissue culture method is believed to be adequate. Toxicity evaluation for an implantable device is usually addressed first as one of the fundamental screening processes for biocompatibility.

The tissue culture method as an effective evaluation of toxicity for polymeric materials was introduced in 1965 (Rosenbluth, 1965; Guess, 1965) and later standardized by ASTM (American Society for Testing and Materials, ASTM, 1988; Brown, 1983). It has been well established that the tissue culture methods show very good correlation with animal assays and are frequently more sensitive to toxic moieties(ASTM, 1988; Brown,1983; Johnson,1985).

There are two types of interactions between cells and polymers. One is commonly recognized as the polymer toxicity which is caused by the leachable chemicals from the polymers such as monomers, oligomers and various additives used in the polymer manufacturing process. It is here referred to as indirect interaction because the toxic chemicals released from the polymer react with the cells through the medium. The second is the direct interaction between the polymer surface and the cells which is characterized by the attachment of the cells to the surface when the surface is exposed to the cells in the culture medium (Tamada, 1986).

In establishing the cell culture tests it was found that this technique is a convenient tool for obtaining an initial evaluation of the sensor toxicity. It enables one to locate the source of toxic release in a multi-component biosensor and to visualize the degree of toxic effect and the removal of the toxicity from the sensor through different treatments.

The conventional cell culture test procedures used previously (Rosenbluth, 1965; Guess, 1965; ASTM,1988; Brown, 1983, etc.) were found not to be sensitive enough to test our needle-type microsensor. Because of its small size it was necessary

to develop toxicity test procedures with sufficient sensitivity to be suitable for sensor evaluation.

Experimental

Materials

ATCC standard L929 mouse fibroblast cell line, originally purchased from American Type Culture Collection, Rockville, Maryland, USA was a gift from Professor P. Kitos. Dulbecco's Modified Eagle's Medium (DMEM) was purchased from Sigma Chemical Company. Dulbecco's phosphate buffer saline solution A (PBSA) was prepared according to Freshney,1988. Trypsin (0.1% solution in PBSA with 0.1% EDTA) and cell culture tested $NaHCO_3$ and agar were from Sigma. Cellulose acetate (39.8% acetyl content) was obtained from Aldrich Chemical Company,Inc. and Polyurethane (Tecoflex[R] ,SG 85A) from Thermedics Inc., Woburn, MA, USA. Sterile 6-well cell culture plates with 3.5 cm well diameter and 75 cm^2 cell culture flasks were purchased from Corning. Latex rubber tubing of various diameters were Fisher products. Silicone rubber tubing and silicone rubber glue were purchased from Aldrich and Dow Corning, respectively. The ethylene oxide sterilizer was a closed gas chamber (10 liter capacity and 100 psi max. pressure at 394 K) manufactured by Millipore Corp. (Bedford, Mass. 01730,USA) with inlet linked to an ethylene oxide cylinder.

Cells were maintained in an incubator (310 K, 4-6% CO_2, 90% relative humidity) and all manipulations were carried out in a laminar flow hood. An Olympus Model CK2 inverted microscope with camera adaptor was used for cell culture evaluation.

Procedures

Preparation of L-929 cell monolayer

Fibroblast cells grown to a confluent monolayer in a 75 cm^2 culture flask were rinsed with PBSA and trypsinized with 0.1% trypsin solution. The detached cells were diluted into a 10 ml culture medium and then transferred into a 15 ml centrifuge tube and centrifuged at 230 G for 5 min. The supernatant was discarded and the cells resuspended in 10 ml of medium which contained about 1x10^6 cells. Cell wells of the 6-well culture plate were each filled with 2 ml of culture medium and three drops of the fibroblast cell-containing suspension were added. The cells were mixed with the medium by carefully shaking the plates with circular motion. The plates were then placed in the incubator. A near confluent monolayer usually formed in two to three days.

Toxicity Tests

(I) Direct Contact Cell Culture Toxicity Test

The cell monolayer was first microscopically examined and any cell well exhibiting abnormal morphology such as incorrect confluency or granular/sloughing cells was rejected. The medium was replaced with fresh medium. A single test specimen was placed on top of the cell monolayer in each of the cell wells. The plates were returned to the incubator and evaluation was made after 24 h (ASTM,1988).

(II) Agar Diffusion Cell Culture Toxicity Test

The cell monolayer were prepared in the wells as above. Agar solution was prepared by autoclaving 2% agar solution in PBSA at 394 K for 15 min followed by cooling in a 318 K water bath. A 2xDMEM (medium of double concentration) solution was also warmed to 318 K and equal volumes of the agar and 2xDMEM were mixed and allowed to cool to approximately 310 K. The culture medium in the cell wells in which the cell monolayers were grown was quickly replaced with the newly prepared 1% agar medium. The agar culture medium became solidified in 2 min and a single test

75

specimen was placed on top of the agar gel in each well. The plates were placed into the incubator for 24 h and results were assessed (ASTM,1988).

(III) Modified Agar Diffusion Toxicity Test

When very tiny specimens with limited toxicity were tested, the above two procedures did not yield definitive results, thus necessitating an alternative approach. The test specimens were carefully placed directly on top of the cell monolayer in the cell well from which the medium had been withdrawn. A few drops of agar solution (310 K) were used to "glue" the specimens to the cell layer to protect the adjacent cells from being scratched off by further movement of the test material. The remaining agar solution (total volume 2.0 ml in each cell well) was poured into the culture dishes when the first few drops were solidified. The cell culture plates were then incubated for 24 h in the incubator and the results evaluated. This procedure is referred to as "modified agar diffusion" to distinguish it from the agar overlay methods in which the specimens are placed on top of the agar medium.

Sterilization of the Test Materials

Ethylene oxide(EO) sterilization was carried out with a gas sterilizer. The test specimens were cut to the required size(except for sensors which were tested as whole assemblies) and sealed into a gas sterilizing pouch (Propper MFG Co. Inc., Long Island City, NY 11101) and then exposed to EO gas in the sterilizing chamber at 1 atm EO pressure for about 12 h in a closed ventilation hood. The specimens in the pouch were allowed to degas in the air to get rid of the adsorbed EO for at least 24 h. The time required for complete desorption is different for different materials (Autian,1975; Bruck, 1974; Bruck,1971; Boretos,1973).

Ethanol solution (70%) was also used to sterilize polymer samples and other raw materials such as Pt wire, Teflon tubing,etc. The specimens were soaked in the solution

from 15 min to 1 h and then dried in a stream of aseptic air followed by thorough rinsing with sterile saline buffer. The ethanol solution was also used as an extracting solvent in treating the polymer materials.

Evaluation of the Cell Culture Tests

The grading for Procedure II was accomplished using the zone index (region of dead cells) according to ASTM Procedures (ASTM, 1988). There were six basic qualitative grades: 0, no detectable zone; 1, zone limited under specimen; 2, zone extends 0.5 cm beyond specimen; 3, zone extends 0.5 - 1.0 cm beyond specimen; 4, zone extends beyond 1.0 cm; 5, zone spreads entire dish. The toxicity measurements for Procedure III were tracked by microphotographing the cell cultures and measuring the spatial distribution or morphological change of the lysed cells. A toxic band as narrow as 50 μm (200x magnification) reflecting the cell lysis or change in cell morphology could be clearly discerned.

Results and Discussion

Sensor Design

The diagram of the glucose sensor is shown in Figure 5-1. The sensing element is located on the side of the sensor in the form of a cylindrical cavity. The Ag/AgCl reference electrode is present to the left of the cavity in the form of a coil. The cavity is first coated with cellulose acetate and glucose oxidase is immobilized by crosslinking with glutaraldehyde. The whole sensor including the reference electrode is finally coated with polyurethane (Bindra, 1991).

Sterilization

The sensors were sterilized with EO because the ethanol treatment changed the surface properties of the polymer membrane on the sensors. The effect of EO on sensor

performance was examined. Normal sensors having stable response to glucose were checked before and after EO sterilization. The results are shown in Table 5-1. Essentially no change in glucose sensitivity or hydrogen peroxide sensitivity was observed, indicating that the EO treatment did not alter either the polymer permeability or the enzyme activity. Sensors were degassed for at least 48 h in the sealed pouch after EO sterilization. Polymer samples were allowed to degas for more than three days. There was no evidence of any residual EO contamination from the

Table 5-1. Effect of EO Sterilization on Sensor Response

	Sensor #1		Sensor #2	
	Before	After	Before	After
Sensitivity to glucose (nA/mM)	2.2	2.3	1.8	1.8
Sensitivity to H_2O_2 (nA/mM)	50	53	70	62

sterilized materials during the cell culture tests. This was verified consistently by the negative tests of EO sterilized silicone rubber and nontoxic sensors. Since the preparation of a uniform confluent cell monolayer in the well took three days, it was possible to start the sample treatment and the cell culture preparation at the same time. In fact, the sterilization can be done any time prior to the cell culture tests because the sterile pouch keeps the samples sterile until needed.

The effect of ethylene oxide sterilization was demonstrated by keeping the EO

sterilized sensors in the pouch for three months followed by testing with Procedures II and III under prolonged incubation (three or four days). No bacterial growth was observed. On the contrary, sensors that did not undergo sterilization showed bacterial contamination in the cell culture after two day's incubation.

The Control Materials

Latex and silicone rubber are generally used as positive and negative controls respectively(ASTM,1988). Rubber from various manufacturers has been tested by cutting the sample into strips 25 mm in length and different thicknesses. Latex showed positive toxicity without exception while silicone had no effect on cell growth although in a few cases minor toxicity was observed for parts of the silicone test strips. It was assumed to be due to the local contamination of the rubber during its manufacturing or handling processes. The results were consistent with the existing literature (Brown,1983). Subsequent experiments were carried out with the Latex and silicone rubber standards occupying two of the cell wells in a 6 well plate, while the remaining 4 wells were allocated to the test specimens. Any sign of toxicity in the silicone rubber test well would lead to the rejection of the whole plate.

It is necessary to adjust the size of the Latex standard to yield significant but not complete cell lysis. For example, 24 h direct contact culturing of the L929 cells with a 2x2x25 mm Latex rubber strip resulted in cell lysis throughout the well. In contrast a strip of 1x1x25 mm had much less severe toxicity. It is found that Latex rubber strips of this latter size have toxicity comparable to the freshly made untreated sensors so this size was then used throughout the experiments. The obvious advantage of this size is that the zone index created in the cell layer can be clearly photographed with reasonable magnification. Larger samples make rating the degree of toxicity difficult.
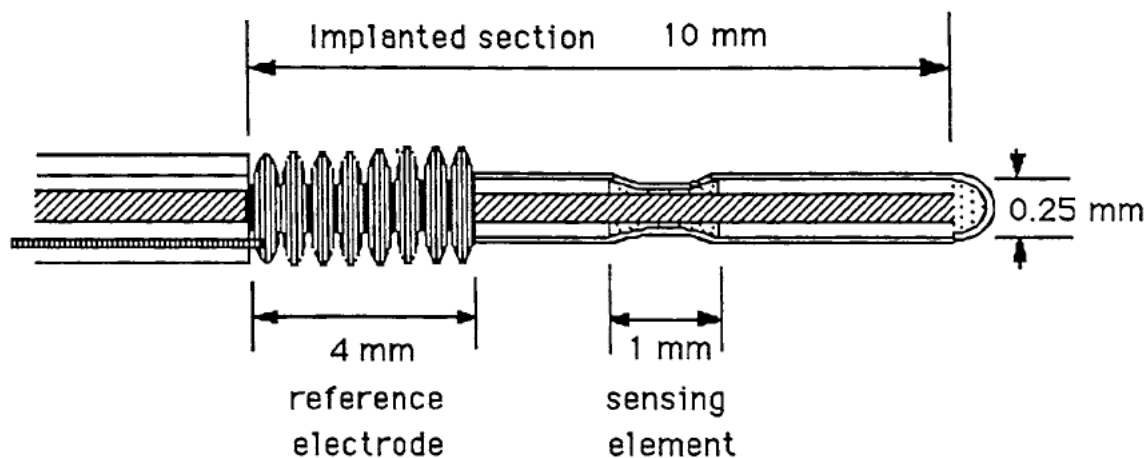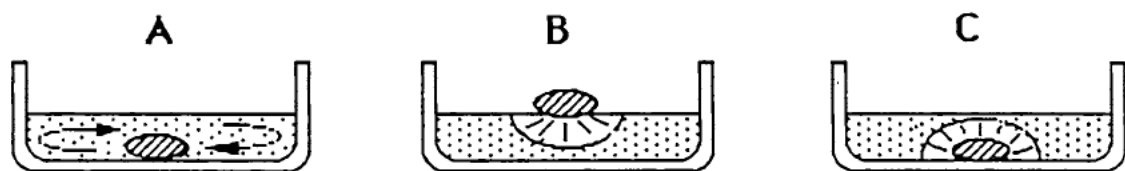
Figure 5-1. Diagram of the Glucose Sensor

Figure 5-2. Diffusion Patterns of the Three Cell Culture Tests

I. Direct contact----Free diffusion around the whole cell well.

II. Agar overlay---Diffusion across the entire agar medium is required

and the cell monolayer is not affected.

III. Modified agar overlay---The toxic effect is highlighted.

Comparison of Toxicity Measurement Procedures

Identical sensors of minor toxicity were tested using the three procedures described in the Experimental Section. The only one giving positive results was the modified agar diffusion (Procedure III). ASTM Procedures I and II, which were originally designed to evaluate bulk test materials, were unable to detect toxicity. The difference in the diffusion pattern of the toxic release is illustrated in Figure 5-2, where a,b, and c correspond to Procedures I, II and III respectively. The low sensitivity of Procedure I was due to the fact that the leached toxic substances could diffuse freely throughout the culture thus diluting the toxic effect. Figure 5-3 shows a definite difference between Procedures II and III. The photographs were taken for the tests with identical 1x1x25 mm Latex strips in 2 ml total volume of agar culture medium. These results support the pattern of Figure 5-2.

Removal of Toxicity

Toxicity removal was demonstrated by extracting the Latex rubber in ethanol and phosphate buffer. The results again showed size dependent behavior. A 2x2x25 mm strip still had significant toxicity left after soaking in ethanol for 120 h. The 1x1x25 mm strip, on the other hand, had no remaining toxicity after only 22 h of extraction. The efficiency of toxic substance removal from the rubber was higher for smaller sizes because the surface to volume ratio was larger. This was further substantiated by monitoring the loss in weight during ethanol extraction as shown in Table 5-2.

A similar effect was also observed for phosphate buffer extraction. However, the time for complete toxicity removal was extended to two weeks for the 1x1x25 mm Latex rubber and more than a month for the larger size. It is reasonable to presume that
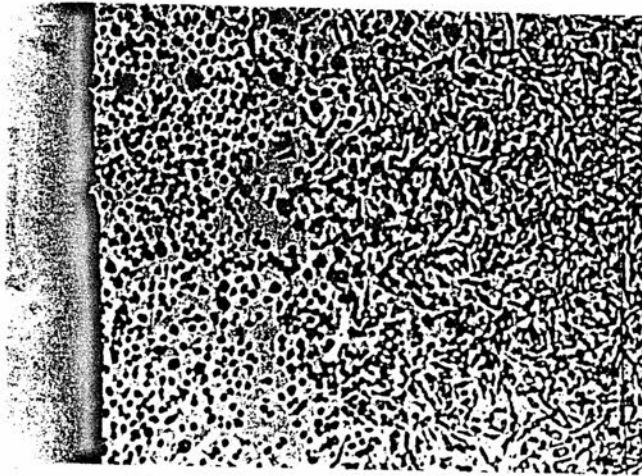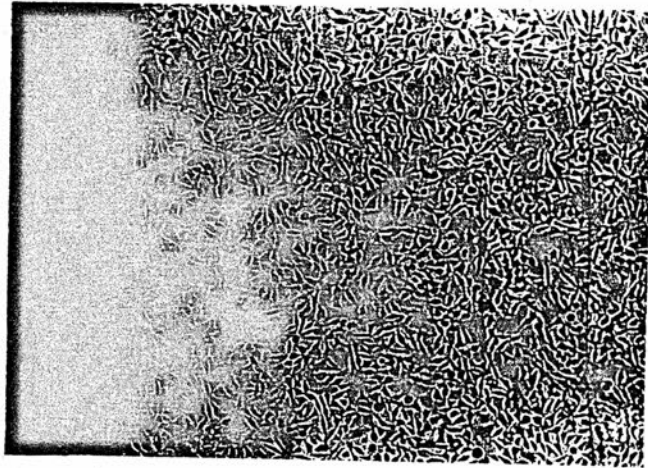
Figure 5-3. Results of the Two Different Agar Culture Procedures

    a. Procedure II---Monolayer is not affected.

    b. Procedure III---Toxic effect is observed.

Table 5-2. Weight Loss for Latex Rubber after Ethanol Extraction

hours in	weight (mg)			
70% ethanol	1x1x25 mm strips		2x2x25mm strips	
	sample 1	sample 2	sample 1	sample 2
0	23.3	25.2	67.6	70.5
10	22.9	24.8	67.4	70.2
22	22.8	24.7	67.2	70.0
64	22.7	24.7	67.0	69.8
120	22.8	24.7	66.9	69.7
% weight loss	2.1%	2.0%	1.0%	1.0%

the ethanol solution has much higher extracting power than phosphate buffer. The buffer extraction is a more appropriate though less efficient treatment for sensors to get rid of residual solvents and leachable reagents and to stabilize membrane structure.

These tests on the control materials show that care must be taken to control the sizes and pretreatment protocols to establish reproducible positive controls.

Applications in Sensor Development

The untreated polyurethane pellets (approximately 1.5x1.5x2 mm) had a toxicity grade of 2 if Latex of similar size were graded at 5 (Procedure II, Zone Index, ASTM,1988), which means that the pellets show low to moderate toxicity. A freshly

made sensor coated with a solution of the same polyurethane, however, was much less toxic and can be detected only by Procedure III. Figure 5-4 shows a series of sensors at different stages of the buffer extraction treatment. Figure 5-4a is a new sensor and 5-4b is a sensor after three days in phosphate buffer while 5-4c is a sensor which has been soaked in buffer for a week. These experiments illustrate clearly that toxicity can be removed relatively effectively in the case of the sensor because the polymer layers are thin (total thickness about 10 - 15 μm). Based on these results we conclude that the sensor should be conditioned in buffer for about seven days. The buffer treatment is also an important step in stabilizing the polymer structure and hence the sensor sensitivity.

The new cell culture technique also permits the evaluation of the relative toxicity of various parts of a multi-component sensor. It is of great help in accurately visualizing the degree and source of toxicity. Figure 5-4b clearly demonstrates that the sensing element is the source of toxic release.

To identify the toxic substance, all the materials involved in the sensor fabrication including Ag and AgCl wires, Pt/Ir wire, Teflon tubing, cellulose acetate, hydrogen peroxide, glutaraldehyde, glucose oxidase, polyurethane and silicone rubber glue were individually tested. None of the metal or polymer materials were found toxic when pre-treated with sterile PBSA. But all three reagents, hydrogen peroxide, glutaraldehyde and glucose oxidase testedpositive when they were directly added to the cell culture at various concentrations. The morphology of the cell monolayers produced by the three reagents is shown in Figure 5-5. It is interesting to note that the different reagents cause different morphological characteristics.It is not clear what makes glucose oxidase toxic. It could be due either to the H_2O_2 production catalyzed by the enzyme or to oxygen depletion in the culture medium which contains 5 mM glucose as well as
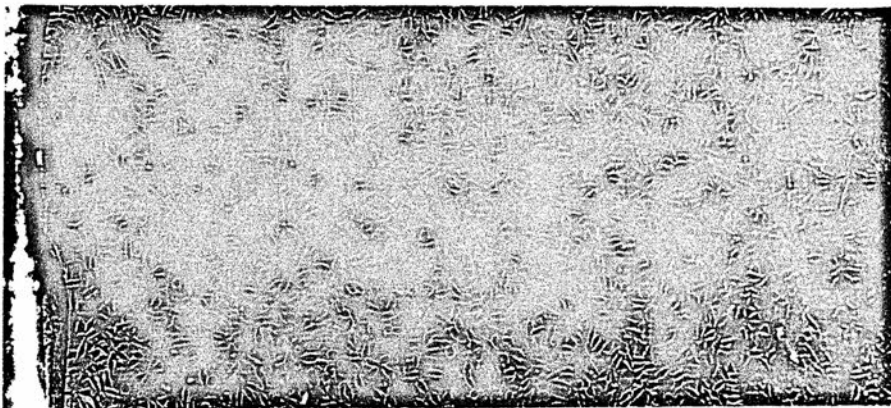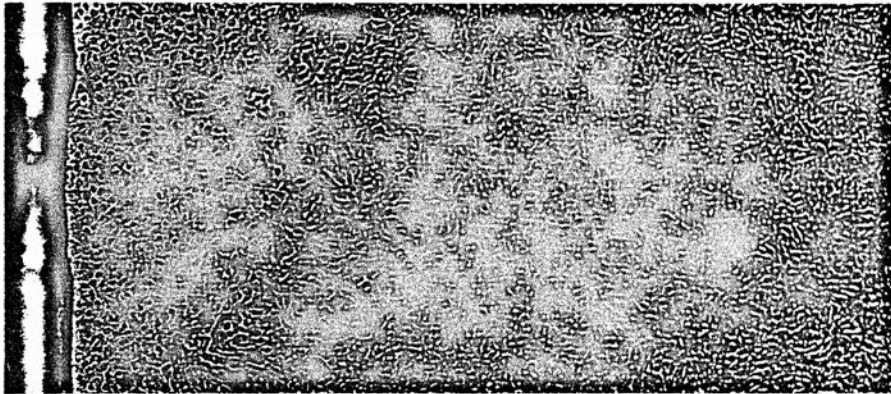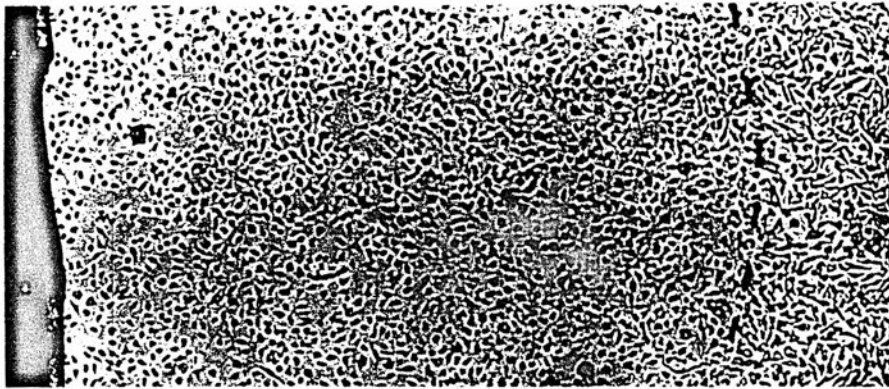
Figure 5-4. Sensors in Relative Toxic States

a. High toxicity.
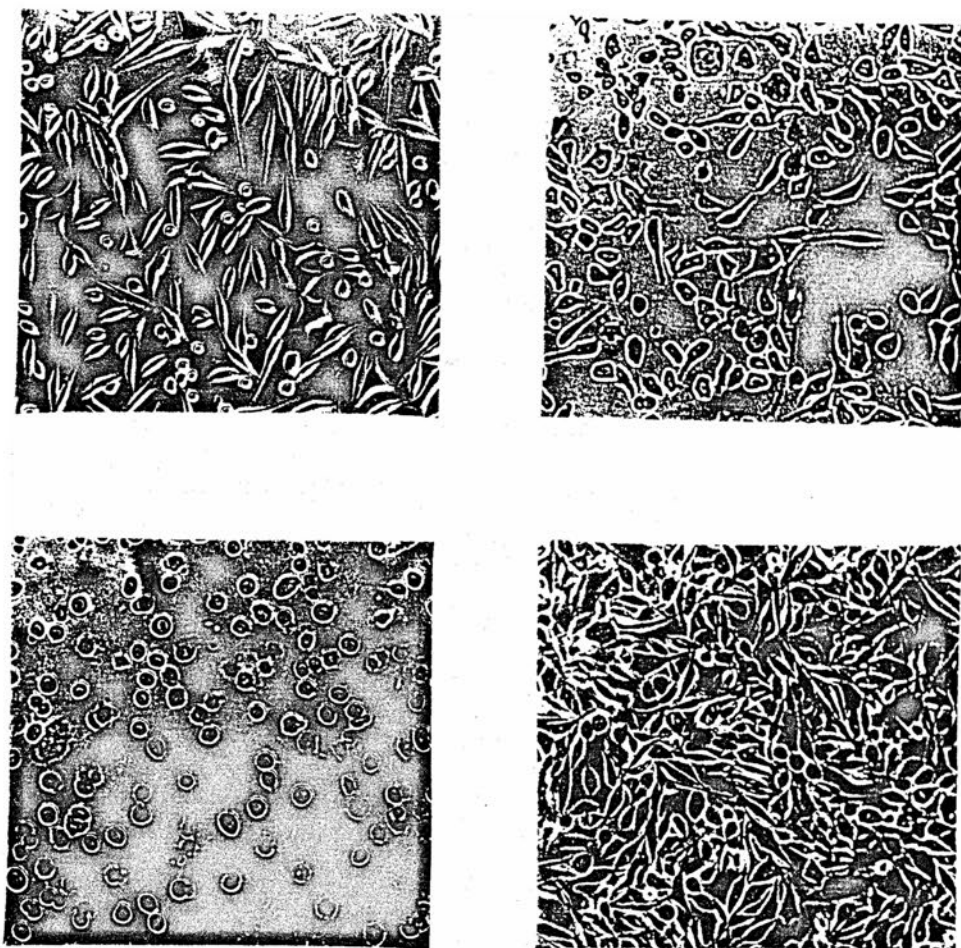b. Medium toxicity.
c. Non-toxic.

Figure 5-5. Different Morphologies Produced by (a) H_2O_2,

(b) Glucose oxidase, (c) Glutaraldehyde and (d) Normal culture.

dissolved oxygen.

The toxic effect of solvents was separately tested with "reagent free" sensors that did not contain glucose oxidase and glutaraldehyde. Blank sensors were coated with a 4 % solution of polyurethane (in tetrahydrofuran containing 2 % dimethylformamide) and were subjected to cell culture test. The only possible toxic substance released (if any) from sensors thus made would be either polymer impurities or residual solvents. All freshly made sensors were shown to have low toxicity without exception while sensors dried in aseptic air for four days mostly tested negative, indicating that the toxic effect for fresh sensors was mainly due to the solvents because polymer additives and impurities were not volatile and could not be eliminated by air drying. The same effect of toxicity removal was also observed for phosphate buffer treated "reagent free" sensors and the buffer extraction was more efficient than air drying. Two day's soaking in buffer eliminated the solvent toxicity completely.

Glucose oxidase did not create detectable toxicity when it was incorporated into the sensors. The polyurethane membrane apparently entraps the enzyme effectively. Although H_2O_2 has been shown to have toxic effct on the cells, the whole sensor tests (containing glucose oxidase which produces H_2O_2) were not observed to have detectable toxicity. It was assumed that the amount of H_2O_2 produced by the sensors was not high enough to induce the cell change or the H_2O_2 produced was destroyed by catalase present in the culture medium.The enzyme activity in the sensors was examined by checking the sensor response before and after the cell culture tests and no significant change in sensitivity was observed. This confirmed that the enzyme activity was maintained.

The toxicity of glutaraldehyde was the most serious problem. The overall toxicity of a whole sensor far exceeded that of a "reagent free" sensor, which meant that the solvent toxicity was not the major toxic source. A series of sensors incorporated with

different amount of glutaraldehyde were dried in aseptic air for four days (to remove the solvent toxicity) andtested. The degree of toxicity was approximately proportional to the total loading of glutaraldehyde. The removal of residual glutaraldehyde from the sensors usually took more than four days in phosphate buffer. The sensors were all tested negative after one week in buffer.

Repeated experiments over a period of one year have shown consistent results. New sensors have moderate toxicity (mainly from glutaraldehyde) and the toxic effect can be removed by extracting the leachable substances with phosphate buffer for 4-8 days. A typical photograph of a non-toxic sensor is shown in Figure 5-4c.

The Ag/AgCl reference electrode, which is an integral part of the sensor, is a potential source of toxicity. Newly made references were sometimes found toxic, but the toxicity could be removed by buffer. Therefore the initial toxic substances were neither Ag^+ nor AgCl, but were assumed to be impurities that were taken up during the Ag anodization. It is possible that the reference electrode could generate toxicity after a prolonged *in vivo* implantation under current flow. The passage of current through the reference electrodes was shown not to create any observable toxic effect after 4.0 mC cathodic charge was passed through them. This amount of charge is equal to that passed by a sensor monitoring normal glucose levels for ten days. Figure 5-6 shows the toxicity tests of reference electrodes in different states. The fresh electrode shows toxic release. The conditioned sensors with or without current passage are non-toxic.

Conclusion

The cell culture toxicity test has been shown to be an effective way to locate the source and visualize the degree of sensor toxicity. The effectiveness of various treatments can be monitored. It should be pointed out, though, that this toxicity test can provide only acute assessment of cytotoxicity on qualitative basis. The sensitivity of
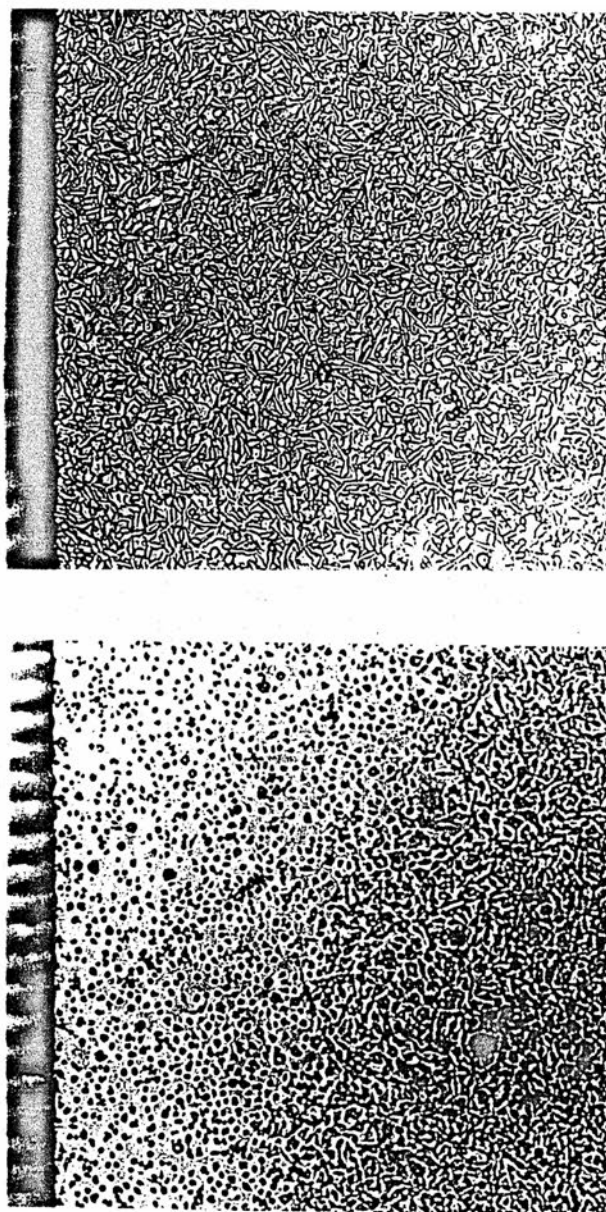
Figure 5-6. The Toxicity Tests for the Reference Electrode

(a) Newly prepared reference electrode.

(b) Buffer treated reference electrode.

this method is based on the observation of the cell morphology. The affected cells are shown to form a clearly defined boundary with the surrounding normal cells, which indicates the diffusion front for toxic substances. This means that the observable morphological change can be induced only by the toxic materials at a concentration higher than a "critical value" which causes cell death. The critical concentration is the limit of this method. Thus the simplicity of this method rests in the estimation of the width of the toxic zone. The results is even independent of the state of the cell confluency because the cell death and lysis within the toxic zone occur whenever the toxic concentration is above the critical value regardless of the number of cells present. This is an advantage of the proposed method. Since the sensitivity of this *in vitro* test has generally proven to be higher than the *in vivo* test, a negative result does increase the likelihood that *in vivo* applications are feasible. Long term implantation tests for biocompatibility are necessary and intensive *in vivo* investigations are currently underway.

Chapter 6. Characterization of a Miniature Needle-type Oxygen Sensor and *In Vivo* Measurements of P_{O_2} and pH in Rat Subcutaneous Tissue

Abstract

In order to evaluate the oxygen effect on the glucose sensor, a monopolar needle-type oxygen sensor was constructed to monitor the oxygen partial pressure in subcutaneous tissue. The *in vitro* charaterisics of this oxygen sensor which had two layers, cellulose acetate and polyurethane, was studied. The combination of these two films effectively blocked electrochemical interference and the outer polyurethane membrane was favorable for oxygen diffusion. *In vivo* measurement of oxygen in rat subcutaneous tissue suggested that the tissue P_{O_2} was ~22 ± 5 mm Hg. A 25 Gauge commercial pH sensor was also used to measure the pH in subcutaneous tissue and it was found that the fluctuation in tissue pH was within ±0.05 unit, e.g. 7.4 ± 0.05.

Introduction

The electrochemistry of oxygen in aqueous solution has been one of the most intensively studied systems. Its properties and measurements are all well documented (Hoare, 1968; Fatt, 1976; Hitchman, 1978; Gnaiger, 1983; Linek, 1988). Yet active studies are still being undertaken to further understand its role in especially life science and energetics. The measurement of oxygen in living organisms is an important aspect because of the significance of oxygen in physiological processes and clinical treatments.

Measurement traces back to early 1940's when an oxygen cathode was used to measure oxygen in animal tissue (Davis and Brink, 1942). It was not until 1956, however, that the tissue oxygen measurement became reliable when the "Clark" electrode was developed (Clark, 1956). Major advances towards oxygen sensor development and tissue oxygen measurement were made in the late 1950's and 1960's

(Cater, 1957-1966; Silver, 1966, 1973; Jamieson, 1963, 1965; Fatt, 1964, 1976), which greatly enriched the knowledge of tissue oxygenation and oxygen transport in the physiological processes.

The development of the polarographic oxygen sensor has undergone several phases since the first membrane covered oxygen electrode was introduced by Clark (Clark, 1951)· The first category is the two electrode system in which the working electrode and reference electrode (usually Ag/AgCl that serves also as counter electrode) are separate and current has to pass through the measuring medium. This type of construction has wide application mainly in micro electrodes (Whalen,1967; Staub,1961; Bicher, 1970; Crawford,1985) and is still the major configuration for tissue microsensors. The second category is the so called "Clark electrode" (Clark,1956) which combines both working electrode and reference electrode within a closed chamber and carries its own internal electrolyte. The outer hydrophobic membrane is permeable only to O_2 so that other electrochemical interferents in the test environment are not likely to interfere. The Clark electrode has found major application in both *in vivo* and *in vitro* measurements. The third category of oxygen electrode has the configuration of a three electrode potentiostat (Lucisano, 1987) and all the three electrodes are housed inside a gel filled compartment which is covered with a hydrophobic membrane. It is electrochemically stable and less susceptible to interference. Its sophisticated configuration, on the other hand, makes it bulky and difficult to miniaturize. The initial design, therefore, was not for the purpose of tissue oxygen measurement.

The *in vivo* measurement of oxygen partial pressure faces two major challenges. The first is how to construct an adequate sensor to achieve dependable measurements. The second is how to interpret the data of *in vivo* measurements by relying on *in vitro* characteristics considering that it is essentially impossible to make

an *in vivo* calibration. There have been hundreds of different sensor designs (Silver, 1966; Cater, 1966; Gnaiger, 1983; Fatt, 1976) in terms of shape, size, configuration and purpose. Many factors such as the variation in diffusion coefficient, effect of stirring, response time, consumption of oxygen by the sensor, electrochemical interferences and change in surface permeability all influence the results (Hitchman, 1983; Baumgartl, 1983). The tissue inhomogeneity, on the other hand, adds some more complexities to the problem. The tissue is not uniform in the scale of microns and therfore the sensor surface does not experience an uniform medium. The physiological fluid in the tissue is not static but its pattern of flow or circulation is unknown. More importantly, the oxygen tension in the tissue is not uniform. There is oxygen gradient between capillaries. To achieve a specific goal, compromise has to be made in constructing the sensor in order to obtain a relatively more accurate estimate.

In the process of developing a glucose oxidase based implantable glucose sensor in our laboratory it was raised that the oxygen dependence of the glucose sensor should be evaluated because the sensor worked on the enzymatic oxidation of glucose. This reaction needs oxygen as the co-substrate to proceed, which requires that the supply of oxygen should be relatively abundant such that the overall process is not affected by the fluctuation in oxygen pressure. Two factors affect oxygen levels at the sensor / tissue interface: the subcutaneous oxygen availability and the oxygen demand by the implanted glucose sensor. The first aspect can be approached by making statistical measurements in the subcutaneous tissue with appropriate oxygen sensors while the second aspect can be addressed only by simultaneously measuring both O_2 and glucose in the living organism.

The glucose sensor which was designed and tested both *in vitro* and *in vivo* for subcutaneous glucose measurement in ours and our collaborator's laboratories (Bindra, 1991; Moatti, 1991) is based on electrooxidative detection of H_2O_2, the

product of glucose enzymatic reaction. Factors having potential effect on the performance of this glucose sensor are P_{O2}, pH, temperature and electrochemical interferences from the physiological fluid. The purpose of this chapter is to address oxygen availability and the pH stability at the implantation sites in subcutaneous tissue. Other factors such as interferences, applied potential, H_2O_2 electrode oxidation, toxicity and *in vivo* performance have been discussed elsewhere (Chapters 3, 4 and 5; Moatti,1991). The properties of various membranes and their thickness vs permeability are not the focus of this work and therefore have not been investigated in detail.

To validate the results of the subcutaneous oxygen measurement, identical geometry and configuration of the oxygen sensor to that of a glucose sensor were used. The same monopolar detection mode as that used for glucose measurement (separate reference electrode) which passes current through the tissue is also adopted because the passage of current could have some physiological effect on the surrounding tissue and therefore influence the O_2 transport. The O_2 sensor also uses the same Pt/Ir wire and identical polymer coatings (Bindra,1991) except that the enzyme layer is eliminated. This configuration enables the O_2 sensor to experience the same *in vivo* environment and, more importantly, to see the same amount of accessible O_2 in the surrounding tissue. The measured O_2 level is, therefore, a more reliable estimate of the available oxygen for the glucose sensor.

In this report the fabrication of the oxygen sensor, its *in vitro* characterization and *in vivo* measurement of oxygen partial pressure in subcutaneous tissue of anesthetized rats are discussed. The simultaneous measurement of subcutaneous pH with a commercial needle pH sensor is also conducted.

Experimental

Oxygen Sensor Fabrication

The sensors were made from the Teflon coated Pt/Ir wire (0.17 mm o.d., Medwire Co., NY) that was used for the glucose sensor fabrication. A cylindrical cavity was created on each electrode as shown in Figure 1. Cellulose acetate (CA) (Aldrich, 39.8 % acetyl content) and polyurethane (PU) (SG 85A, Thermedics Inc., Woburn, MA) membrane coatings were described elsewhere (Chapter 3). The sensors were dried in air at room temperature for ~ 30 minutes and then put in to 0.1 M phosphate buffer of pH 7.4 containing 0.15 M NaCl. A complete sensor is shown in Figure 6-1.

Oxygen Sensor Characterization

In vitro characterization and calibration of the O_2 sensors were conducted in a closed single compartment cell which had the capacity of 20 ml buffer and similar volume for the gas phase. Nitrogen and air were introduced from tanks through two separate flow meters (Cole Parmer, Chicago, IL)) which had flow rate scale ranges in 1   10 ratio (with higher flow rate for N_2 to achieve low P_{O2} levels) and mixed before bubbling into the cell. The P_{O2} levels in the gas phase could be adjusted between 0 and 160 mmHg. The solution was constantlt stirred with a stirring bar.

Voltammetry was performed with a Cypress Systems Model CYSY-1R (Lawrence, KS) potentiostat and amperometric measurements were made with a PAR Model 400 (EG&G Princeton Applied Research) electrochemical detector. Ag/AgCl reference electrodes for *in vivo* measurements were made from a silver wire of 0.25 mm o.d. with an implantable length of 15 mm, anodized in 2 M KCl solution at a constant current of 0.1 mA for 10 minutes . The same pH 7.4 phosphate buffer containing 0.15 M NaCl was used throughout the experiment.

pH Sensor Calibration

A needle type pH sensor (25 G, 0.5 mm o.d. with sensing unit at the tip of the needle) was purchased from World Precision Instruments, Inc. (Cat.# SA1B, New

Haven, CT). An external Ag/AgCl reference electrode described above was used. The pH sensor was fully hydrated in pH 7.4 phosphate buffer. The calibration was performed by the following procedure. Two buffer solutions of 0.1 M phosphate containing 0.15 M NaCl were prepared from reagent grade Na_2HPO_4 and KH_2PO_4. The pH of the buffers was measured with a Fisher Accumet Model 910 pH meter and adjusted with 5 N NaOH or HCl to pH 7.40 and 5.38 respectively. The pH sensor was then calibrated in these two Cl-containing buffer solutions vs the Ag/AgCl reference. The drift of the sensor output was also monitored in pH 7.40 buffer against a BAS (BioAnalytical Systems, Inc.) Ag/AgCl reference electrode and the output in mV was plotted vs time.

In vivo Experiment

An anesthetized (chloral hydrate, 35 mg / 100 g bodyweight, ip) rat (Sprague Dawley, body weight ~400 g) was placed on a 37 ^{O}C thermostat pad and the hair on the back of the neck was shaved. The pH sensor was directly inserted into the subcutaneous tissue while the reference electrode, the anodized Ag wire, was implanted through a 23 Gauge syringe needle. The needle which served as a catheter was pulled out of the tissue, leaving behind the reference electrode in the subcutaneous tissue parallel to the sensor. The sensor and reference were then connected to the pH meter and the mV output was monitored for about 4 - 8 hours. The sensor was pulled out of the tissue at the end of the experiment and rinsed with buffer. Calibration was carried out again using the same pH 7.4 and pH 5.38 buffer solutions vs the same Ag/AgCl wire reference electrode.

The *in vivo* measurements of O_2 in rats followed the same procedure for subcutaneous pH measurement except that an amperometric detector was used to measure the O_2 electroreduction current at a constant applied potential of -550 mV vs Ag/AgCl .

Alternatively, inhalation anesthesia with halothane was used to compare the effect of anesthesia on the tissue oxygenation. Halothane was administered through a three flowmeter system. O_2 (containing 5 % CO_2) and air were regulated by two separate flowmeters to achieve various ratio before being mixed. Part of the gas mixture was controlled to bubble through a halothane tube and then rejoin the main stream which was inhaled by the rats. The O_2:air ratio and halothane dosage could all be regulated freely by the flowmeters.
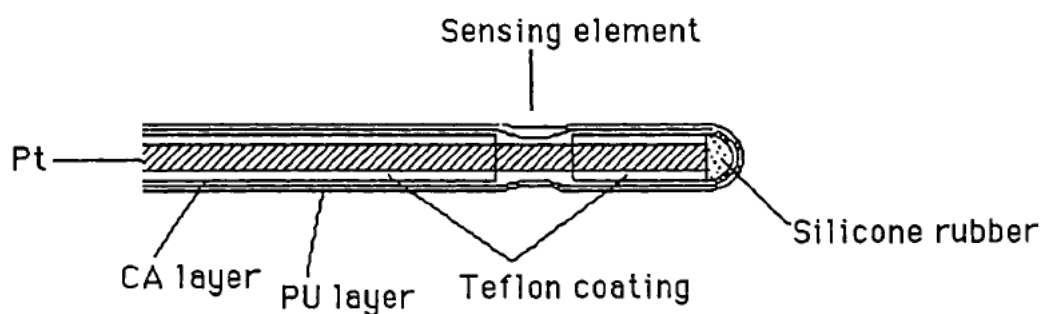
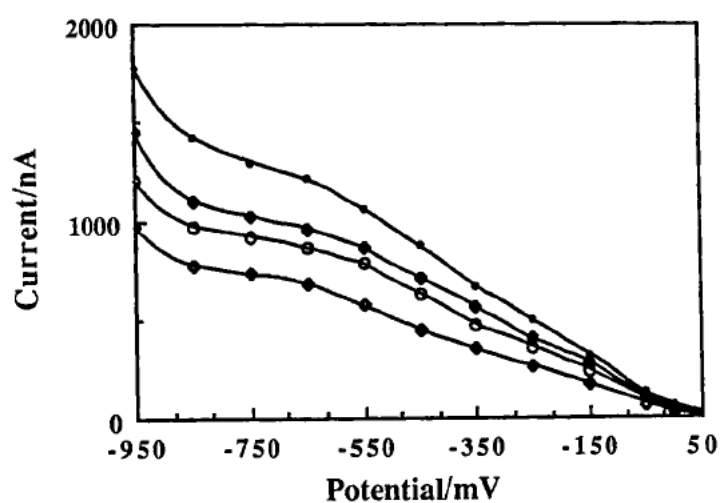**Figure 6-1.** Schematic Diagram of the Oxygen Sensor

Figure 6-2. Reduction of Oxygen on Bare Pt/Ir Electrode

(•: 50 °C; ◆: 36 °C; O : 30 °C; ◇: 20 °C.)

Results and Discussion

I. *In Vitro* Characterization

(a) Reduction of Oxygen on Bare and Polymer Covered Pt-Ir Electrodes

On bare Pt/Ir wire electrodes oxygen reduction reaches a limiting current at about - 500 mV vs Ag/AgCl and H_2 evolution starts at about - 650 mV to -850 mV. The potential for the diffusion current, however, varies somewhat with scan rate. To ensure a steady state current, the i-E curves were measured in the amperometric mode on bare electrodes at various temperatures, The results are shown in Figure 6-2.

Hydrogen evolution was measured on both bare and PU covered electrodes at approximately zero P_{02} in pH 7.4 buffer. Figure 6-3 shows curves which indicate that there is no substantial H_2 evolution on the polyurethane covered electrode even at 950 mV while it occurs at 700 mV on a bare electrode.

When the electrode was covered only with a cellulose acetate membrane, the O_2 diffusion was partially hindered but the H_2 evolution was not affected. The presence of the PU membrane caused H_2 evolution at a more negative potential but had much less effect on inhibition of oxygen diffusion. The i-E curves of complete sensors (having a PU layer on top of CA) exhibited the combined effect of each of the individual membranes as observed in Figure 6-4. Curve a represents a the response of a bare sensor. Curve b has only an PU membrane and Curve c has CA only and Curve d is a complete sensor. This sensor has wider potential window than a bare electrode and the overall sensitivity is controlled by the inner CA membrane and the existence of the PU layer serves only as protection and also prevents H_2 from forming at its normal potential.

(b) Interferences

Cystine, Dulbecco modified Eagle's cell culture medium (DME) and bovine

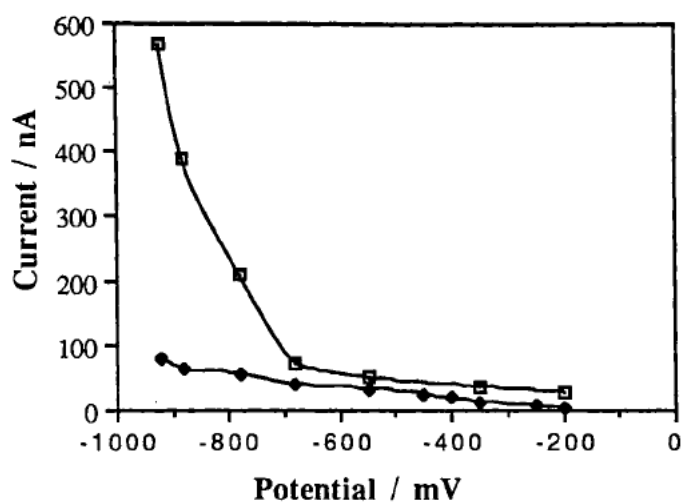**Figure 6-3.** Hydrogen Evolution on Bare and PU Coated Sensors
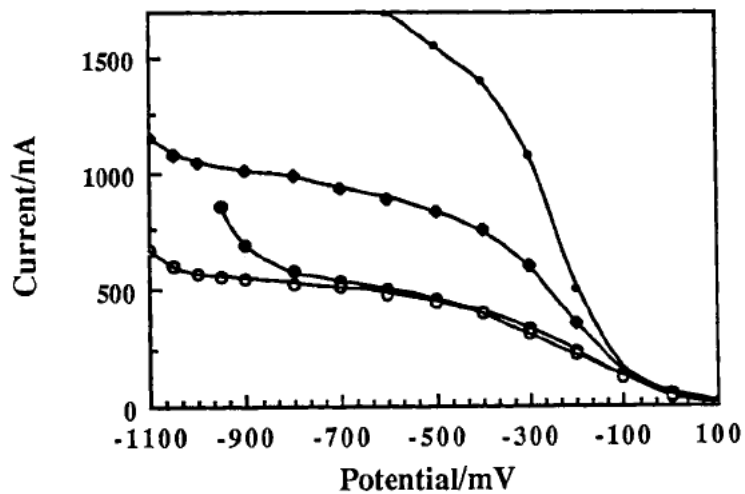
a. Bare electrode; b. PU coated electrode

Figure 6-4. Reduction of Oxygen on Bare, PU and CA+PU Cated Sensors

(• : Bare; ◆ : PU cated; ● : CA coated; ○ : CA+PU coated.)

serum (BS) were chosen to test the potential interferences to the sensors. They were assumed to simulate the complex background for *in vivo* operation. The experiment was carried out with two electrodes, one coated with PU and the other coated with CA+PU, in the same closed cell and oxygen was removed by constantly bubbling the buffer with nitrogen until a steady state current (~0-10 nA) at the sensor output was observed. Cystine, DME and bovine serum were then sequentially injected and their corresponding response was recorded as shown in Figure 6-5. The CA+PU film apparently had the function to discriminate some of the interfering species as compared to the PU coated electrode. The PU film, however, had indeed the function of eliminating electrode fouling. Bare electrode had a decreased response to oxygen when tested in buffer containing 3% serum while the PU coated electrode did not show any current decrease after 24 hour in the same serum solution.

The bare, PU and CA+PU coated electrodes were also examined in a two-electrode system in which Ag coils anodized in chloride were used as the anodes and 550 mV was applied between the Ag/AgCl anode and the sensor. The buffer was saturated with air and stirred constantly. A decreasing current was observed for the bare electrode and a layer of silver black was deposited on the Pt-Ir surface after 12 hours. But no signal decrease occurred on the other two polymer coated sensors and no observable change took place when the sensors were examined under microscope.
(c) Stirring Effect

It has been a tradition for oxygen sensors to exhibit a stirring effect except for the ultramicro and recessed types. In this study the stirring effect was tested by comparing the three different electrodes, bare, PU and CA+PU coated sensors. Figure 6-6 illustrates the stirring effect of the three sensors. The output of the bare sensor had almost proportional dependence on the stirring rate. The current at static state was only 35 % of that at maximum rate (stirrer's upper limit). The membrane coated sensors, on
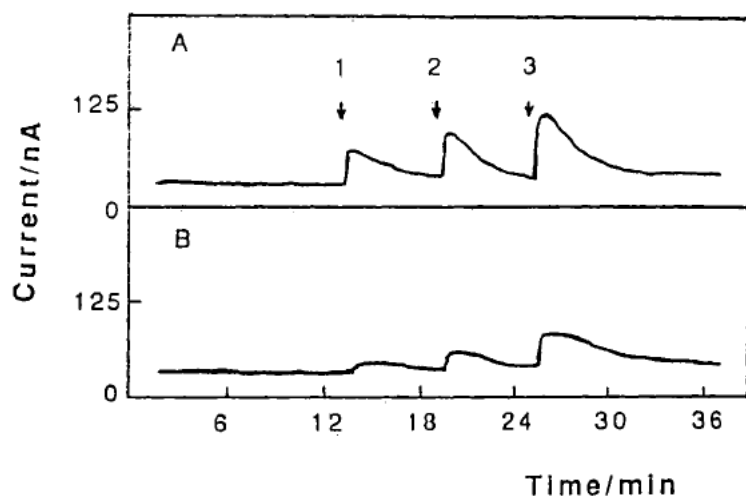
101

Figure 6-5. Effect of membranes on Interferences

A. PU coated; B.CA+PU coated.

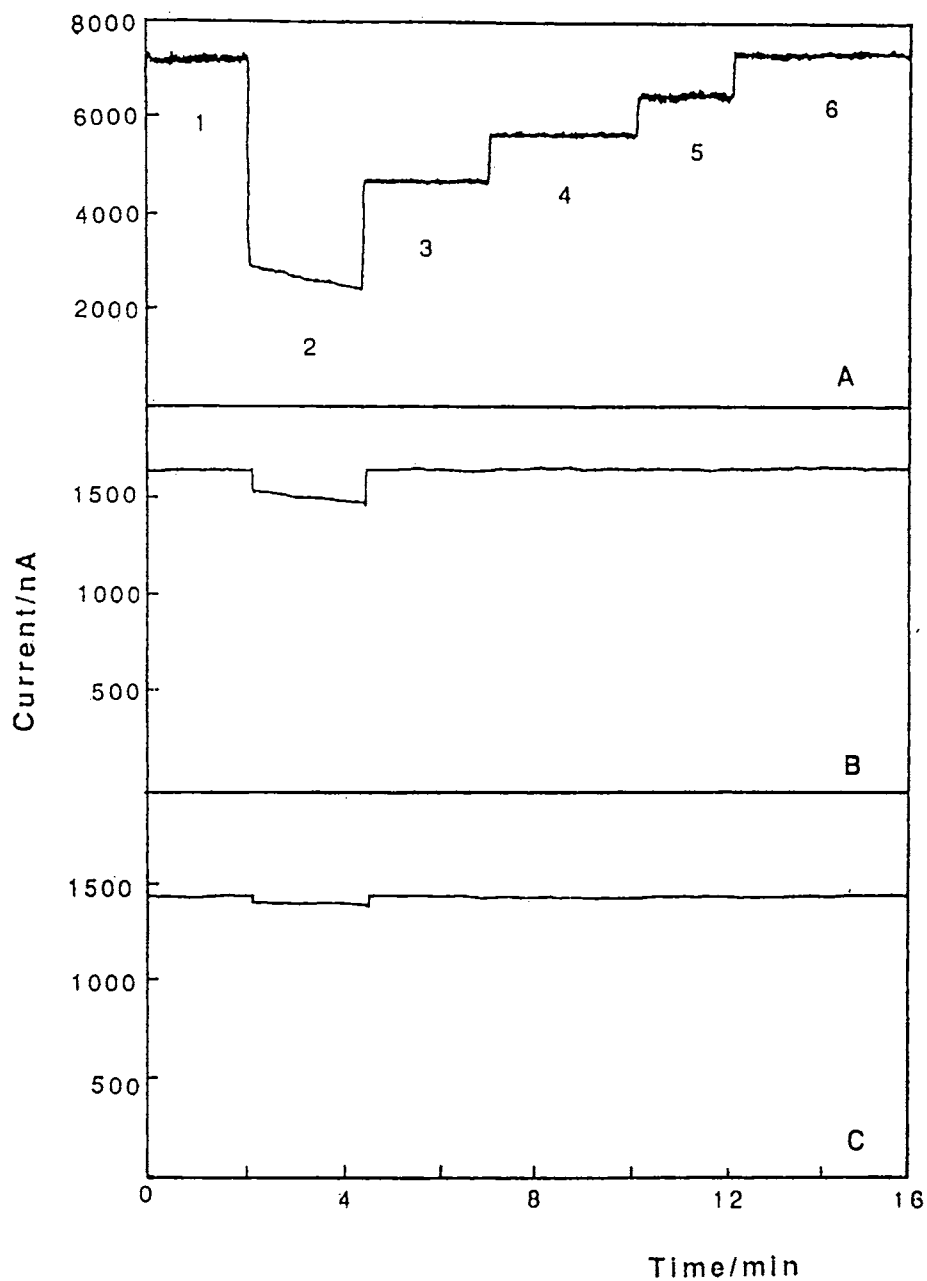(1) Injection of 0.5 mM cystine; (2) 3% DME and (3) 3% bovine serum.

Figure 6-6. Stirring Effect on Bare, PU and CA+PU Coated Electrodes

A. Bare; B. PU coated; C. CA+PU coated.

(1) and (6) Maximum stirring rate; (2) Unstirred; (3)Minimum stirring rate;

(4) and (5) Intermediate stirring rates.

103

the contrary, had a different pattern. The output was not stirring rate dependent. They behaved like a flip-flop device, having a constant static response and another constant stirred response as shown in Figures 6-6b and 6-6c. The differences between these two levels were 6 % for PU coated and 2 % for CA+PU coated sensors.

(d) Temperature Effect

The reduction of O_2 on the Pt/Ir electrode is affected by temperature with a coefficient of ~2%/$^\circ$C. Both the bare and coated sensors have the same temperature coefficient which suggests that the temperature affects only the electrochemistry of O_2 reduction. O_2 diffusion through the membrane is not substantially influenced by temperature.

(e) *In Vitro* Calibration

The *in vitro* calibration was carried out using the procedure described in the Experimental Section and most of the sensors coated with only polyurethane had a linear output up to 40 - 100 mm Hg Po_2. The air Po_2 (~ 150 mm Hg in vapor saturated cell) was beyond the dynamic range. The CA+PU coated sensor, however, had much better linearity and the air point was within the dynamic range. Figure 6-7 shows the calibration curves of these two types. It is not clear why the PU coated sensor has shorter linearity. Nevertheless, the high linearity of the CA+PU coated sensor greatly simplifies its use because a two-point calibration (N_2 and air) is feasible.

II. *In Vivo* Measurement of Po_2

(a) Effect of Membranes

Only transient *in vivo* measurements were performed, varying from three to eight hours. All the sensors examined have shown very stable output in the subcutaneous tissue of anesthetized rats although the current scale varies greatly from
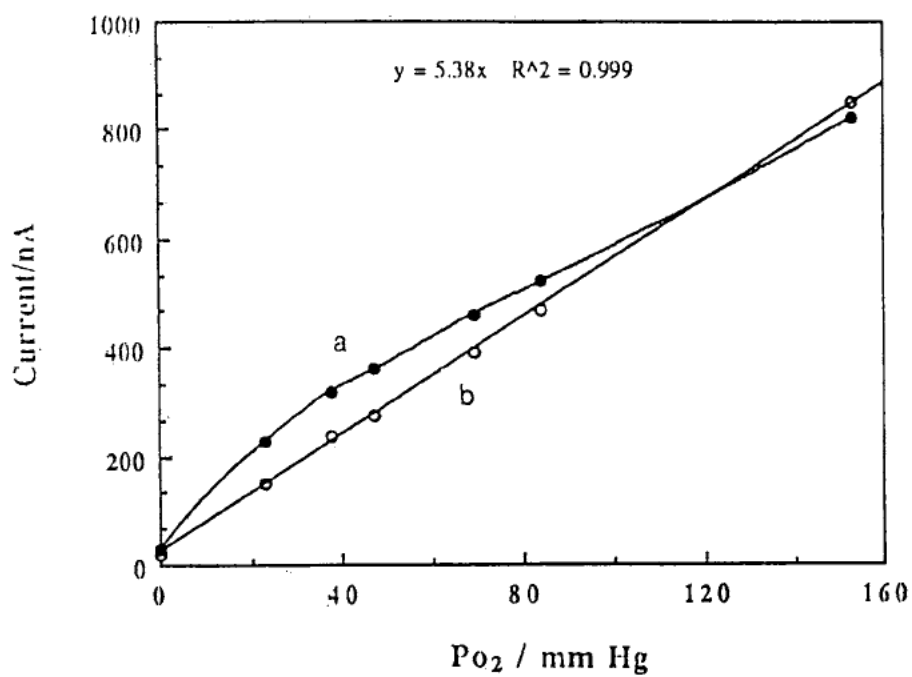
Figure 6-7. Calibration Curves of PU and CA+PU Coated Sensors

(a). PU coated; (b). CA+PU coated.

~20 nA to ~300 nA. The *in vivo* background current was determined by sacrificing the rats at the end of the experiments. In every case, the sensor output current dropped to zero O_2 level in a few minutes when the rats died.

In order to examine the membrane permeability, some sensors with only PU coating were implanted and the background current was obtained after the death of the subjects. The *in vivo* background current for this type of sensor was usually very high. It was comparable to the signal for oxygen in some measurements as shown in Figure 6-8. The inability of polyurethane alone to eliminate electrochemical interferences in tissue was clearly demonstrated by the high background. Six PU coated sensors were tested and the results were similar. Figure 6-8 illustrates the output of two of the PU sensors during the experiments. The background currents indicated at death were 283 nA and 142 nA respectively.

The complete sensors with the inner CA film, however, had excellent performance (Figure 6-9). Zero background was observed for all the sensors tested (n =13). This is consistent with the *in vitro* results which showed that the cellulose acetate layer functioned more efficiently as the diffusional barrier to the electrochemical interferents than polyurethane. Although a certain degree of interference from DME and serum was observed for the CA+PU sensors *in vitro* (Figure 6-5), their *in vivo* background was negligible. This is an indication that there are less electroreducible species in the living tissue than in the culture medium and serum.

(b) Significance of the Measured Results

An important observation for tissue O_2 measurement is that different sensor sizes give different results (Jamieson,1965) for the measured O_2 levels. An ultramicrosensor (< 5 μ) gives the P_{02} at the specific point of implantation because the
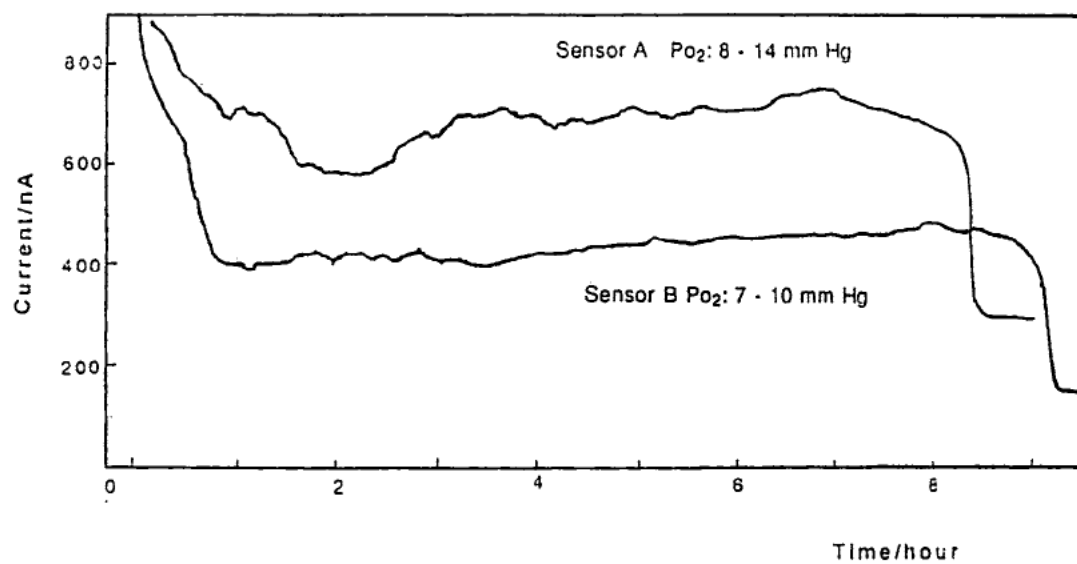
106

Figure 6-8. *In vivo* Output of PU Coated Sensors

107

oxygen consumption by the sensor is insignificant and the size of the sensor is smaller than adjacent capillaries (Silver, 1966; Metzger, 1973). This kind of measurement will yield varied P_{O2} values (or the true P_{O2} values) because of the P_{O2} gradient in the tissue. Sizeble sensors, however, such as the ones used in this experiment (0.17 mm o.d. and 0.3 - 1.0 mm in length) usually yield an average of the tissue oxygen tension because the exposed sensor surface area is larger than the P_{O2} gradient scale(the distance between adjacent capillaries). To verify this point some sensors were implanted several times in different rats and typical results were overplotted in Figure 6-9 (designated sensor C and D). It is shown that the detected oxygen levels are indeed averaged and stable, i.e. the current output for the same sensor was similar in different rats because the average oxygen tension in the same tissue was similar. The measurements performed with these sensors, therefore, give the average availability of oxygen at the location of implantation. This is favorable for the oxygen dependent glucose sensor that requires a stable supply of oxygen.

Thirteen measurements were made with 8 complete sensors in rats anesthetized with chloral hydrate (ip). The variation in oxygen level was usually within the range of 5 - 8 mmHg as shown in Figure 6-9. The length of the experiments was 6 ± 2 h and no common trend of decreasing or increasing in oxygen level was observed. The measured P_{O2} values were between 15 and 30 mm Hg.

(c) Effect of anesthetics

The above experiments were performed with rats anesthetized with chloral hydrate through ip injection. Tissue oxygen levels were stable and no significant fluctuation was observed. Inhalation anesthesia with halothane was further tested. It was found that the inhalation anesthesia significantly influenced the oxygen uptake by the animals. The subjects suffered hypoxia in most of the cases when breathing normal air. It was very difficult to maintain the rats in deep anesthesia for more than four
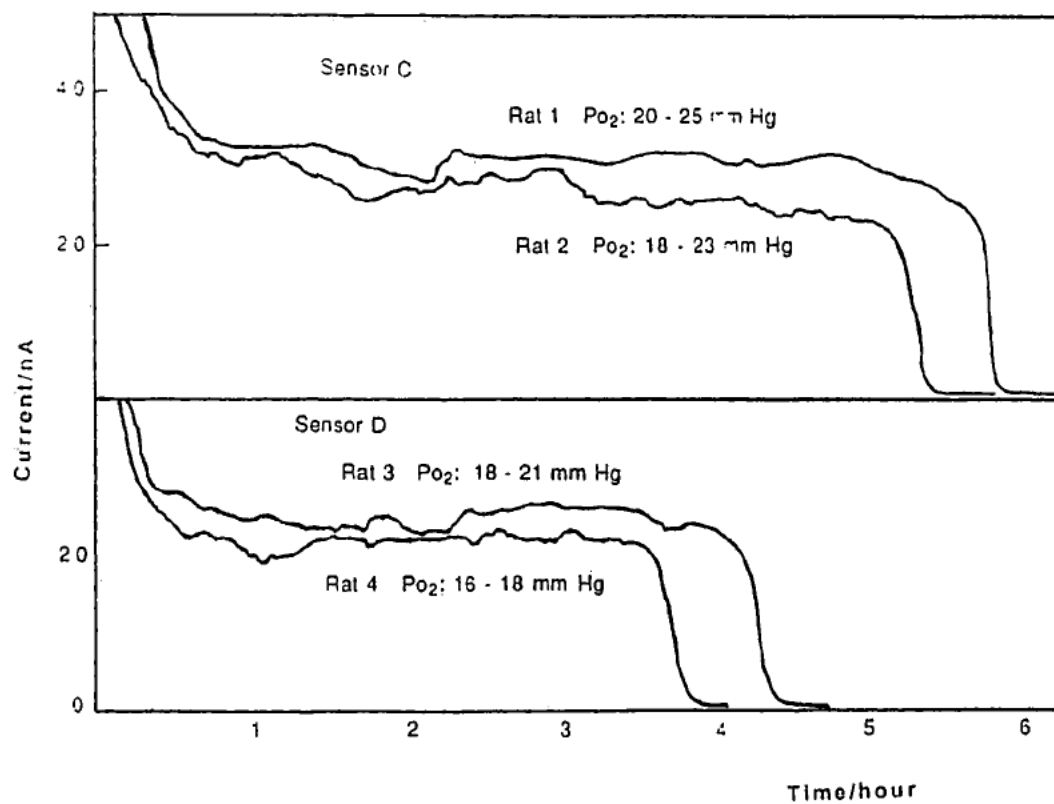
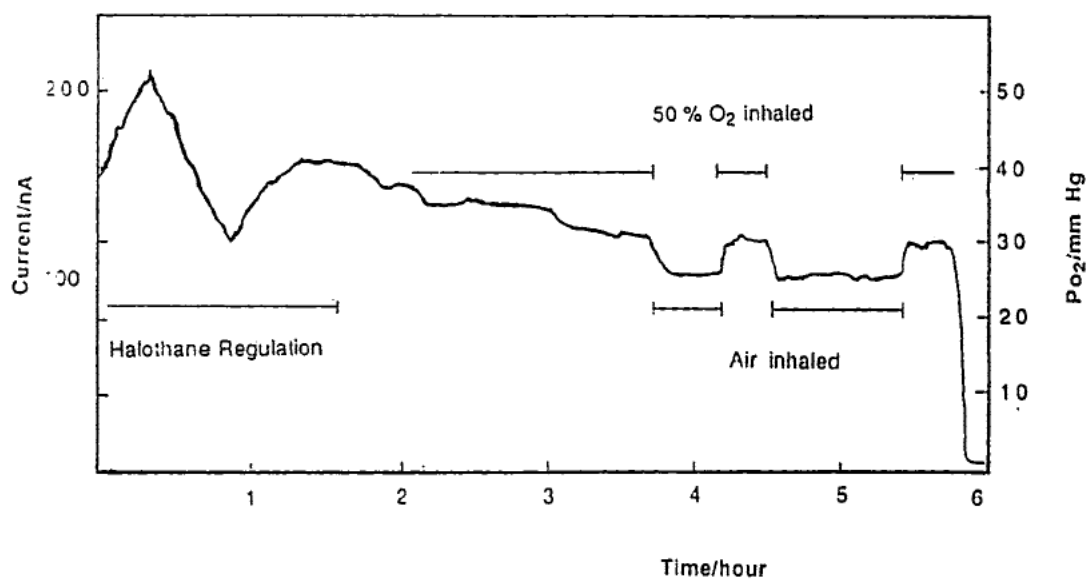**Figure 6-9.** *In vivo* Output of CA+PU Coated Sensors

109

hours when only air was used. An additional oxygen (containing 5 % CO_2) supply was provided which was regulated by a separate flowmeter. A gas mixture of 40 - 60 % O_2 was supplied to the rats and the experiment could be carried out smoothly. The rats could resume normal activities in 3 - 5 minutes when the halothane was stopped even after 8 to 10 hour's anesthesia. With inhalation anesthesia the tissue oxygen level could be changed easily by merely changing the halothane dosage. But the problem with the halothane anesthesia was that the normal oxygen tension was not easy to define because the subjects were not breathing normal air. The oxygen sensor output indicated the tissue oxygen tension anywhere from 15 mm Hg to 60 mm Hg and the tissue Po_2 was closely related to the degree of anesthesia. Figure 6-10 shows a typical sensor output during a 6 hour experiment in which the rat was inhaling air and 50 % O_2 alternatively. The tissue Po_2 during air breathing was around 25 mm Hg and was above 30 mm Hg for oxygen rich gas breathing.

III. *In Vivo* pH measurement

The two-point calibration of the pH sensor gave a fairly reproducible output with a slope of -66 mV/pH. The sensor took about four hours to hydrate from its dry state and the output was very stable thereafter. The drift in output was about 3 mV in ten hours.

The sensor output showed some fluctuation during the first 20 - 30 minutes after implantation and then remained stable for prolonged times. Four measurements were made in different rats. Results for two of the measurements are shown in Figure 6-11. The subcutaneous pH level was stable as indicated by the sensor, varying within the limit of pH 7.4 ± 0.05 range during the entire period of experiment.

The after *in vivo* measurement calibration was carried out vs the same

Figure 6-10. *In Vivo* Output of CA+PU Coated Sensor
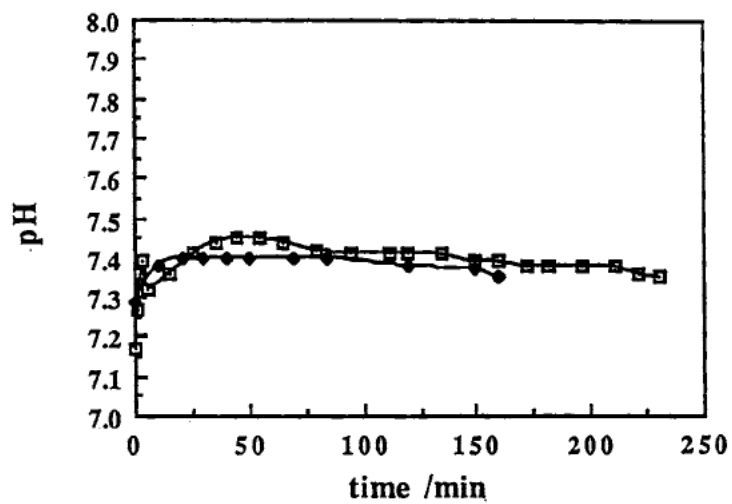
in Halothane Anesthetized Rat

Figure 6-11. *In vivo* Measurement of pH in Rats

112

reference electrode in the pH 7.40 and pH 5.38 buffer solutions immediately after removal of the sensor from the tissue. An identical slope was observed for both before and after the implantation.

Conclusion

The oxygen sensors characterized *in vitro* and tested *in vivo* have shown that this monopolar probe could be used to measure the oxygen availability in the subcutaneous tissue. The cellulose acetate film was able to effectively screen off electrochemical interferences so that the *in vivo* background current was essentially negligible. The polyurethane layer, although was not a good diffusion barrier to interferences, played another useful role to cause delayed hydrogen evolution, which widened the window for oxygen detection. It was also an effective surface modifier to protect the electrode from fouling.

The *in vivo* measurements of Po_2 in rat subcutaneous tissue highlighted the difference between the PU and CA+PU modified sensors. Comparison between Figure 8 and Figure 9 revealed that the measured Po_2 values were lower for PU coated sensors (7 - 14 mm Hg). This is because the polyurethane film was more permeable to oxygen which resulted in excessive oxygen consumption and a more pronounced gradient was created at the sensor surface. The sensors, therefore, experienced a lowered oxygen tension. The CA+PU coated sensor, on the other hand, had better performance *in vitro* as was shown in Figures 4, 5 and 7. Its *in vivo* application was also satisfactory due to its low background feature. The output of these sensors in Figures 9 and 10 were within the range of 16 - 27 mm Hg for air breathing rats. This was in good agreement with documented values (Cater, 1966; Jamieson, 1965).

Many authors have discussed the issue that high oxygen consumption can cause lower result because the rate of oxygen supply to the tissue is lower than the rate

of sensor consumption. A gradient of Po_2 will be extended into the tisssue and the sensor experiences a lowered oxygen level. Observation for this specific design and size concluded that an *in vivo* output higher than 250 nA was likely to yield significant error. This necessarily requires that the sensor sensitivity should be under 10 nA/mm Hg. Usually the sensitivity can be conveniently controlled by changing the electrode surface area (the length of the sensing cavity) and the thickness of the cellulose acetate membrane. The thickness of the polyurethane membrane essentially does not affect the sensitivity due to its high permeability to oxygen.

The tissue oxygen profile is uneven as was first proposed by Krogh (Krogh,1918) and later proved experimentally by others (Silver,1966; Metzger, 1973). The capillaries in the tissue have an average diameter between 10 to 30 microns and an average distance of 100 to 200 microns. The oxygen tension has a maximum value at the wall of the capillary and decreases to minimum somewhere between two adjacent capillaries. This oxygen gradient in tissue can be measured only with sensors of a few microns diameter. Larger sensors (>30 μ) can measure only the average tension which has been shown to be stable. The measurements in this investigation did not give an accurate indication of Po_2 at the point of implantation, but rather a measure of oxygen availability averaged through distance and time, which is indeed the purpose of this work.

The level of oxygen measured with oxygen sensors has also much to do with the sensor size for reasons other than the averaging effect discussed above. Jamieson and Vanden Brenk reported that 60 μ sensors yielded 23 $\pm$ 3 mm Hg (n = 33) while 330 μ sensors gave 31 $\pm$ 2 mm Hg (Jamieson,1965). The authors ascribed this phenomenon to excessive damage to the capillaries introduced by larger sensors. More oxygen supply was therefore available to the larger sensors than to smaller ones.

114

The observation in our experiments gave an approximate subcutaneous tissue P_{O_2} range of 21 $\pm$ 5 mm Hg (250 μ sensor, n= 18) for air breathing rats. This was much lower than the reported value in dogs (Fischer, 1989, 800 μ sensors, 54 $\pm$ 13 mm Hg). Although there was difference between animal species and the state of anesthesia, the size effect could still exist.

Because the oxygen availability is closely related to the sensor size, the oxygen dependent glucose sensor will also have a size limitation. A very small sensor (e.g. less than 20 μ) could have oxygen deficiency and malfunction simply because it is implanted at a low P_{O_2} point in the tissue. This question was in fact raised by some early investigators (see Discussion Section, Clark, 1973). To ensure the proper functioning of the glucose sensor, the sensor must be large enough to achieve a distance averaged oxygen supply. The size of a glucose oxidase based sensor, therefore, cannot be reduced infinitely.

Chapter 7. *In Vivo* and *In Vitro* Evaluation of Oxygen Effects on a Glucose Oxidase Based Implantable Glucose Sensor

Abstract

The oxygen effect on the needle-type glucose sensor was evaluated both *in vitro* and *in vivo* by simultaneously measuring glucose and oxygen with glucose and oxygen sensors developed in this laboratory. Glucose sensors of high sensitivity were found to be oxygen dependent while low sensitivity sensors were essentially not affected by fluctuation in P_{O_2} at normal tissue oxygen levels. This study demonstrated that for amperometric implantable glucose sensors high sensitivity is not a required feature and sensitivity control is crucial for the reliable functioning of the sensor.

Introduction

An implantable needle-type glucose sensor has been developed in our laboratories and its performance has been characterized intensively both *in vitro* (Bindra,1991) and *in vivo* (Moatti,1991; Poitout,1991). Studies concerning the *in vivo* environment in the subcutaneous tissue have been also undertaken to further understand the physiological situation around the implanted sensor and the interactions between the tissue and the sensor.

It is generally understood that the process of tissue response to an implanted foreign object (depending on the degree of tissue damage) includes inflammation, immune response and wound healing (Black,1981). Changes in local pH, P_{O2}, electrolyte concentration and rate of metabolism are also expected. From a physiological point of view, there could be a concentration gradient at the interface due to changes in microcirculation. Merely decreasing the sensor consumption will not improve the sensor performance because it is not a problem of consumption vs supply. This is in fact an inflammation phenomenon and should be considered as a

biocompatibility problem. To reduce those effect the sensor size and proper method of implantation are very important.

Since the glucose oxidase based sensor requires oxygen as the co-substrate to carry out the glucose oxidation, oxygen supply can influence sensor output. It is therefore important to examine the tissue oxygenation and its effect upon the *in vivo* performance of the sensor. This approach necessitates understanding of the balance between the absolute demand for oxygen by the sensor and the relative availability of oxygen in the physiological environment.To meet the needs of oxygen measurement in subcutaneous tissue, a needle-type oxygen sensor has been constructed and its characterization and *in vivo* oxygen measurement have been conducted (Chapter 6).

The method of *in vitro* calibration of oxygen sensors, for *in vivo* measurements, is subject to some serious limitations. Since the oxygen solubility in the solution is affected by many factors as discussed in Chapter 6, it is not practical to simulate the physiological fluid by mixing known species together and assuming that a measurement in such a medium is valid. This approach, in reality, raises more problems than it solves because organic species, especially proteins, alter the solution viscosity which causes changes in oxygen diffusion coefficient. For example, addition of 2.5 % serum proteins to the buffer caused a 15 % decrease in sensor response, which was verified to be due to the increase in viscosity instead of decrease in oxygen solubility (Cater, 1960). The difference between the *in vitro* and *in vivo* calibration, however, will be ignored in this study because the problem of solution viscosity has been minimized (Chapter 6) and our goal is to evaluate the oxygen demand by the glucose sensor and the availability of oxygen in the subcutaneous tissue. Comparison is based on the assumption of the same oxygen sensor sensitivity in both *in vitro* and *in vivo* measurements. Even an error of 10 % will still give reasonable conclusion, e.g. 20 $\pm$ 2 mm Hg in oxygen partial pressure is accurate enough to evaluate the

performance of the glucose sensor.

This chapter deals primarily with the oxygen effect on the glucose sensor. Simultaneous measurements of glucose and oxygen were conducted both *in vitro* and *in vivo* with glucose and oxygen sensors that had identical geometries and sizes. Since the sensor size is larger than the average capillary distance, the measured P_{O_2} should be stable and reproducible in similar tissue. It has been observed previously (Chapter 6) that the oxygen partial pressure in nearby tissue was similar because of the averaging effect so that an oxygen sensor implanted next to the glucose sensor could reflect approximately the oxygen availability to the glucose sensor.

Experimental

(I). Glucose and Oxygen Sensor Construction

Glucose sensor fabrication has been reported earlier (Chapter 3). The electrode is a Pt-Ir (10 % Ir) wire of 0.17 mm diameter. The sensing layer consists of a cellulose acetate inner membrane, an enzyme layer of glucose oxidase crosslinked with glutaraldehyde and an outer membrane of polyurethane. The sensor sensitivity is essentially controlled by the thickness of the outer membrane. The overall diameter is 0.25 mm for the sensing element and 0.45 mm including the reference element. The oxygen sensor has the same configuration as the glucose sensor except that the enzyme-glutaraldehyde layer is eliminated (Chapter 6). The oxygen sensor had a typical sensitivity of 2 - 7 nA/mm Hg when calibrated in pH 7.4 phosphate buffer.

(II). *In vitro* Study

A closed-single compartment cell with the capacity of 20 ml of solution and a similar volume for the gas phase was used. Experiments were performed in 0.15 M phosphate buffer of pH 7.4 containing 0.15 M NaCl with 0.1 % NaN_3 as the

preservative. Oxygen equilibrium in the cell was achieved by bubbling the buffer with an air N$_2$ mixture whose ratio was regulated by two separate flow meters (Cole Parmer, Chicago, IL) at a flow rate of approximately 100 ml / min while the solution was stirred constantly. The whole unit was submerged in a 37 ^{o}C water bath (Fisher, Isotemp, Refrigerated circulator, Model 900). Both glucose and oxygen sensors were installed in the cell each with its own Ag/AgCl reference electrode and Pt wire counter electrode. The output was monitored with BAS (BioAnalytical Systems Inc.) LC-4A Amperometric Detectors and recorded with Kipp & Zonen BD-40 chart recorders.

To correct for the volume error caused by buffer evaporation, the gas mixture was bubbled through two separate mixing bottles containing phosphate buffer at 37 ^{o}C before being introduced into the cell chamber. Calibration of the oxygen sensor was also performed similarly in the absence of the glucose sensor.

(III). *In vivo* Study

A Sprague Dawley rat (body weight 350 - 450 g) was anesthetized with halothane through inhalation and placed on a thermostated plastic cushion which had constant circulation of 37 ^{0}C water. The top portion of the body was illuminated with a table lamp of 100 W to warm the body surface which had been observed otherwise to decrease in temperature after prolonged anesthesia and leading to hypoxia. Anesthesia from 4 to 10 hours was maintained by regulating a gas mixture of air and O$_2$ bubbling through halothane. The body oxygen level was also controlled by feeding the rat with different air : O$_2$ ratios.

Glucose and oxygen sensors were implanted through a 20 Gauge catheter into the subcutaneous tissue on the back of the neck and the output of glucose sensor was monitored at 600 mV vs Ag/AgCl constant potential. Oxygen sensor output was monitored at -550 mV. The output of the two sensors were recorded simultaneously

with chart recorders.

Both sensors were calibrated before and after the *in vivo* experiments as stated above in the Experimental Section.

Results and Discussion

In Vitro Experiment

18 sensors were fabricated purposely to possess different sensitivities and linearities in order to test their oxygen effect. Generally, high sensitivity denotes >3.0 nA/mM and low sensitivity corresponds to the range of 0.5 - 1.5 nA/mM. *In vitro* measurements were performed in the closed electrochemical cell with three sensors (two glucose and one oxygen sensors) and each sensor had its own amperometric detector and chart recorder. The environment for all the sensors was thus identical and the two glucose sensors experienced the same P_{O2} in the same buffer solution. Comparison between different sensors could therefore be made with confidence.

Figure 7-1 shows the i - C curves of two sensors measured under different oxygen tensions. Sensor A had a sensitivity of ~ 5 nA/mM and a dynamic range of ~ 8 mM glucose in air saturated buffer. Sensor B was linear up to 30 mM glucose in air saturated buffer and sensitivity of 0.58 nA/mM. It is clearly shown that sensor A was quite oxygen dependent while sensor B was affected little by oxygen. At a glucose concentration of 15 mM, for example, the change in sensor B output was only 5% when P_{O2} changed from 150 mm Hg to 7.6 mm Hg. On the contrary, sensor A had a 30 % decrease in current due to the same P_{O2} change.

To further clarify the relationship between sensor sensitivity and oxygen effect, the system was first equilibrated with air and the baselines of the glucose sensors were stabilized. Two consecutive injections of glucose were made, with each injection giving 5 mM concentration in the system, to create a total glucose
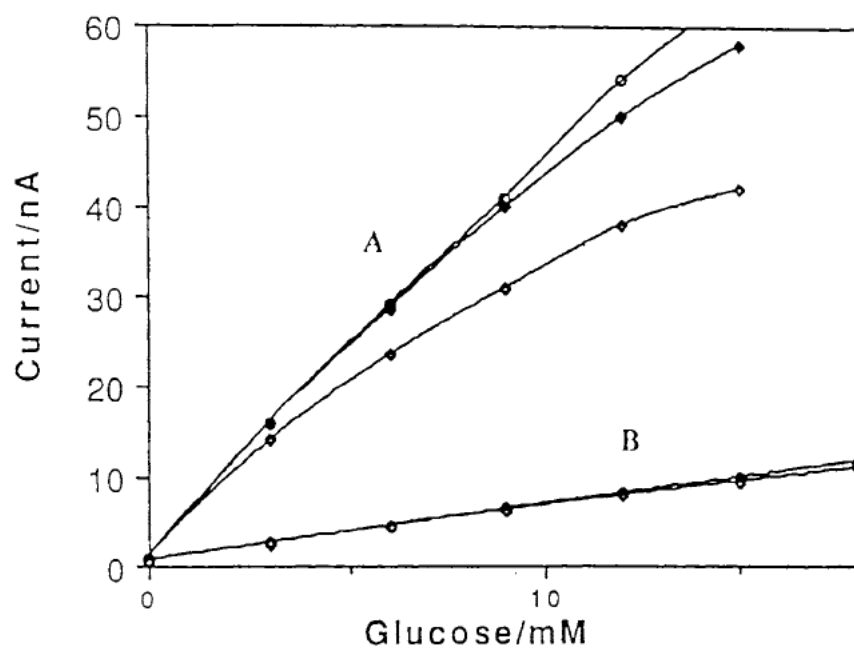
Figure 7-1. Oxygen Effect on Sensors of Different Sensitivity

A. High sensitivity; B. Low sensitivity
Po_2 changes: 150, 40, 8 mm Hg

concentration of 10 mM which was 3 - 5 mM higher than the normal blood glucose level. When the glucose sensors assumed stable current, a smooth stream of N_2 gas was introduced into the solution to reduce the oxygen tension. This process was carried out slowly and the solution was constantly stirred to ensure the oxygen equilibrium throughout the cell. The oxygen partial pressure was monitored with the oxygen sensor. After the oxygen effect was observed at a low P_{02} level, the N_2 flow was partly shut down to allow a gradual build-up of oxygen in the system, which enabled the glucose sensors to resume normal functioning. The numerical values of the oxygen sensor output on the amperometric detector LCD was also recorded simultaneously in order to obtain an accurate P_{02} value at very low oxygen tension (as illustrated in Figure 7-2A). Figure 7-2 is one of the typical data sets observed in the above experiment. Figure 7-2A is the oxygen partial pressure obtained with a calibrated oxygen sensor. Figure 7-2B is the direct current output of a low sensitivity glucose sensor (0.94 nA/mM; linearity, 25 mM) responding to 10 mM glucose and Figure 7-2C is the output of a high sensitivity glucose sensor (3.2 nA/mM; linearity, 12 mM). It is interesting to note that in Figure 4b the sensor did not exhibit any oxygen effect until the oxygen tension dropped to 5 mm Hg which indicated that this value was the critical point for this sensor. This value was confirmed again when P_{02} rose to 5 mm Hg. The sensor started to function at that point and quickly turned over the accumulated glucose which had been trapped inside the enzyme layer due to the lack of O_2 supply, giving a peak current and then resuming the normal steady state current. The high sensitivity sensor in Figure 7-2C had similar behavior except that the current began to decrease at much higher oxygen tension. It occurred around $P_{02} = 12$ mm Hg.

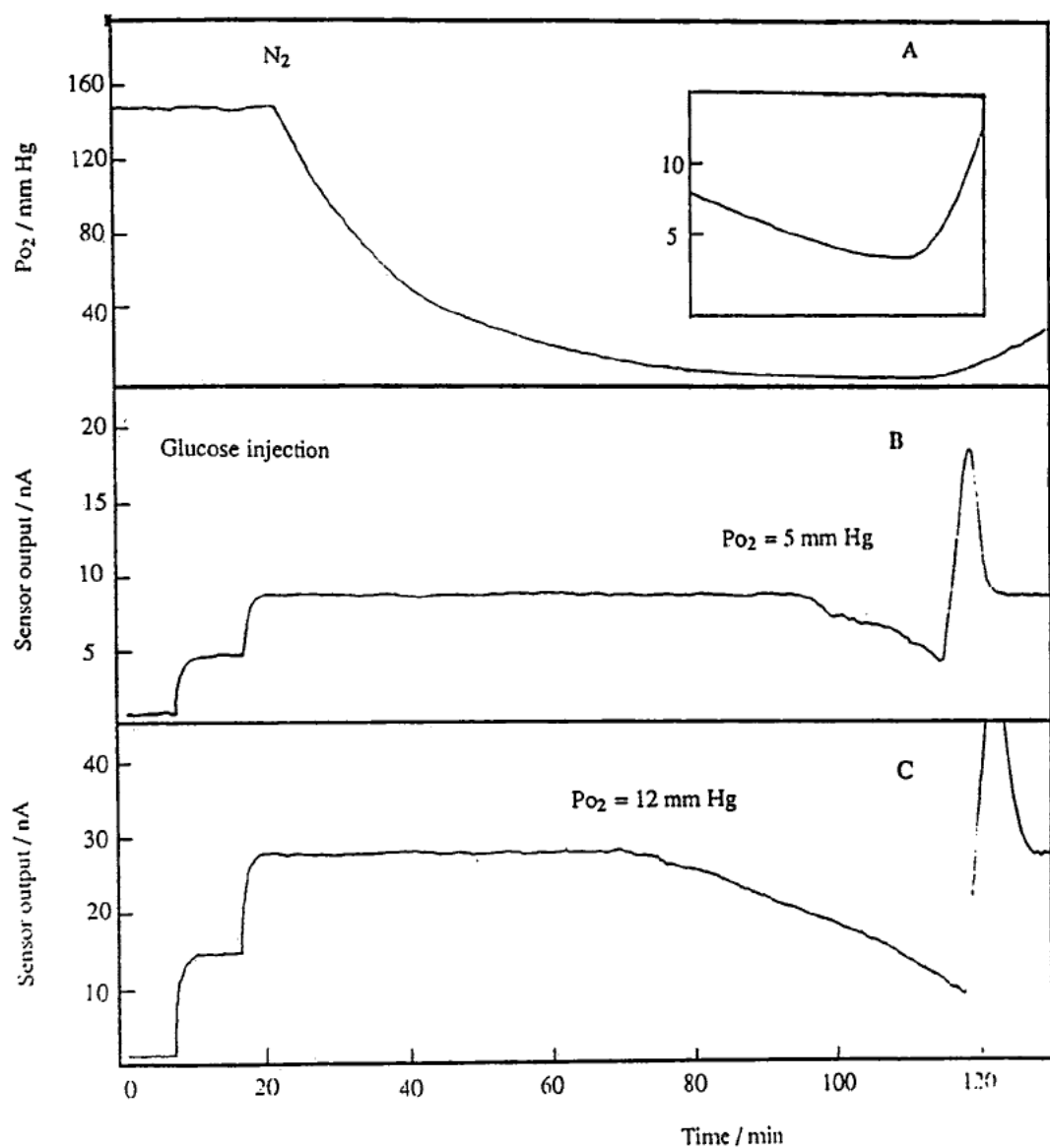Table I gives the characteristics of 9 glucose sensors and their corresponding

Figure 7-2. Oxygen Effect on Sensors of Different Sensitivity

A. Po₂ in the System; B. Low sensitivity Sensor;
C. High sensitivity Sensor

critical P_{02} values, from which a general rule can be drawn to ensure the proper functioning of the glucose sensors. The sensor sensitivity should not be higher than 2 nA/mM; The sensor linearity should be higher than 12 mM and under no circumstances should the sensors be used at $P_{02} < 7$ mm Hg.

Table I. Critical P_{02} Values vs Sensitivity and Linearity

# of sensor	1	2	3	4	5	6	7	8	9
Sensitivity (nA/mM)	0.54	0.90	0.94	1.1	2.5	2.6	3.2	4.0	5.4
Linearity (mM)	30	25	25	20	12	13	12	7	8
Critical P_{02} (mm Hg)	3	6	5	8	16	17	12	30	40

In Vivo Experiment

Glucose sensors of different sensitivities and linearities were implanted in rat subcutaneous tissue and oxygen sensors were implanted parallel to the glucose sensors about 2 cm apart from each other. One glucose sensor and one oxygen sensor were implanted in each rat. A total of 12 glucose sensors were tested in rats. Glucose sensors having high sensitivity were observed to have oxygen dependence. Figure 7-3 shows one of those extremes which were totally dependent on the tissue oxygen fluctuation. This sensor shown in Figure 7-3B had an *in vitro* sensitivity of 4.0 nA/mM (Sensor sensitivity denotes only the *in vitro* sensitivity because *in vivo* sensitivity is different (Velho, 1989; Moatti,1991)) and dynamic range of 0 - 7 mM. Other linear sensors with linearity higher than 12 mM and sensitivities less than 2 nA/mM were not observed to have oxygen dependency. Figure 7-4 illustrates a typical example in which three sensors (two glucose and one oxygen sensors) were simultaneously monitored in order to compare the difference between linear and non-
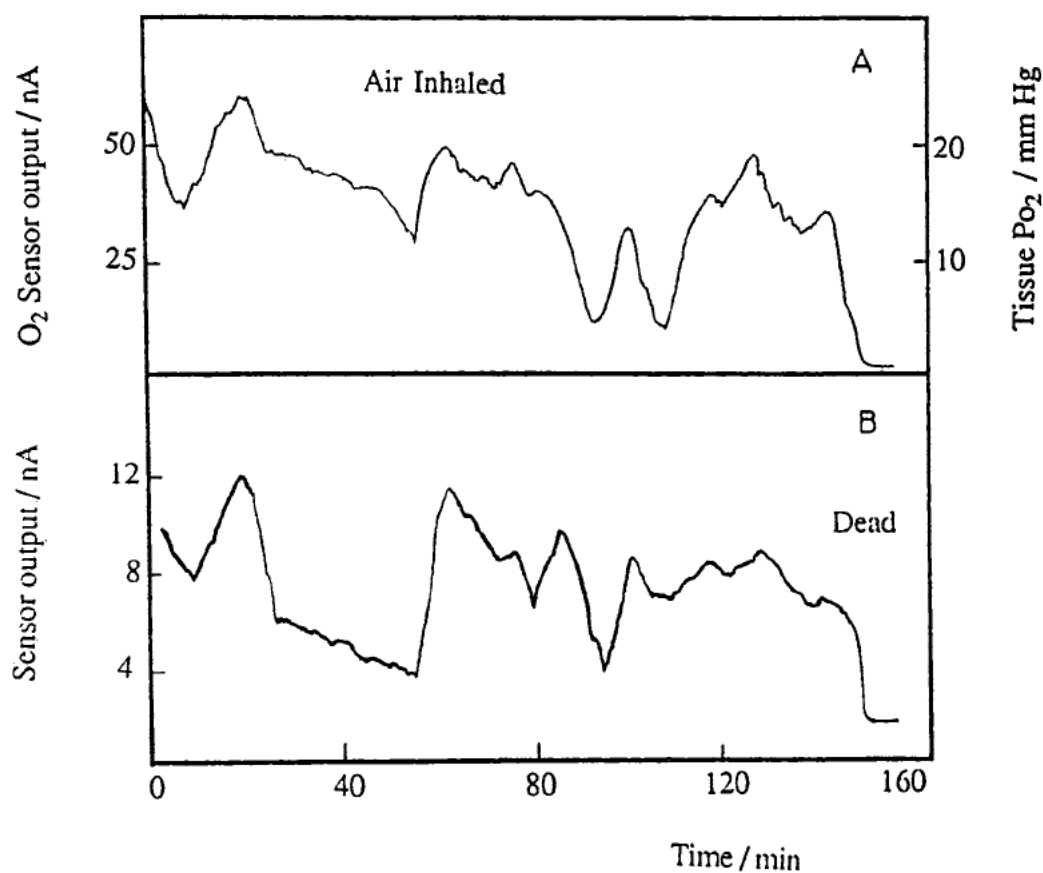
Figure 7-3. *In Vivo* Response of a High Sensitivity Sensor

A. Oxygen Sensor Output; B. Glucose Sensor Output

linear sensors under identical oxygen conditions. Figure 7-4A is the response of the oxygen sensor. The fluctuation in P_{02} level was manipulated by changing the composition of the air/O_2 mixture inhaled by the rat through the mask. The oxygen level of air inhalation corresponded to ~ 20 mm Hg in the subcutaneous tissue. The oxygen level was equivalent to 26 - 30 mm Hg when the rat was inhaling 60 % oxygen. It should be pointed out, though, that the tissue oxygen level is affected by the amount of anesthetics administered The tissue oxygen level can be altered by merely changing the flow of halothane while keeping the air/O_2 ratio constant. Figure 7-4B shows the output of a non-linear sensor (2.2 nA/mM; linearity, 6 mM) while Figure 7-4C is that of a linear sensor (1.1 nA/mM; linearity 12 mM). Figure 7-4D shows the corresponding blood glucose change measured *in situ* with a Boehringer Mannheim Accu-Chek IIm blood glucose test kit. The blood sample was drawn from the end of the rat's tail.

The *in vivo* oxygen effect on the sensor was also demonstrated by an experiment shown in Figure 7-5. Figure 7-5A is the tissue oxygen and Figure 7-5B is the glucose sensor output and Figure 7-5C the blood glucose. Two injections of 30 % d-glucose were administered ip during the experiment and the glucose level was reflected by the sensor while no oxygen effect was observed. In order to obtain the critical P_{02} value the rat was sacrificed at the end by increasing the dose of halothane, which was followed by a sharp decrease in tissue oxygen. As soon as the oxygen effect was observed at the glucose sensor, oxygen was quickly supplied to the rat through the mask and the tissue oxygen returned instantly to its original level, a condition which lasted for a few more minutes. This manipulation left a small defect in the glucose sensor curve (Figure 7-5B) and a critical point of P_{02} for this sensor was determined to be ~ 8 mm Hg.
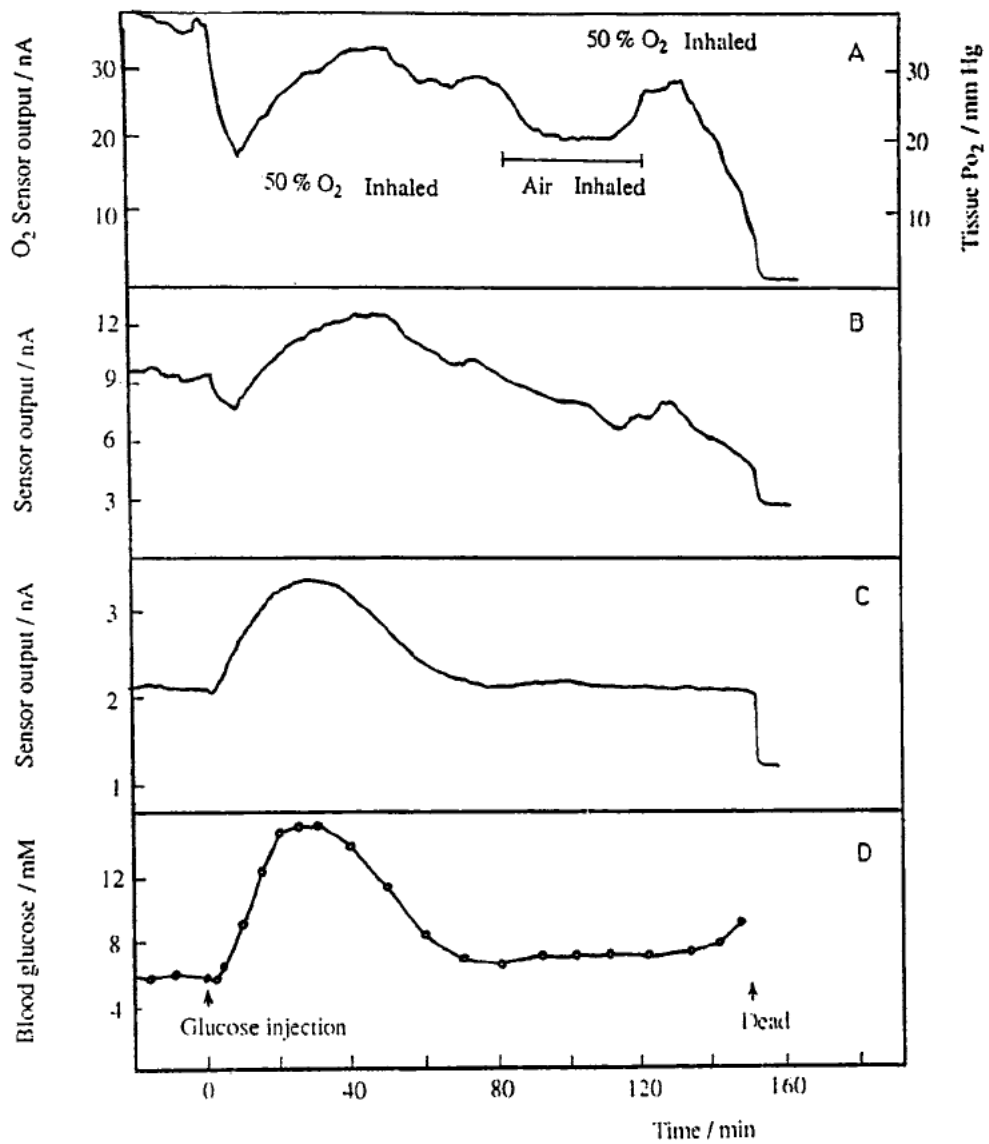
Figure 7-4. *In Vivo* Performance of Glucose Sensors of Different Sensitivity

A. Oxygen Sensor Output;   B. High Sensitivity Sensor Output.
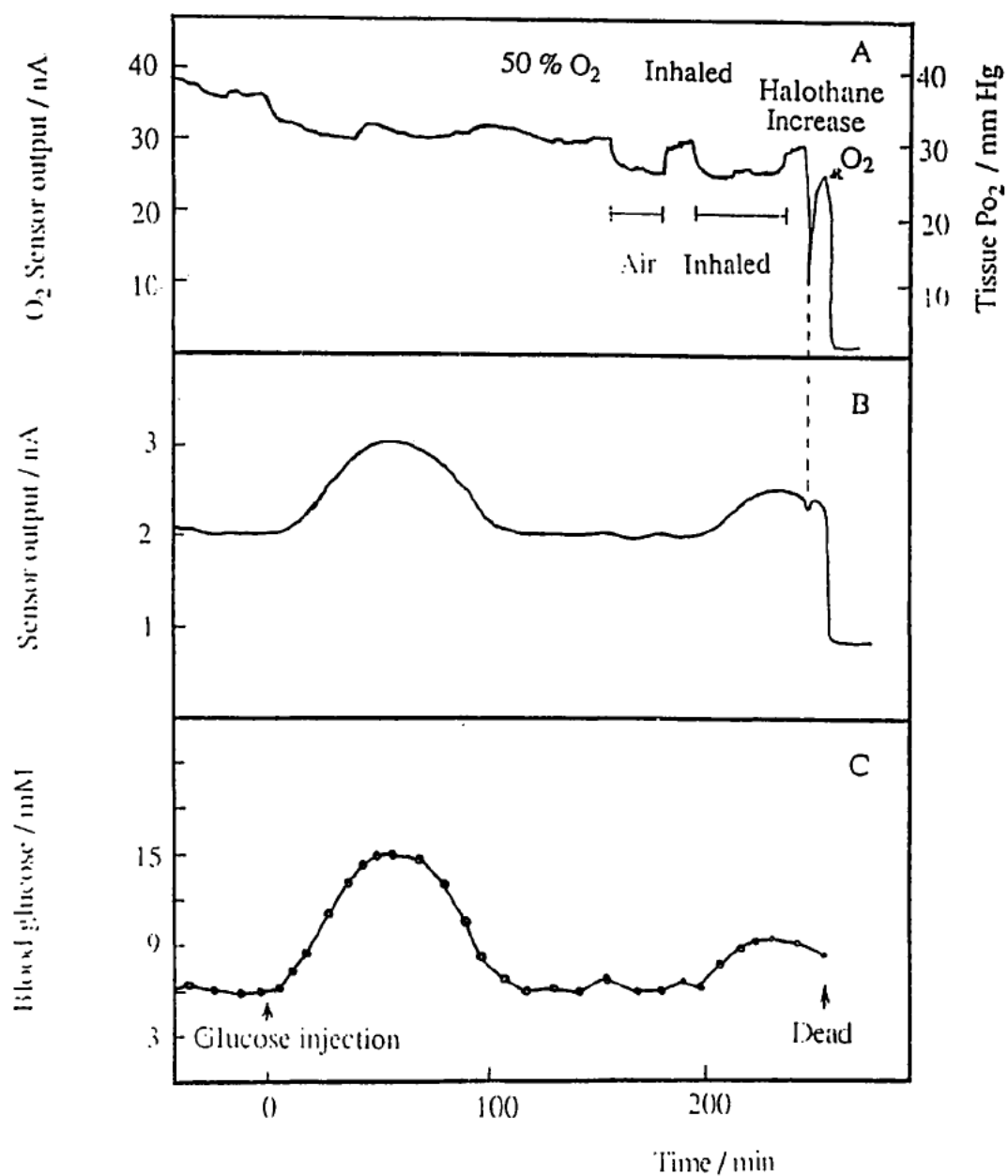C. Low Sensitivity Sensor Output, D. Plasma Glucose

Figure 7-5. Critical Po₂ Point Measurement *In Vivo*

A. Oxygen Sensor Output;   B. Glucose Sensor Output;
C. Plasma Glucose.

128

Conclusion

The oxygen dependence of the glucose sensors, as has been demonstrated in this experiment, can be designed to fit the requirement for *in vivo* implantation. The demand for oxygen by the sensor is primarily determined by its sensitivity because the absolute current output is a direct measure of the rate of the catalytic reaction and therefore oxygen consumption. The oxygen effect can also be less significant when the enzymatic reaction rate is much faster than glucose mass transfer through the outer membrane. This is the case for linear sensors. A slight fluctuation in oxygen partial pressure will not affect the glucose diffusion controlled process and a linear response is maintained.

The criteria for an *in vivo* type glucose sensor with given geometry and surface area are thus set as the following: (a) The sensitivity should be kept in the 0.5 - 2.0 nA/mM range; (b) The dynamic range should be at least 0 - 15 mM in air saturated buffer and (c) the sensors should not be used in the situation where the oxygen tension is below 7 mm Hg.

Sensors with *in vitro* sensitivity of 2 - 3 nA/mM have been observed to exhibit oxygen dependence in the 10 - 13 mm Hg oxygen range. Although this value is not expected in normal subcutaneous tissue (common observation for rat subcutaneous tissue is 23 ± 3 mm Hg (Cater (1966) and in this report (Fig 7-4 &7- 5) P_{02} between 20 and 30 mm Hg), heterogeneity of tissue environment must be considered because local P_{02} level can be perturbed by trauma and inflammation.

All the *in vivo* tests were conducted with anesthetized rats. The subcutaneous P_{02} was constantly monitored while the air : O_2 ratio and the dosage of anesthetic were adjusted. In deep anesthesia, air breathing rats had typical oxygen levels of 17 - 25 mm Hg. Rats breathing high content oxygen (60 % O_2) usually had the value above 30 mm

Hg. Lightly anesthetized rats, however, showed larger fluctuations and higher levels of oxygen in the range of 30 - 50 mm Hg when fed with high oxygen gas. From these experiments and other reports (Fischer, 1989) it is expected that conscious animals will have slightly higher oxygen levels which is more favorable for the oxygen dependent glucose sensor.

Chapter 8. Future Directions

A series of investigations of the implantable glucose sensors have been carried out , starting from the basic signal transducing process, the electrooxidation of H_2O_2, through sensor fabrication, *in vitro* and *in vivo* characterization, initial toxicity screening and the evaluation of oxygen influence on the sensor functioning. A needle-type tissue oxygen sensor was also developed and characterized during this process. We have been able to provide quantitative control for the fabrication of the miniature sensors and a success rate of higher than 80 % was achieved. The G3 sensor has been shown to function reliably in rats for up to twenty days while the G6M sensor provided a potential device for direct implantation by the patients.

The small size and the overall cylindrical geometry of this sensor seems to be responsible for the good *in vivo* performance because the inflammation and consequent encapsulation have been shown not to "blind" the sensor. On the contrary normal tissue reactions in fact stabilize the surrounding physiological environment and help to realize constant sensor *in vivo* sensitivity.

The method of ethylene oxide sterilization was demonstrated to be compatible with dry storage. The process of manufacturing can therefore be commercialized (or automated) to meet the requirement of industrial production. The sensor can be prepared, stabilized, sterilized and packed. A slight modification will be made to the sensor design in order to meet the requirement for human test. Figure 8-1A illustrates the overall configuration of the sensor packed in a sterile envelope. The reference electrode which is a wrapped 0.05 mm Ag wire covers majority of the sensor body. There is no lead wire connected to the Pt/Ir electrode to keep the overall diameter (0.35 mm) uniform. This sensor is incorporated into a thin wall 23 Gauge needle which is
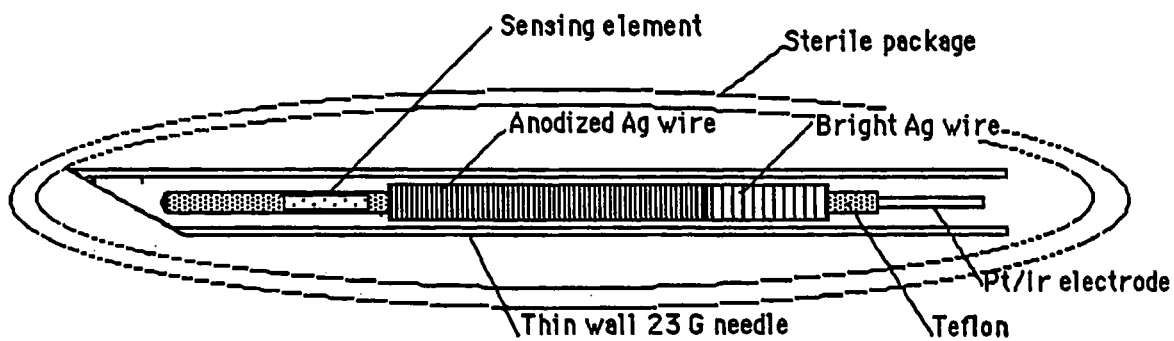
A. Sterile Package of the Sensor in a 23 G Needle
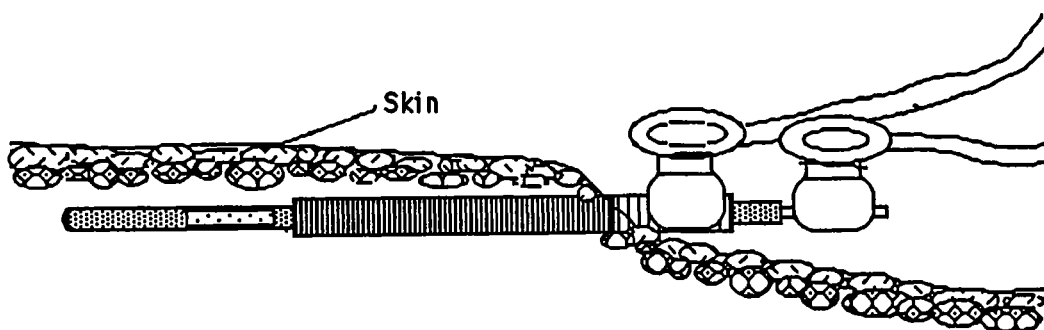
B. Sensor Implanted in Tissue

Figure 8-1. The Sensor Design, Packaging and Implantation for Human

132

directly sterilized and packed. Implantation can be made directly by inserting the needle into subcutaneous tissue and pulling it out, leaving the sensor in the tissue. The exposed Ag wire wrap and the Pt/Ir end are connected to the monitor unit with two mini clamps as shown in Figure 8-1B and continuous monitoring is conducted.

The major disadvantage of implanted sensors seems to be the rather long run-in time (3-5 hours). Initial study in Chapter 4 indicated that the sensitivity decrease was one of the reasons and it was presumably caused by surface adsorption. There are two possible strategies to deal with this problem. One is to modify the polyurethane surface with more compatible materials to reduce the degree of tissue reaction. The other is to use long width pulses to alternatively polarize the electrode to get rid of possible adsorption induced by the electrical field.

The first application of this sensor is to serve as an alarm system for hypoglycemia which is an immediate threat to diabetics. A portable monitoring unit has been developed and the hypoglycemic alarm device will be expected without major obstacle. The final goal of the sensor, the artificial pancreas, will depend on the effectiveness of glycemia regulation by the automatic insulin delivery driven by the sensor output and especially the reliability of the sensor.

References

Abel,P., Miller,. A. and Fischer, U., (1984), **Biomed. Biochim. Acta., 5**, 577.

Adams,R.N.,(1969), "**Electrochemistry at Solid Electrodes**", Marcel Dekker, NY.

Albisser, A.M., Leibel, B.S., Ewart, G., Davidovac, Z., Botz, C.K., Zingg, W., (1974), **Diabetes, 23**, 389.

Armour, J. C., Lucisano, J.Y., McKean, B.D. and Gough, D.A., (1990), **Diabetes, 39**, 1519.

ASTM, (1988). **Annual Book of ASTM Standards,** Vol. 13.01, Medical Devices, American Society for Testing and Materials, Philadelphia, PA., F 813-83, , pp. 262-5 and F 895-84, pp. 276-9.

Autian, J. (1975). Biological Model Systems for the Testing of the Toxicity of Biomaterials, In **Polymers in Medicine and Surgery**, Kronenthal,R.L., Oser,Z. & Martin,E., eds, Plenum Press, NY, pp.181.

Bard,A.J. and Faulkner,L.R., (1980), **Electrochemical Methods, Fundamentals and Applications**, John Wiley & Sons, NY.

Baumgartl,H. and Lubbers, D.W., (1983), in **Polarographic Oxygen Sensors**, Gnaiger, E. and Forstner, H. eds, Springer-Verlag, Berlin.

Bessman, S.P., Thomas, L.J., Kojima, H., Sayler, D.F. and Layne, E.C., (1981). **Trans. Am. Soc. Art. Int. Org. 27**, 7.

Bicher,H.I. and Kinsely,M.H., (1970), **J.Appl.Physiol., 28**, 3,387.

Bindra,D.S., Zhang,Y., Wilson,G.S., Sternberg,R., Thevenot,D.R., Moatti,D. and Reach,G., (1991), **Anal.Chem.**, in press.

Black, J, (1981). **Biological Performance of Materials**, Marcel Dekker Inc., NY.

Bockris,J.O'M. and Oldfield,L.F.(1955) **Trans.Faraday Soc., 51**, 249.

Boretos,J. W., (1973). **Concise Guide to Biomedical Polymers**, Charles C. Thomas, Springfield, IL.

Brown, S. A., ed. (1983). **Cell Culture Test Methods**, ASTM STP 810, Philadelphia, PA.

Bruck, S. D., (1980). **Properties of Biomaterials in the Physiological Environment**, CRC Press,Inc., Boca Raton, Florida.

Bruck, S.D., (1974).**Blood Compatible Synthetic Polymers**, Charles C. Thomas, Springfield, IL.

Bruck, S. D., (1971), **J. Biomed. Mater. Res., 5**, 139.

Brunstein,E., Abel,P., Gens,A., Eich,K. and Woedtke,T.V., (1989), **Biomed. Biochem. Acta., 48**, 11/12, 911.

Caligara,F. and Rooth,G, (1961), **Acta Physiol. Scand., 53**, 114.

Cater,D.B., Phillips,A.F. and Silver,I.A., (1957), **Proc. Roy. Soc. B, 146**, 289.

Cater.D.B., Silver,I.A. and Wilson,G.M., (1959), **Proc. Roy. Soc. B, 151**, 256.

Cater,D.B., Garattini,S. Marina,F. and Silver,I.A., (1962), **Proc. Roy. Soc. B, 155**, 136.

Cater,D.B., Hill,D.W., Lindop,P.J., Nunn,J.F. and Silver,I.A., (1963), **J. Appl. Physiol. 18** (5) 888.

Cater,D.B., (1963), "The Measurement of P_{02} in Tissue", in **Oxygen in the Animal Organism**, Dickens,F and Neil,E., eds., The MacMillan Co.

Cater,D.B., (1966), "The Significance of Oxygen Tension Measurements in Tissue", in **Oxygen Meassurements in Blood and Tissue**, Payne,J.P. and Hill,W. eds., J&A. Churchill Ltd.

Chialvo,A.C., Triaca,W.E. and Arvia,A.J.,(1983), **J.Electroanal.Chem., 146**, 93.

Claremont,D.J., Sambrook,I.E., Penton,C., and Pickup,J.C., (1986) **Diabetologia, 29**, 817-852.

Clark,L.C.Jr., Wolf, R., Granger,D. and Laylor, Z., (1953), **J. Appl. Physiol., 6**, 189.

Clark,L.C.Jr., (1956), **Trans.Am.Soc.Artif. Intern.Organs., 2**, 41.

Clark,L.C.Jr. and Clark,E.W., (1973), " Differential Anodic Enzyme Polarography for the Measurement of Glucose " in **Oxygen Transport to Tissue**, Bicher and Bruley, eds, Plenum Press.

Clark, L.C. Jr. and Duggan, C.A., (1982), **Diabetes Care, 5**, 174.

Crawford,D.W. and Cole,M.A., (1985), **J.Appl.Physiol., 58**(4) 1400.

Davis,P.W. and Brink,F., (1942), **Rev.Scient. Instr., 13**, 524.

135

Fatt,I., (1964), **J.Appl.Physiol., 19.** 2, 326.

Fatt,I., (1976), **Polarographic Oxygen Sensors:** Its Theory of Operation and Its Application in Biology, Medicine, and Technology, CRC Press.

Fischer,U., Hidde,A., Herrman,S., Woedtke,T.V., Rebrin,K and Abel,P., (1989), **Biomed. Biochem. Acta., 48,** 11/12, 965.

Freshney,R.I., (1988). **Culture of Animal Cells:** A Manual of Basic Technique, Alan R. Liss, Inc., NY.

Galloway, J.A., Potvin, A.H. and Shuman, C.R. eds, **Diabetes Mellitus,** (1988), Eli Lilly and Co., Indanaplis, IN.

Geise,R.J., Adams,J.M., Barone,N.J. and Yacynych,A.M., (1991) **Biosensors & Bioelectronics, 6,** 151.

Gnaiger,E and Forstner,H.,(1983), **Polarographic Oxygen Sensors.** Aquatic and Physiological Applications, Springer-Verlag.

Gough, D.A., Armour, J.C., Lucisano, J.Y., Brian, D.M., (1986), **Trans. Am. Soc. Int. Org., 32,** 148.

Hitchman,M.L., (1978), **"Measurement of dissolved oxygen"**, John Wiley & Sons.

Hitchman,M.L.,(1983), in **Polarographic Oxygen Sensors,** Gnaiger, E. and Forstner, H. eds, Springer-Verlag, Berlin.

Hoare,J.P., (1968), **The Electrochemistry of Oxygen,** John Wiley & Sons, Inc.

Hoare,J.P., (1974), "Oxygen", in A.J.Bard,ed., **"Encyclopedia of Electrochemistry of the Elements"**, Vol. II, II-5, Marcel Dekker, NY.

Hoare,J.P., (1965), **J.Electrochem.Soc., 112,** 608.

Honda,M., Kodera, T. and Kita,H.,(1983) **Electrochim.Acta., 28,** 727.

Hsuch,K-L. and Chin,D-T., (1983), **J.Electroanal.Chem., 153,** 79.

Huang,J.C., Sen,R.K. and Yeager,E., (1979), **J.Electrochem.Soc., 126,** 786.

Hudson,J.A. and Cater,D.B., (1964), **Proc. Roy. Soc. B, 161,** 247.

Hudson,J.A., (1967), **Med.& Biol. Engineering, 5,** 207.

Hughes, S. and Johnson,D.C., (1981), **Anal. Chim. Acta, 132,** 11.

Itaya,K., Sugawara,S., Sashikata,K. and Furuya,N., (1990), **J.Vac.Sci.Technol. A, 8,** 515.

Jamieson,D and Vanden Brenk,H.A.S., (1963), **Int.J.Rad.Biol., 6**(6) 529.

Jamieson,D and Vanden Brenk,H.A.S., (1965), **J.Appl.Physiol.20**(3) 514.

Johnson,H.J., Northup,S.J., Seagraves,P.A., Atallah,M., Garvin,P.J., Lin,L.& Darby,T.D., (1985), **J. Biomed. Mater. Res., 9,** 489.

W.R. Lacourse, W.A. Jackson and D.C. Johnson,(1989), **Anal. Chem., 61,** 2466.

Linek,V., Vacek,V., Sinkule,J., Benes,P. and Chalmers,R.A., (1988), **Measurement of Oxygen by Membrane-covered Probes:** Guidline for Application in Chemical and Biochemical Engineering, Ellis Horwood Ltd.

Longmuir,I.S.,(1963), "The oxygen electrode", in **Oxygen in the animal organism,** Dickens,F and Neil,E., eds., The MacMillan Co.

Lucisano,J.Y., Armour,J.C and Gough,D.A., (1987), **Anal.Chem., 59,** 736.

Kaska,S.M., Sarangani,S. and Giner,J., (1989), **J.Electrochem.Soc., 136,**75.

Koudelka,M., Rohner-Jeanrenaud,F., Terrenttaz,J., Bobbioni-Harsch,E., de Rooij,N.F. and Jeanrenaud,B., (1991), **Biosensors and Bioelectronics, 6,** 31.

Krogh, A., (1919), **J.Physiol.(London), 52,** 409.

Matthews,D.R., Beck,T.W., Plotkin,E., Lock,L., Gosden,E. and Wickham,M., (1988) **Diabetic Medicine, 5,** 248.

Metzger,H., (1973), "Polarographic oxygen tension measurements in microstructure of living tissue", in **Chemical Engineering in Medicine,** Advances in Chemistry Series, Gould, R.F., Ed., American Chemical Society, Washington D.C.

Moatti,D., Capron,F., Poitout,V., Reach,G., Bindra, D.S., Zhang,Y., Wilson,G.S., Thevenot,D.R., (1991) **Diabetologia.** Submitted.

Montgomery,H. and Horwitz,O., (1950), **J.Clin.Invest, 29,** 1120.

Osaka,T., Hirokawa,T., Miyamoto,H. and Oyamo,N., (1987) **Anal. Chem. 59.** 1758.

Pickup, J.C. and Claremont, D.J., (1985), **Diab. Res. Clin. Prac. Suppl., 1,** 447.

Pickup,J.C., Shaw,G.W. and Claremont,D.J., (1989) **Diabetologia, 32,** 213.

Poitout,V., Moatti,D., Velho,G., Reach,G., Sternberg,R., Thevenot,D.R., Bindra,B.S., Zhang,Y. and Wilson,G.S., (1991), **Trans. Am. Soc. Int. Art.**

Org., in press.

Prabhu,V.G., Zarapkar,L.R. and Dhaneshwar,R.G.,(1981), **Electrochim. Acta.**, **26**, 725.

Quess,W.L., Rosenbluth,S.A., Schmidt,B. & Autian,J.,(1965). **J. Pharm. Sci.**, **54**, 1545.

Reach, G., (1990), **Intern. J. Artif. Org.**, **13**. 329.

Rebrin,K., Fischer,U., Woedtke,T.V., Abel,P. and Brunstein,E., (1989), **Diabetologia**, **32**, 573.

Rosenbluth,S.A., Weddington,G.R., Guess,W.L., &Autian,J.,(1965). **J. Pharm. Sci.**,**54**, 156.

Sandler,Y.L. and Pantier,E.A., (1965), **J.Electrochem.Soc.**, **112**, 929.

Santiago, J.V., (1988), in **Diabetes Melitus**, Gallway, J.A., et al. eds, Eli Lilly and Co., Indianaplis, IN.

Schuldiner,S. and Roe,R.M., (1963) **J.Electrochem.Soc.**, **110**, 1142.

W.C.Schumb, C.N.Satterfield and R.L.Wentworth, (1955), "**Hydrogen Peroxide**", Reinhold Publishing Co., NY.

Shaw,G.W., Claremont,D.J. and Pickup,J.C., (1991), **Biosensors & Bioelectronics**, **6**, 401.

Shichri,M., Yamasaki,Y., Kawamori, R., Hakui,N. and Abe,H., (1982) **Lancet, ii**, 1129.

Shichiri,M., Hakui,N., Yamasaki, Y. and Abe,H., (1984) **Diabetes, 33**, 1200.

Silver,I.A.,(1966), "The Measurement of Oxygen Tension in Tissues", in **Oxygen Meassurements in Blood and Tissue**, Payne,J.P. and Hill,W. eds., J&A. Churchill Ltd.

Silver, I.A.,(1973). " Problems in the Investigation of Tissue Oxygen Microenvironment", in **Chemical Engineering in Medicine**, Advances in Chemistry Series, Gould, R.F., Ed., American Chemical Society, Washington D.C.

Sittampalam,G. and Wilson,G.S., (1983) **Anal. Chem. 54**, 1608.

Staub,N.C., (1961), **J.Appl.Physiol.**, **16**,1, 192.

Sternberg,R., Barrau,M-B., Gangiotti,L., Thevenot,D.R., Bindra,D.S., Wilson,G.S., Velho,G., Froguel,P. and Reach,G., (1988) **Biosensors, 4**, 27.

Tamada,Y. and Ikada, Y., (1986). "Cell Attachment to Various Polymer surfaces," **Polymers in Medicine II**, Chiellini,E., Giusti,P., Migliaresi, C., Nicolais,L.,

eds, Plenum Press, NY., p.101.

Urbach,H.B. and Bowen,R.J., (1969), **Electrochim.Acta., 14,** 927.

Velho,G., Froguel,P., Thevenot, D.R. and Reach,G., (1989), **Biomed. Biochim. Acta., 48,** 11/12, 957.

Velho,G., Froguel,P., Sternberg,R., Thevenot,D.R. and Reach,G., (1989), **Diabetes, 38,** 164-71.

Whalen,W.J., Riley,J. and Nair,P., (1967), **J. Appl. Physiol., 23,** 5, 798.

Wilson, G.S., (1986), in **Biosensors. Fundamentals and Applications.,** Turner, A.P.F., Karube, I. and Wilson, G.S., eds., Oxford University Press.

Wilson, G.S., Reach, G. and Thevenot, D.R., (1991), **Biochem. Soc Trans., 19,** 9.

65 - 857